

Drug targeting delivery systems for treatment of Raf-1 induced lung tumors in mice

DISSERTATION

zur Erlangung
des naturwissenschaftlichen Doktorgrades
der Julius-Maximilians-Universität Würzburg

vorgelegt von
Samar Afify
aus Doha/Qatar

Würzburg 2007

Eingereicht am:

bei der Fakultät für Chemie und Pharmazie

1. Gutachter:

2. Gutachter:

der Dissertation

1. Prüfer:

2. Prüfer:

3. Prüfer:

des Öffentlichen Promotionskolloquiums

Tag des Öffentlichen Promotionskolloquiums:

Doktorurkunde ausgehändigt am:

Die vorliegende Arbeit wurde auf Anregung und unter Anleitung von

Herrn Prof. Dr. Ulf Rapp

Institut für Medizinische Strahlenkunde und Zellforschung
der Julius-Maximilians-Universität Würzburg

und

Frau Prof. Dr. Petra Högger

am Lehrstuhl für Pharmazeutische Chemie
des Instituts für Pharmazie und Lebensmittelchemie
der Julius-Maximilians-Universität Würzburg angefertigt.

Meiner Familie

Teile der vorliegenden Dissertation wurden bereits an folgenden Stellen veröffentlicht

Original Publication

Afify S., Rapp UR., Högger P.: **Validation of a liquid chromatography assay for the quantification of the Raf kinase inhibitor BAY 43-9006 in small volumes of mouse serum.** *J Chromatogr B Analyt Technol Biomed Life Sci* 2004, **809**(1):99-103.

Poster

Afify S., Rapp U., Högger P., **Validation of HPLC method for the determination of BAY 43-9006 in mouse serum**, DPhG-Meeting, 2003, Würzburg.

ACKNOWLEDGEMENT

*I wish to express my hearty appreciation and feeling of gratitude to Prof. Dr. **Ulf Rapp**, for suggesting the subject, for his instructive supervision and unlimited continual help that he kindly offered throughout the development of this work.*

*I would like to express my sincere thanks to Prof. Dr. **Petra Högger**, for giving me the chance to express myself in my research, for support and helpful advices.*

*A very special thank to PD Dr. rer. nat. **Rudolf Götz**, our group leader, Institut für Medizinische Strahlenkunde und Zellforschung, Würzburg University, for his help.*

*Also I am profoundly grateful to Dr. **Boris Kramer**, Children Clinic, Würzburg, for his great effort and help in the instillation of mice by the intratracheal technique.*

*I would also like to express my thanks to Dr. **Camarero Guadalupe**, Institut für Medizinische Strahlenkunde und Zellforschung, Würzburg University, for her help in immunohistochemistry staining and for her advices.*

*I am particularly indebted and grateful to Dr. **Manfred Ogris**, Pharmaceutical Biology-Biotechnology, Department of Pharmacy Ludwig-Maximilians-University München, for supplying me with the cationic vectors.*

*My thanks are expressed to Prof. Dr. **Georg Krohne**, Department of Electron Microscopes, for using his scanning electron microscope and to **Dr. Ursula Rdest**, Microbiology Department, for performing centrifugation, Theodor-Boveri-Institut, Faculty of Biology, Würzburg University.*

*Also I am deeply grateful to AR Dr. **Sascha Zügner**, Department of Pharmaceutical Technology, Julius-Maximilians University, Würzburg, for employing the coulter counter.*

*Very special thank to **Roswitha Skrabala** for excellent technical assistance by HPLC analysis and my thanks are expressed to **Angelika Schäfer** for her support and help during my research, Department of Pharmaceutical Chemistry, Institute of Pharmacy and Food Chemistry, Julius-Maximilians University, Würzburg.*

I would like also to thank Doris, Tamara, Maureen, Alla and Nikolaj for their wonderful technical assistance and also to Hilde for her help for supplying me with mice. Special thanks for Tamara for her help in understanding mouse language and culture, Institut für Medizinische Strahlenkunde und Zellforschung, Würzburg University.

Also I am deeply grateful to all my colleagues at Institute of Pharmacy and Food Chemistry, Julius-Maximilians University, Würzburg, for their understanding sincere cooperation and encouragement which enable this work to be completed.

*It is difficult to express in few sentences the gratitude for my family, for their love and support. The greatest acknowledgement I reserve for my husband **Mohamad**, supporting me every time either mentally or in reality, to whom I dedicate this dissertation.*

Table of contents

1. Introduction.....	2
1.1 Meaning of cancer.....	2
1.1.1 Tumor cells and the onset of cancer.....	2
1.1.2 Lung cancer.....	3
1.1.2.1 Aetiology.....	4
1.1.2.2 Symptoms of lung cancer.....	5
1.1.2.3 Stages of lung cancer.....	5
1.1.2.4 Treatment of lung cancer.....	7
1.2 Sorafenib (BAY 43-9006, Nexavar[®]) structure	8
1.2.1. Sorafenib mechanism of action.....	8
1.2.2 Preclinical sorafenib studies.....	10
1.2.2.1 <i>In vitro</i> cellular studies.....	10
1.2.2.2 Sorafenib studies in mice	11
1.2.3 Sorafenib studies in humans	12
1.2.3.1 Sorafenib adverse effects.....	14
1.2.3.2 Sorafenib combination studies	15
1.3 The aim of the present project.....	16
2. Results and discussion	18
2.1 Sorafenib delivery to treat lung adenoma	18
2.1.1 Emulsions as carrier systems for lipophilic drugs	18
2.1.2 Preparation and characterization of a sorafenib emulsion	22
2.2 Development and validation of a HPLC method	22
2.3 Serum concentration of sorafenib after peroral treatment of wild type mice ..	23
2.4 Pharmacological effects on lung adenomas after peroral treatment with	
sorafenib emulsion	24
2.4.1 Histological examination of hematoxylin and eosin stained BXB-23 lung	
tissues after the treatment period	25
2.4.1.1 Effect of oral sorafenib treatment on the lung morphology	26

2.4.1.2 Effect on the tumor area and foci number/mm ²	28
2.4.1.3 Effect on the lung weight	30
2.4.2 Effect of sorafenib (2 mg) peroral treatment on proliferation and apoptosis ...	31
2.4.2.1 Effect of sorafenib treatment on proliferation.....	31
2.4.2.2 Effect of sorafenib treatment on apoptosis	32
2.4.3 Sorafenib concentration in mice serum after oral treatment.....	34
2.5 Conclusion about sorafenib oral treatment	34
2.6 Targeting the lung	36
2.7 Liposomes as carrier system for sorafenib.....	37
2.7.1 Advantages of liposomes	37
2.7.2 Liposome structure	38
2.7.3 Interaction of liposomes with cell surfaces.....	39
2.7.4 Lyophilization as a sorafenib liposome preparation method.....	40
2.7.5 Characterization of the sorafenib liposome	42
2.7.5.1 Liposome size determination	42
2.7.5.2 The entrapment efficiency of sorafenib liposome.....	44
2.7.5.3 Stability of sorafenib liposomal dispersion.....	45
2.7.5.4 Release test of sorafenib from liposome suspension by dialysis	47
2.7.5.5 Release of sorafenib from the liposomal suspension in cell culture	50
2.8 Treatment of BXB-23 mice intratracheally with sorafenib liposomes	53
2.8.1 Advantages and disadvantages of intratracheal instillation.....	53
2.8.2 The difference between intratracheal instillation and inhalation.....	54
2.8.3 Delivery of liposomes via intratracheal instillation.....	55
2.9 Pharmacokinetics of sorafenib after intratracheal administration	56
2.10 Antitumor effects of liposomal sorafenib	58
2.10.1 Histological examination of the lung sections.....	59
2.10.2 Effect of intratracheal instillation sorafenib treatment on the tumor area	62
2.10.3 Effect on the number of foci/mm ²	63
2.10.4 Effect on the ratio of lung weight to body weight (mg/g)	64
2.10.5 Immunohistochemistry for lungs of BXB-23 mice after intratracheal administration of sorafenib liposome	66
2.10.5.1 Effect on proliferation (PCNA assay)	66
2.10.5.2 Effect on apoptosis (caspase-3 assay).....	68

2.10.6 Determination of sorafenib concentration in the lung tissues and blood samples after intratracheal treatment	71
2.10.7 Evaluation of multidrug resistance induction by sorafenib	73
2.10.7.1 Multidrug resistance phenomena.....	73
2.10.7.2 Immunohistochemistry detection of MDR expression in lungs of BXB-23 mice after intratracheal administration of sorafenib liposome	75
2.11 Microspheres as carrier system for sorafenib	79
2.11.1 Microspheres preparation.....	79
2.11.2 Microspheres characterization	80
2.11.2.1 Particle size and size distribution determination.....	80
2.11.2.2 Morphology of microspheres	82
2.11.2.3 Yield and encapsulation efficiency of sorafenib microspheres.....	83
2.11.2.4 <i>In vitro</i> release study of sorafenib from the microspheres	84
2.12 Gene delivery and cationic vectors.....	87
2.12.1 Polyethylenimine (PEI) as a cationic polymer for gene delivery	89
2.13 <i>In vivo</i> application of transfection complex of a reporter gene using different vectors and different routes in tumor bearing BXB-23 mice.....	92
2.13.1 Examination of GFP (Green Fluorescent Protein) reporter gene expression after systemic application via tail vein using PEI as a cationic vector	93
2.13.2 Examination of LacZ (β -galactosidase) expression in lung tissues using PEI as a cationic vector	94
2.13.2.1 Examination of LacZ expression after intravenous injection.....	94
2.13.2.2 Examination of LacZ expression after intratracheal instillation	96
2.13.2.3 Examination of LacZ expression after systemic application of two polyplexes.....	98
2.13.2.4 Immunohistochemical detection of EGF receptors in BXB-23 mice lung and adenoma foci.....	101
3. Experimental procedures	105
A. Frequently used chemicals and materials.....	105
B. Frequently used devices	105
C. Kits	106

D. Solutions and buffers.....	106
3.1 Preparation of sorafenib (BAY 43-9006) emulsions.....	111
3.1.1 Materials and devices.....	111
3.1.2 Preparation of an emulsion containing 2 mg/ml sorafenib	111
3.1.3 Preparation of an emulsion containing 20 mg/ml sorafenib	111
3.2 Treatment of mice with sorafenib emulsions p.o.....	111
3.2.1 Animals.....	111
3.2.2 Pharmacokinetic experiment.....	112
3.2.3 Pharmacological effect of sorafenib emulsion.....	112
a. Transgenic drug treatment group	112
b. Transgenic placebo treatment group	112
c. Transgenic control group	112
3.3 HPLC analytics of sorafenib in serum samples	113
3.3.1 Materials and devices.....	113
3.3.2 Samples preparation.....	113
3.3.3 HPLC conditions.....	113
3.3.4 Validation of the HPLC method	114
3.3.4.1 Selectivity.....	114
3.3.4.2 Linearity	115
3.3.4.3 Accuracy and precision	116
3.3.4.4 Sensitivity.....	117
3.3.4.5 Relative recovery	118
3.3.4.6 Extraction efficiency	118
3.4. Histopathological evaluation of lungs from SP-C-craf BXB-23 mice.....	119
3.4.1 Materials	119
3.4.2 Preparation and staining of the lung tissues.....	119
3.4.3 Immunohistochemistry	120
3.4.3.1 Proliferation test (Proliferating Cell Nuclear Antigen) (PCNA)	120
3.4.3.2 Caspase-3 staining for apoptosis.....	120
3.5. Preparation and characterization of sorafenib liposomes	121
3.5.1 Materials and devices.....	121
3.5.2 Procedure of liposome preparation	122
3.5.3 Characterization of the liposomal suspension	122

3.5.3.1 Particle size measurement	122
3.5.3.2 Determination of encapsulation efficiency.....	123
3.5.3.3 Stability of the liposomal suspension.....	123
3.5.3.4 <i>In vitro</i> release of sorafenib from liposomes in a dialysis assay	123
3.5.3.5 <i>In vitro</i> release of sorafenib in a cell culture assay	124
3.5.3.5.1 SDS-PAGE and Western blot analysis (Detection of p-ERK inhibition by sorafenib)	124
3.6. Treatment of mice with sorafenib liposome intratracheally.....	126
3.6.1 Animals and materials.....	126
3.6.2 Pharmacokinetic experiment.....	126
3.6.3 Pharmacological effects of sorafenib liposome	127
3.6.4 HPLC analytics of sorafenib in lung samples.....	127
3.6.4.1 Samples preparation	127
3.6.4.2 HPLC conditions	128
3.6.5 Immunohistochemistry for multidrug resistance (MDR) in BXB-23 lungs ...	128
3.6.5.1 Materials.....	128
3.6.5.2 Immunohistochemistry protocol.....	129
3.7 Preparation and characterization of sorafenib microspheres	129
3.7.1 Materials and devices.....	129
3.7.2 Preparation of sorafenib PLGA microspheres	130
3.7.3 Sorafenib microspheres characterization	131
3.7.3.1 Determination of particle size distribution.....	131
3.7.3.2 Morphological studies of sorafenib microspheres.....	131
3.7.3.3 Determination of the actual drug loading and microspheres yield.....	132
3.7.3.4 <i>In vitro</i> release study of sorafenib from the microspheres preparation...	132
3.8. <i>In vivo</i> application of transfection complex of a reporter gene using different vectors and different routes in tumor bearing BXB-23 mice.....	133
3.8.1 Materials and devices.....	133
3.8.2 Preparation of the transfection complex	134
3.8.3 Determination of GFP (Green Fluorescent Protein) reporter gene expression after systemic application via tail vein.....	134
3.8.3.1 Animals	134

3.8.3.2 <i>In vivo</i> transfection efficiency in tumor bearing lungs using PEI (polyethylenimine)/GFP complex.....	134
3.8.4 Determination of LacZ (β -galactosidase) reporter gene expression after systemic application via tail vein.....	135
3.8.4.1 Maxi-preparation of plasmid DNA (LacZ).....	135
3.8.4.2 Measurement of DNA concentration.....	136
3.8.4.3 Electrophoresis of DNA on agarose gel.....	136
3.8.4.4 Animals.....	137
3.8.4.5 <i>In vivo</i> transfection efficiency in tumor bearing lungs after intravenous injection of PEI/LacZ complex.....	137
3.8.5 Determination of LacZ reporter gene expression after intratracheal instillation.....	137
3.8.5.1 Animals.....	137
3.8.5.2 <i>In vivo</i> transfection efficiency in tumor bearing lungs after intratracheal instillation of PEI/LacZ complex.....	138
3.8.6 Determination of LacZ reporter gene expression after systemic application of two polyplexes via tail vein.....	138
3.8.6.1 Animals and materials.....	138
3.8.6.2 Preparation of transfection complex (EGF targeted polyplexes).....	138
3.8.6.3 <i>In vivo</i> transfection efficiency in tumor bearing lungs using EGF/PEI and EGF/PEG/PEI as cationic vectors.....	139
3.8.6.4 Immunohistochemistry for EGFR in BXB-23 lungs.....	139
4. Tables.....	142
4.1 Treatment of BXB-23 mice with sorafenib emulsion peroral.....	142
4.1.1 Sorafenib concentration in mice serum after peroral treatment.....	142
4.1.2 Pharmacological effects on the lung adenoma after peroral treatment of BXB-23 mice with sorafenib emulsion.....	142
4.2 Characterization of sorafenib liposome preparation.....	145
4.3 Pharmacokinetics of sorafenib after intratracheal instillation.....	147
4.4 Antitumor effect of liposomal sorafenib after intratracheal instillation.....	148
4.5 Characterization of sorafenib microspheres.....	150

4.6 Validation of sorafenib HPLC method	152
5. Summary	155
6. Abbreviations	162
7. Bibliography	165

1. Introduction

1. Introduction

1.1 Meaning of cancer

Very occasionally, the superb controls that regulate cell multiplication break down. Consequently, this cell starts to grow and divide in an unregulated fashion, regardless the body's need for this type of cells. Subsequently, a clone of cells is able to expand indefinitely as a result of cell proliferation without responding to regulation [1]. Finally, a mass called a tumor may be formed by this clone of unwanted cells. Spreading of those cells throughout the body usually cause the disease. Cancer is caused by mutations, but there are two key differences between cancer and genetic diseases. First, somatic cells mutation mainly causes cancer. Second, a single mutation in genes that normally regulate cell multiplication does not result in cancer, but rather from the accumulation of as few as 3 to perhaps as many as 20 mutations, depending on the type of cancer. Because years can be required for many mutations to accumulate, cancer is mainly a disease of the aged [1].

1.1.1 Tumor cells and the onset of cancer

Benign tumors are small in size, localized and arise frequently in older animals and humans. It is usually obvious when a tumor is benign because it contains cells that closely resemble and may function like normal cells. Serious medical problems can be developed only if the sheer bulk of benign tumors interferes with the normal functions or if they secrete excess amounts of biologically active substances like hormones.

In contrast, the cells composing a malignant tumor, or cancer, express some proteins characteristic of the cell type from which it arose. In addition, a high fraction of the cells grow and divide more rapidly than normal. Carcinoma in situ in the ovary or breast is an example of malignant tumors which remain localized and encapsulated at least for a time [1]. In contrast, some malignant tumors do not remain in their original site and invade surrounding tissues, get into the body's circulatory system and form areas of proliferation away from the site of their original appearance. The spread of tumor cells and establishment of secondary areas of growth is called metastasis. Most malignant cells eventually acquire the ability to metastasize. Thus, the major characteristics that differentiate metastatic (or malignant) tumors from benign ones are their invasiveness and

spread. Malignant tumors are classified as carcinomas if they derive from endoderm or ectoderm and sarcomas if they derive from mesoderm [1].

1.1.2 Lung cancer

Lung cancer is associated with a 90 % death rate within the first year of diagnosis [2]. Lung cancer accounted for 34 % and 21 % of cancer death in men and women [3], respectively. It was investigated that in 2004, there were 173.770 cases of lung cancer and 160.440 deaths related to lung cancer in the U.S. alone, with >80 % being non-small cell lung cancer (NSCLC). Only 14 % of patients diagnosed with NSCLC survive >5 years. In early stages of lung cancer, surgery has been the mainstay of treatment. However, most patients (>75 %) are not surgical candidates due to their advanced lung cancer stage. Therefore, medicinal therapy or radiations are their only options [2].

Lung cancer is classified according to histology of the cancer cells into small cell lung cancer (SCLC) and non-small cell lung cancer (NSCLC) [4].

The NSCLC frequently appears as glands or with an epidermoid architecture and the cells have an abundant cytoplasm with pleomorphic nuclei and often prominent nucleoli. Non-small cell lung cancers include approximately 75 % of all lung tumors and comprise large cell, squamous cell, and adenocarcinoma cell types. Pulmonary adenocarcinomas are classified into four subtypes: acinar, papillary, bronchioloalveolar and solid. Although the cell of origin has not been established definitively, the four subtypes of adenocarcinomas are thought to be stemmed from epithelial cells lining the distal regions of the respiratory tract, including type II alveolar cells, mucin-producing cells and non-ciliated bronchiolar cells [3].

The incidence of adenocarcinoma is increasing in the United States and it is the most frequent lung cancer in non-smokers and women. Pulmonary adenocarcinoma diagnosis is complicated due to the lack of clinical signs and symptoms until the disease is well advanced. In addition, the pulmonary adenocarcinomas are generally refractory to the conventional antitumor therapies.

SCLC is characterized by diffuse sheets of cells with a scant cytoplasm and small hyperchromatic nuclei with indistinct nucleoli [5]. SCLC is believed to be malignant end of spectrum of tumors showing neuroendocrine differentiation. These tumors consist of highly anaplastic small cells with a high nuclear:cytoplasmic ratio. They have metastasized

virtually by the time of diagnosis and are highly malignant. Small cell tumors represent approximately 25 % of lung cancers. For most SCLC patients the prognosis is very poor and 5-years survival for patients with SCLC is only 5 %. Due to the poor prognosis of SCLC patients, it is important in research to develop new therapies, such as gene therapy for lung cancer [5]. Small cell lung cancer patients are generally treated with combinations of chemotherapeutic drugs.

Many tumors possess mixed components similar to those of small cell and non-small cell carcinoma but they behave generally as a small cell carcinoma. After chemotherapy, small cell components often show a good response leaving residual non-small cell tumor. Therefore, consolidation radiotherapy should be taken into account for the residual tumor after standard small cell chemotherapy [6].

Alveolar adenoma is an unusual pulmonary neoplasm first described by Yousem and Hochholzer in 1986 [7]. It is a rare, benign tumor that is usually determined as a solitary pulmonary nodule in asymptomatic patients, more frequently in the middle-aged women [8]. Alveolar adenoma represents a benign proliferation of both alveolar epithelium and septal mesenchyma [9]. It is well delineated with multiple cystic spaces containing a granular material. Most of the epithelial cells lining the cystic spaces are type 2 pneumocytes [10].

1.1.2.1 Aetiology

Although there are different causes for lung cancer, cigarette smoking is the main cause and the number of lung cancer cases entirely due to other carcinogens is uncommon. Among the environmental factors associated with lung cancer such as active smoking of tobacco (responsible for 80 % of all cases of lung cancer), passive smoking, asbestos (several minerals that occur naturally as fibers, float in air and inhaled, where they can lodge in the lungs, damaging cells and increasing the risk for lung cancer), urban pollution, arsenic and radon gas (radioactive gas that occurs naturally in soil and rock). Also, lung disease such as tuberculosis and some types of pneumonia could result in lung cancer. The other cause of lung cancer can be due to personal and family history [6].

1.1.2.2 Symptoms of lung cancer

The classic symptoms of lung cancer are haemoptysis, cough (does not go away and gets worse over time), dyspnoea, constant chest pain, shortness of breath and recurrent or persistent chest infections (such as bronchitis and pneumonia). Lung cancer mainly occurs in elderly smokers, all of whom have a smoker's cough and frequent fits of bronchitis with associated sputum production and frequently haemoptysis. Many have breathlessness due to emphysema and chest pain due to ischemic heart disease [6].

1.1.2.3 Stages of lung cancer

A. Small cell lung cancer staging

Most patients with small cell cancer have systemic metastatic disease at the time of diagnosis and hence the treatment and prognosis are independent on locoregional tumor as in the case of non-small cell cancer. Indeed, the patients' performance status has more relevance to the treatment manner to which they are most adapted [6]. Disease is therefore classified as limited or extensive (Table 1).

Table 1: Stages of small cell lung cancer

Limited stage	The cancer is only in one lung and in lymph nodes on the same side of the chest.
Extensive stage	The cancer has spread to the other lung, to lymph nodes on the other side of the chest, or to distant organs. Many physicians consider cancer that has spread to the fluid around the lung to be extensive stage as well.

B. Non-small cell lung cancer staging

In NSCLC, treatment and prognosis are completely dependent on accurate staging (Table 2). Stage I tumors are small and readily considerable with good prognosis. The standard treatment is surgery and also radical radiotherapy is an option. Stage II tumors have local lymph node metastasis which lead to a reduced prognosis due to their node metastasis. Stage III tumors are locally advanced and heal with surgery alone is uncommon [6]. The staging components consist of descriptions of the extent and location of the primary tumor, the presence or absence of regional lymph node involvement and the incidence of distant metastasis.

Stage grouping combines the anatomic subsets with generally similar treatment options and survival expectations into stages, such that the survival experience of each group is unique, with stage I reflecting the best prognosis and stage IV is the worst [11, 12].

Table 2: Stages of non-small cell lung cancer

Stage 0	The cancer is limited to the lung and is found in a few layers of cells only. It has not grown through the top lining of the lung. Stage 0 is also called carcinoma in situ.
Stage I	The cancer is in the lung only, with normal tissue around the tumor. Stage I is divided into stages IA and IB, based on the size of the tumor.
Stage II	The cancer has spread to nearby lymph nodes or to the chest wall. Stage II is divided into stage IIA and stage IIB, based on the size of the tumor and whether it has spread to the lymph nodes.
Stage III	<p>The cancer has either:</p> <ul style="list-style-type: none"> • Spread to the lymph nodes in the <i>mediastinum</i> (middle area between the lungs that contains the heart, major blood vessels and other structures). or • Spread to the lymph nodes on the opposite side of the chest or in the lower neck. <p>Stage III is divided into stage IIIA (which is sometimes treated with surgery) and stage IIIB (which is rarely treated with surgery).</p>
Stage IV	The cancer has spread to other parts of the body or to another lobe of the lungs.

1.1.2.4 Treatment of lung cancer

The treatment options for lung cancer include best supportive care, surgery, chemotherapy, radiation therapy and photodynamic treatment, either alone or in combination, depending on the type and the stage of cancer [6].

1.2 Sorafenib (BAY 43-9006, Nexavar[®]) structure

In collaboration between Onyx Pharmaceuticals (Emeryville, CA, USA) and Bayer (Leverkusen, Germany), the Raf kinase inhibitor BAY 43-9006 (now called sorafenib) was developed [13-15]. Recently, sorafenib was marketed under the name Nexavar[®] [16]. Sorafenib is a bis-aryl urea, namely, 4-(4-(3-(4-chloro-3-trifluoromethylphenyl) ureido) phenoxy) pyridine-2-carboxylic acid methylamide (Figure 1). Furthermore, it was the first molecule of its class to undergo clinical development. Sorafenib and related ureas have been described as inhibitors of several other kinases including p38 and Cdk4 [17].

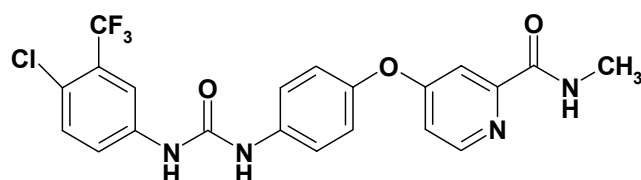


Figure 1: Chemical structure of sorafenib (BAY 43-9006): c-Raf inhibitor.

1.2.1. Sorafenib mechanism of action

Sorafenib is an antineoplastic agent that functions by inhibiting the Raf kinase constituent of the classical mitogen-activated protein kinase (MAPK) signaling cascade [13]. It is an orally bioavailable Raf kinase inhibitor, which inhibits Ras-dependent human tumor xenograft models [14].

Although sorafenib was initially developed as an orally available potent Raf kinase inhibitor through blockade of Raf/MEK/ERK pathway, sorafenib can also target several other important tyrosine kinase receptors, including VEGFR (Vascular endothelial growth factor receptor), EGFR (Epidermal growth factor receptor) and PDGFR (Platelet-derived growth factor receptor) kinases as described in several earlier studies [18-20]. Therefore, sorafenib is considered as a novel dual-action Raf kinase and VEGFR inhibitor that inhibits tumor cell proliferation and angiogenesis [21, 22] Figure 2.

Raf-1 is serine/threonine kinase and it is a downstream effector of Ras (it is a monomeric GTP-binding protein that plays an important role in MAPK signal transduction pathway)

signaling cascade. Both proteins are highly oncogenic when mutationally activated. Both Raf-1 and Ras proteins play a pivotal role in controlling normal and transformed cell growth. In MAPK pathway, Ras is activated by a variety of growth factors and cytokines. Subsequently, the MAPK signal transduction pathway is activated. Raf binds directly to Ras and such binding leads to membrane-translocation and activation of Raf kinase activity. Activated Raf phosphorylates the kinase MEK (mitogen-activated protein kinase kinase) resulting in MEK activation. In turn, activated MEK phosphorylates the kinase ERK (extracellular signal-regulated kinase) leading to translocation of ERK to the nucleus (Figure 2). ERK phosphorylates and activates a variety of transcription factors which control cell transformation, cell growth and proliferation [23, 24]. Inhibition of the MAPK pathway through inhibition of Raf kinase using sorafenib results in anti-proliferative effects with slowing or inhibition of tumor cell proliferation (Figure 2).

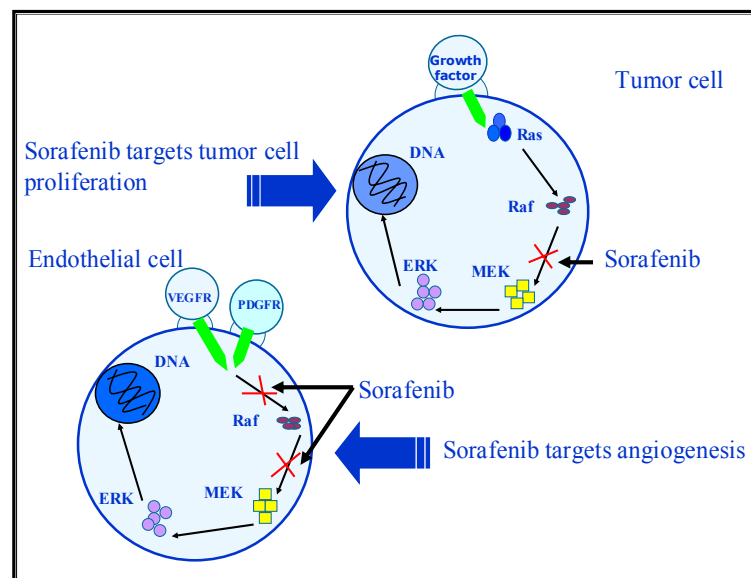


Figure 2: Sorafenib is the first compound to target both the signaling pathway to inhibit cell proliferation and angiogenesis (modified after Branca [25]).

In endothelial cells, sorafenib exerts an antiproliferative effect by blocking the VEGFR-2 pathway at two levels: upstream by inhibiting the VEGFR-2 receptor and downstream at the level of Raf kinase. These activities were found to be responsible for sorafenib anti-angiogenesis activity in tumor vasculature [24] Figure 2.

1.2.2 Preclinical sorafenib studies

1.2.2.1 *In vitro* cellular studies

Sorafenib was shown to inhibit downstream Raf kinase isoforms (wild-type Raf-1, B-Raf and mutant B-RafV599E) in cell lines. Additional characterization of sorafenib in biochemical assays demonstrated potent inhibition of several receptor tyrosine kinases [20] as shown in Table 3.

Table 3: *In vitro* inhibitory profile of sorafenib

Biochemical kinase assay	<i>In vitro</i> IC ₅₀ value (nM)
Raf-1	6
Wild-type B-Raf	25
Mutant B-Raf V599E	38
Murine VEGFR2	90
Murine VEGFR3	20
Murine PDGFR β	57
FLt-3	33
c-KIT	68
FGFR1	580

VEGFR: Vascular endothelial growth factor receptor, PDGFR: Platelet-derived growth factor receptor, FGFR: Fibroblast growth factor receptor, FLt-3: Fms-like tyrosine kinase-3, c-KIT: stem-cell growth and V599E is a mutant form of B-Raf.

To examine sorafenib efficiency in blocking the activation of mitogen-activated protein kinase (MAPK) pathway, the ERK phosphorylation was measured in several tumor cell lines, including those containing Ras mutations and B-Raf mutations, as well as in wt (wild-type) cells [26]. The results demonstrated that sorafenib inhibited ERK phosphorylation in most of these cell lines, regardless of which mutation caused abnormal activation of the Raf/MEK/ERK pathway [20, 27]. Sorafenib inhibition of p-ERK was also detected in human pancreatic (Mia PaCa and BxPC-3), colon (HCT 116 and HT-29) tumor cells and in the human melanoma (LOX) cell lines. More than 50 % inhibition of VEGFR-2 phosphorylation was achieved at 100 nM sorafenib in human umbilical vein endothelial

cells (HUVEC). Wilhelm et al. [20] reported that sorafenib is a potent inhibitor of VEGFR-2 signaling in cells.

Rahmani et al. [28] studied the effect of sorafenib on apoptosis *in vitro* in human leukaemia cells (U937). Their results indicated that sorafenib treatment led to noticeable induction of caspase activation, mitochondrial injury and apoptosis in human myeloid and lymphoid leukaemia cells through down-regulation of Mcl-1 via inhibition of translation. They described also that exposure of U937 cells to sorafenib was accompanied with a decrease in ERK phosphorylation.

Wilhelm et al. [27] showed that sorafenib hindered the tumor cell proliferation at a dose that inhibits Raf activity in colon (HCT 116) and pancreatic (Mia-PaCa-2) cell lines.

Sorafenib exhibited inhibition of the mitogen-activated protein kinase (MAPK) pathway in colon, pancreatic and breast tumor cell lines expressing mutant K-Ras (Kirsten (K)-Ras which was expressed by K-ras mutant gene) or wild-type or mutant B-Raf, whereas non-small-cell lung cancer cell lines expressing mutant K-Ras were insensitive to inhibition of the MAPK pathway by sorafenib [20].

1.2.2.2 Sorafenib studies in mice

The small molecule Raf-1 kinase inhibitor sorafenib (Raf-1 is a member of the RAF/MEK/ERK signaling pathway) was selected for further pharmacological characterization based on its potent inhibition of Raf-1 and its favourable kinase selectivity profile.

A previous pharmacokinetic study [29] using sorafenib (BAY 43-9006) were first performed in CD-1 mice. Sorafenib was rapidly absorbed after oral administration of various doses and showed a terminal $t_{1/2}$ between 3.2 and 4.2 h whereas t_{max} was reported between 1 and 1.6 h. Furthermore, plasma concentrations correlated well with the various doses. The achieved levels of drug ($> 50 \mu\text{M}$ after a dose of 100 mg/kg) were significantly higher than the reported IC_{50} for *in vitro* HCT 116 colon tumor cell inhibition ($4.6 \mu\text{M}$), suggesting that oral administration of sorafenib was suitable for efficient drug delivery and cellular uptake.

Once daily oral dosing of sorafenib revealed a broad spectrum antitumor activity in colon, breast and non-small-cell lung cancer xenograft models. In two of the three xenograft models examined, the immunohistochemistry showed a close association between

inhibition of tumor growth and inhibition of the extracellular signal-regulated kinases (ERKs) phosphorylation with concomitant inhibition of RAF/MEK/ERK pathway in some but not all models [20]. In addition, a significant inhibition of neovascularization in all three of the xenograft models was demonstrated after microvessel density and microvessel area analyses utilizing the antimurine CD31 antibodies [20].

Moreover, sorafenib was identified as a potent inhibitor of Raf kinase in a biochemical assay and in cellular assays. It revealed an antitumor efficiency when administered orally at doses of 10, 30 and 100 mg/kg/day for 14 days against subcutaneously (s.c.) implanted human colon (HCT 116), pancreatic (MIA-Paca-2), lung (Ncl-H 460) and ovarian (SK-OV-3) xenograft models, a dose-dependent tumor growth inhibition of 45 to 68, 44 to 73, 27 to 56 and 45 to 81 %, respectively, was achieved. Sorafenib exhibited cytostatic anti-tumor efficacy against s.c HCT 116 xenografts when the treatment at a dosage of 30 and 100 mg/kg/dose was prolonged up to 30 days in duration. It also demonstrated cytostatic anti-tumor efficacy against advanced staged s.c. HCT 116 xenografts. The presence of an activated ras oncogene was not required for sorafenib sensitivity *in vivo* [13, 30]. The growth of lung tumors (Ncl-H 460) was inhibited 27 % and 56 % at dosage of 10 and 30 mg/kg/dose of Raf kinase inhibitor, respectively.

Kramer et al. [31] studied the effect of the Raf kinase inhibitor sorafenib and the MEK inhibitor CI-1040 (PDI 84352) on a Raf dependent lung tumor mice model (BXB-23). These mice developed adenomas within 4 months of life and then were treated daily either with 100 mg/kg sorafenib or CI-1040 for further 21 days intraperitoneally. They found that both inhibitors showed equal efficacy *in vitro* utilizing a sensitive Raf/MEK/ERK ELISA. Moreover, the systemic administration of the MEK inhibitor CI-1040 *in vivo* reduced adenoma formation and decreased the proliferation rate. On the other hand, the Raf inhibitor sorafenib did not influence adenoma formation. Karasarides et al. [32] explored that sorafenib targeted B-Raf signaling *in vivo* and induced a considerable growth delay in melanoma tumor xenografts.

1.2.3 Sorafenib studies in humans

Clinical testing of oral tablets of sorafenib in cancer patients started in July 2001 [14, 33]. In contrast to the pharmacokinetics of sorafenib in mice, this compound shows a relatively long terminal half-life of 35 hours in humans [34]. More than 500 patients have been

treated with sorafenib in early phase clinical trials [23]. Early pharmacokinetic observations have proven good oral bioavailability (in a fasted state or with a moderate fat meal). Sorafenib has substantial interpatient variability. Increasing sorafenib dose leads to increase in C_{max} and area under the curve (AUC) values. No clear effect of food on sorafenib bioavailability was observed [23].

Strumberg et al. [35] found that sorafenib toxicity did not seem to be a dose dependent and a high variability in its pharmacokinetics for single and multiple dosing was observed. They concluded that the oral sorafenib could provide some clinical profits and according to their results, sorafenib at 400 mg bid continuous, until disease progression or unacceptable toxicity occurred, is recommended for ongoing and future studies.

Another study [36] determined the pharmacokinetics of sorafenib in patients with advanced, refractory metastatic or recurrent solid tumors. Sorafenib was administered orally in eight doses from 50 mg every fourth day to 600 mg twice daily. The results revealed that the median duration of stable disease was 7.2 months and the stable disease was obtained in 22 % of patients. Sorafenib accumulated on multiple dosing as a result of its observed half-life of ~27 h.

Awada et al. [37] described that sorafenib was rapidly absorbed and steady-state conditions were reached within 7 days. Additionally, increasing sorafenib dosing did not increase its exposure proportionally. Sorafenib administration at doses from 50 to 800 mg bid for 21 days with 7 days off treatment exhibited antitumor activity in patients with advanced, refractory solid tumor.

Another research group [38] explored that sorafenib pharmacokinetic analysis revealed early absorption with subsequent delay of the secondary peaks and slow terminal elimination. The maximum tolerated dose (MTD) of sorafenib was 600 mg bid with a favourable safety profile which supported its development for treatment of solid tumors.

In vitro microsomal data revealed that sorafenib was metabolized in two phases: phase I oxidation negotiated by cytochrome P450 (CYP) 3A4 and phase II conjugation negotiated by UGT1A9 [39]. Furthermore, the effect of ketoconazole mediated CYP3A4 inhibition on sorafenib pharmacokinetics *in vivo* was demonstrated. Thus, co-administration of the two drugs did not result in clinical adverse events or laboratory abnormalities. Furthermore, no increase in the sorafenib exposure was achieved after the blocking of sorafenib metabolism by the CYP3A4. It was concluded that higher therapeutic doses of sorafenib can be safely co-administered with ketoconazole as well as with other inhibitors of CYP3A4 [39].

Ratain et al. [40] studied a phase II randomized clinical trial in patients with metastatic renal cell carcinoma. They found that after 12 weeks treatment period with oral sorafenib 400 mg twice daily, a statistically higher percentage of patients with no disease progression in the sorafenib group as compared with the placebo-treated patients was obtained. Sorafenib showed a significant disease-stabilizing activity in this renal carcinoma and was tolerated with chronic daily therapy [40].

Sorafenib showed promising antitumor activity for advanced renal cell cancer patients in phase II trials, that 70 % of study participants with renal cancer had tumor shrinkage or disease stabilization [41]. Sorafenib (Nexavar[®]) has been recently approved by the FDA for advanced renal cell carcinoma in phase III clinical trials [16]. A recently completed phase III, placebo-controlled study showed that median progression-free survival doubled from 12 weeks to 24 weeks in patients treated with the multi-kinase inhibitor sorafenib (Nexavar[®]) and approximately three-quarters of patients had some degree of tumor regression. Furthermore, 39 % improvement in overall survival in sorafenib treated patients relative to those in placebo treated patients was achieved [42].

1.2.3.1 Sorafenib adverse effects

In the early clinical data of sorafenib in patients with advanced, refractory solid tumors [23], the drug has been generally well tolerated with no dose limiting toxicities yet encountered. The more common toxicities have involved the gastrointestinal tract (diarrhea, nausea, abdominal cramping) and the skin (pruritus, rash, cheilitis).

Another research group [38] determined the maximum tolerated dose (MTD) and safety profile in 19 patients with advanced, refractory solid tumors. The MTD of sorafenib in this study was determined to be 600 mg bid. Sorafenib was generally well tolerated, with mild to moderate toxicities.

Awada et al. [37] and Strumberg et al. [35] showed that the most frequently reported adverse events of sorafenib over multiple cycles were related to gastrointestinal (75 %), dermatologic (71 %), constitutional (68 %), pain (64 %) or hepatic (61 %). A MTD of 400 mg bid sorafenib was defined for patients with advanced, refractory solid tumors.

Others [36] determined in phase I study the maximum tolerated dose (MTD) of sorafenib in patients with advanced, refractory metastatic or recurrent solid tumors. The MTD was 400 mg twice daily. Sorafenib was well tolerated, with mild to moderate toxicities. The

dose limiting toxicities (DLTs) was hand-foot syndrome in three of seven patients receiving 600 mg twice daily.

The safety and efficacy of sorafenib were acquired from four phase I dose-escalation trials [43]. This study confirmed that oral sorafenib monotherapy in patients with advanced solid tumor was safe and well tolerated.

Veronese et al. [44] discussed the incidence, severity and mechanism of blood pressure (BP) elevation in patients treated with sorafenib. They reported that treatment with sorafenib was accompanied with significant and sustained increase in BP.

1.2.3.2 Sorafenib combination studies

When sorafenib used in combination with other agents, it was well-tolerated with evidence of antitumor efficacy. Phase I/II are therefore ongoing, evaluating the following combinations: sorafenib and gemcitabine in advanced ovarian and pancreatic cancers [45] showed no consistent pharmacokinetic drug-to-drug interaction and this combination was well tolerated. Sorafenib and doxorubicin in patients with hepatocellular carcinoma [46], sorafenib and oxaliplatin in colorectal cancer [47] showed that oral sorafenib 400 mg twice daily was safely combined with oxaliplatin without detectable drug interactions and revealed antitumor activity in phase I study. Flaherty et al. [48] and Ahmed et al. [49] studied the activity of sorafenib, carboplatin and paclitaxel combination in patients with melanoma. All doses were well tolerated and toxicity rates did not exceed those expected with carboplatin and paclitaxel in the absence of sorafenib. Carter et al. [50] evaluated the efficiency and tolerability of combinations of sorafenib with agents used to treat non-small cell lung cancer (NSCLC) using preclinical models of that disease. Co-administration of sorafenib and vinorelbine, cisplatin or gefitinib was efficacious as the individual agents alone and was well tolerated. Thus, the development of sorafenib in clinical trials in NSCLC using combinations of both cytotoxic and cytostatic agents is recommended.

Reddy and Bukowski [51] discussed the activity of sorafenib as a single agent or in combination with Interferon-alpha2 in patients with advanced-stage renal cell carcinoma. They concluded that sorafenib exhibited a significant clinical potency in these patients.

1.3 The aim of the present project

The aim of the present project was to use different delivery systems in order to target lung tumors of BXB-23 mice model. Also, determination of sorafenib (example of antitumor agents) antitumor activity orally on the lung adenoma of BXB-23 mice model was investigated. Furthermore, targeting sorafenib directly to the lung and assessing its activity on treatment of the lung adenoma of BXB-23 mice model was studied. The plan was to incorporate sorafenib in different dosage forms as carrier systems and then using different routes of administration. The suggestion was to use the intratracheal instillation as a route of administration in order to target sorafenib directly to the lung of BXB-23 transgenic mice model. Additionally, the pharmacological activity of sorafenib was examined on several parameters in order to investigate the success of the targeted delivery.

The other dosage form used for sorafenib incorporation was microspheres which have been considered as a promising carrier for anticancer drugs.

Another strategy in the present project was to target the lung of BXB-23 mice intravenously and intratracheally using a reporter gene. Therefore, the success of gene delivery to the lung tumor and the ability of polyethylenimine (PEI) as an example of non-viral vector to target the lung bearing tumor of BXB-23 mice was investigated. In order to achieve cell-receptor targeting in the lung tumor, the use of epidermal growth factor (EGF) as a ligand complexed with polyethylenimine (PEI) as a vector was suggested.

2. Results and discussion

2. Results and discussion

2.1 Sorafenib delivery to treat lung adenoma

The aim of the present study was to design different dosage forms as carrier systems to deliver sorafenib to the lung of BXB-23 transgenic mice using different routes of administration. Two dosage forms were used, one of them was an oil-in-water emulsion and the oral route was chosen for this experiment. The other delivery system was a liposome preparation for intratracheal instillation as administration route. The oral route in this case was considered as control experiment because sorafenib was investigated before as an orally potent antineoplastic agent in mice [20, 29] and in human studies [36, 37]. Here in this study it was important to test if sorafenib would be released from the emulsion preparation and then absorbed and exhibiting efficacy when given orally to BXB-23 mice. The other aspect was to assess if using the lung targeting route for sorafenib to treat this kind of mice would improve its efficacy or not.

2.1.1 Emulsions as carrier systems for lipophilic drugs

In this chapter we explored if sorafenib incorporation in an emulsion preparation demonstrated its antitumor effect on lung adenoma of BXB-23 transgenic mice following oral administration.

Sorafenib is a highly lipophilic anticancer agent. In the present investigation the solubility of sorafenib in water was measured using HPLC analysis. Sorafenib has a very low aqueous solubility (2.6 $\mu\text{g/ml}$). It was important for sorafenib delivery in the present study to incorporate it in a formulation in order to administer it to the animals. Thus, for the development of a suitable formulation the key point was to increase its aqueous solubility. Several types of carrier systems e.g. oil in water (o/w) emulsion and liposomes have been suggested as candidates for lipophilic drugs in order to raise the aqueous concentration of the drug as well as to provide good pharmacokinetic properties as described by Kan et al. [52] for paclitaxel, a lipophilic drug.

In cancer chemotherapy, in order to increase the therapeutic concentration of the drug at the site of action and decrease the side effects, many types of carrier systems have been investigated to find a means of delivering antitumor agents to the target site. Those carriers include liposomes [53], lipoproteins [54], and others. Among the emulsion types the lipid

emulsions, especially oil in water (o/w) emulsions, are believed to be appropriate for highly lipophilic drugs [55, 56]. The utilization of lipid emulsions is limited by various instability processes like aggregation, flocculation, coalescence and phase separation [57]. In contrast, emulsions have advantages in terms of high drug loading capacity.

An emulsion has the ability to incorporate drugs with poor water solubility within the dispersed phase and was proposed as a suitable vehicle for water insoluble drugs since increased solubility is achieved due to the presence of an oily phase. An emulsion is a dispersion of two immiscible liquids, one of which is finely subdivided and uniformly distributed as droplets (the dispersed phase) throughout the other continuous phase (Figure 3).

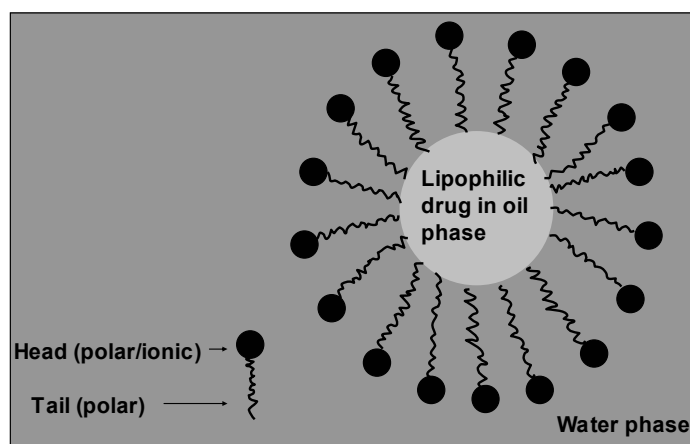


Figure 3: Compounds of an emulsion.
The internal phase is the dispersed phase (oil phase).
The external phase or dispersion medium is the continuous phase (water phase).

As emulsions tend to coalesce, the process of coalescence can be reduced to insignificant levels by addition of an emulsifying agent or emulsifier such as acacia, lecithin, gelatine, or sodium carboxy methyl cellulose to reduce the interfacial tension. They are adsorbed at the oil-water interface, with the hydrocarbon tails in the oil phase and the hydrated polar head groups in the water phase. Fats or oils are suitable for oral administration and the oil in water (o/w) emulsion is formed e.g. to mask unpleasant taste [58]. Several types of emulsions (Table 4) have been described by Nakano [59].

Table 4: Emulsion types

Type of emulsion	Description
Oil-in-water emulsions	Oil-in-water emulsions used as carriers for many oil-soluble drugs. These drugs are enclosed in an oil phase of oil-in-water emulsions.
Lipid emulsions	Emulsions of soybean oil have been employed to deliver drugs parenterally by dissolving drugs in soybean oil. They were originally utilized for supplying vegetable oil parenterally.
Water-in-oil emulsions	Water-in-oil emulsions can be utilized as carriers for water-soluble drugs by dissolving drugs in a dispersed phase (water). Usage of these emulsions is limited because of high viscosity of a dispersion medium (oil) [60].
Self-emulsifying drug delivery systems	They are mixtures of oils and surfactants, sometimes containing cosolvents which emulsify under gentle agitation similar to the one that would be encountered in the gastrointestinal tract [61].
Lipid nanoemulsion	Lipid nanoemulsions (nanospheres) have similar structures and compositions to those of lipid emulsions (microspheres) but their particle sizes (25-50 nm) are smaller (200 nm). They are prepared from purified soybean oil and purified egg yolk lecithin.

Microemulsions	Their particle size range is 8-80 nm. They contain high percentages of both oil and water and high concentrations of surfactants [62].
Solid emulsions	Films of Eudragit RS, a hydrophobic polymer containing polyethylene glycol 14000 after treatment with water, yielded solid emulsions.
Multiple emulsions	Water-in-oil-in-water emulsions
Modified emulsions	a. Electronically charged submicron emulsions for enhanced topical delivery of antifungal drugs [63]. b. Lectin-functionalized multiple emulsions for improved cancer therapy [64].

There are major factors affecting the formulation of emulsions such as: selection of the oil phase, selection of suitable emulsifying agents, rheological properties, preservatives and antioxidants [58].

There are also several methods to evaluate emulsion characterizations such as:

- A. Visual observation, before and after shaking, is relatively simple and useful for examining coalescence and phase separation. Photomicrography can also be a useful technique for testing emulsions for coalescence.
- B. The particle size determination either by coulter or light-scattering methods can be used for emulsion particle size determination and particle size distribution analysis.
- C. Both centrifugation and temperature stress tests have also been utilized for emulsion stability tests [65]. Microwave irradiation can be also used to determine emulsion stability [66].
- D. Phase inversion can usually seen by eyes. However, other tests available include conductimetry (if the water is the continuous phase, the emulsion will conduct electricity) [67]. Alternatively, a few drops of water-soluble dye can be placed on the surface of the emulsion. If the emulsion is o/w, the dye will rapidly diffuse throughout the system, if the emulsion is w/o, the dye will not disperse.

2.1.2 Preparation and characterization of a sorafenib emulsion

The sorafenib emulsion was prepared using a traditional method by dissolving sorafenib in oil phase (olive oil) and then it was emulsified by gum arabic aqueous phase (see experimental part 3.1).

In the present investigation, the emulsion preparation was initially examined by visual observation. It was a homogenous white emulsion. No coalescence or phase separation was observed. Microscopic examination revealed that the particles were round in shape, homogenous and not aggregated. The particle size ranged from 4.5-9 μm which was the same for the plain and sorafenib loaded emulsion. No significant change in droplet size occurred when sorafenib was introduced into the emulsion. This meant that sorafenib did not influence the size of the internal oily phase droplets. It is important to evaluate the emulsion preparation to see if the formulation is stable and has good quality to be suitable to use for further experiments.

2.2 Development and validation of a HPLC method

It was necessary to develop a HPLC method for sorafenib for two reasons. One of them was to see if sorafenib was absorbed after its administration and to determine its concentration in mice serum and lung tissue after treatment with the sorafenib loaded dosage forms. The other reason was that to our knowledge no detailed analytical procedures for sensitive and selective quantification of sorafenib in mice serum had been published so far. Because it was impossible to have a large amount of mice blood, we aimed at the development of a simple method requiring only small volumes of mouse serum. The sample preparation was done using only 30 μl of mouse serum by liquid-liquid extraction method and tolinaftate was chosen as internal standard (see experimental procedures 3.3).

The advantages of this method included the ease of sample preparation and the small volume of serum sample required. The analytical method was validated in terms of selectivity, linearity, precision, accuracy, low limit of quantitation (LOQ), recovery, and extraction efficiency.

The developed HPLC method, validated for sorafenib concentrations in serum ranging from 80-2000 ng/ml, had satisfactory specificity (no interference was observed), linearity,

accuracy, good sensitivity and precision range over the concentration range examined. The LOQ was 80 ng/ml and the relative recovery was 93.3 % [68].

Thus, the developed HPLC method proved to be useful and reliable for the determination of serum concentrations of sorafenib.

2.3 Serum concentration of sorafenib after peroral treatment of wild type mice

The aim of this experiment was to control if sorafenib was absorbed from the emulsion formulation and to determine its concentration in blood samples after oral administration of two different doses. Two wild type mice of the B1/6×D2 strain were used. Although the mice number was small it was enough to confirm that sorafenib was released from the emulsion and absorbed after oral administration. The two mice were from both sex, 3 months old and weighing between 20-30 g. Blood samples were taken after oral administration of 0.2 and 2 mg sorafenib once per animal.

Afterwards 30 μ l serum was analyzed to determine the sorafenib concentration (see HPLC chromatograms in 3.3.4.1).

After single oral administration of 0.2 and 2 mg sorafenib per animal serum concentrations of 999 and 1777 ng/ml, respectively, were determined after 2 h. After 24 h the serum levels declined below the lower limit of quantitation in case of the 0.2 mg dose, while 96 ng/ml were still detectable after administration of 2 mg sorafenib (Figure 4).

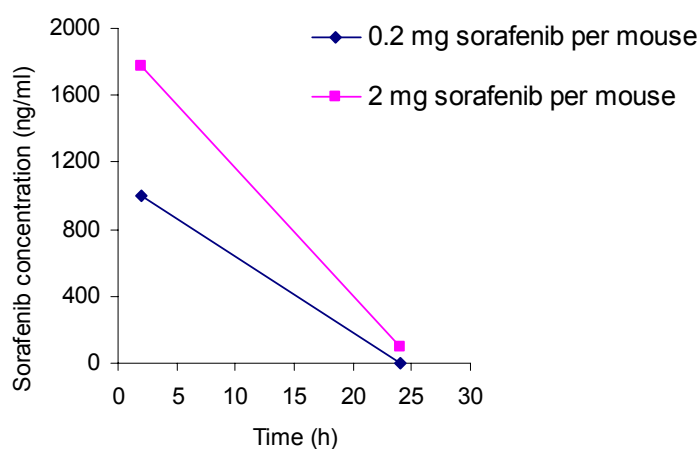


Figure 4: Serum concentrations of sorafenib after peroral treatment of a single mouse with a single dose of a drug-containing emulsion.

The results of the present study showed that the drug was obviously rapidly absorbed with high serum concentration after 2 h and decreasing serum concentration thereafter. Since the higher dose (2 mg) of sorafenib lead to higher serum concentrations it can be concluded that the absorption of the drug is dose dependant. This observation is consistent with the previously described pharmacokinetic profile of sorafenib in CD-1 mice [29]. After oral administration of a range of sorafenib concentrations (10, 30 and 100 mg/kg), sorafenib was rapidly absorbed with t_{\max} of 1-1.6 hours and the sorafenib plasma concentration increased proportionally with higher doses.

In the present investigation elimination was completed after 24 h in case of 0.2 mg sorafenib but there was still a detectable concentration of sorafenib after 24 h after administration of 2 mg sorafenib. Other earlier studies [13, 29] explained that sorafenib showed a terminal $t_{1/2}$ between 3.2 and 4.2 h after oral administration of 10, 30, 100 mg/kg/day for 14 days.

In a previous study of Lathia et al. [39] the elimination process of sorafenib was described. *In vitro* microsomal data indicated that sorafenib was metabolized through two pathways: Phase I oxidation mediated by cytochrome P450 (CYP) 3A4, and phase II conjugation negotiated by UGT1A9. Due to either biliary excretion or lack of absorption, approximately 50 % of an orally administrated dose was recovered as unchanged drug in feces.

To conclude, in the present study sorafenib was absorbed from the emulsion preparation. Thus, pharmacological effects are to be expected and can be further investigated.

2.4 Pharmacological effects on lung adenomas after peroral treatment with sorafenib emulsion

After the successful demonstration of oral absorption of sorafenib, the pharmacological effect was studied on the lung adenoma of BXB-23 mice. The *in vivo* effect of oral administration of sorafenib emulsion was analyzed in the present investigation using Raf dependent lung tumor mice based on the following background:

- The promising previous *in vitro* and *in vivo* results [29], which revealed that in tumor cells, sorafenib inhibited the activation of two downstream Raf effector kinases, MEK and ERK (see introduction). Sorafenib inhibited cellular proliferation and hindered tumor cell proliferation at a dose that inhibited Raf activity.

- The detection of sufficient serum concentrations in the present study (see 2.3) and the previous pharmacokinetic profile of sorafenib [29].

Twenty three mice were used for this experiment, six received a drug free emulsion (placebo), twelve mice received active treatment and five untreated mice served as control. The treated animals were handled with 0.2 or 2 mg sorafenib every second day for one month. The treatment schedule is described in Figure 5.

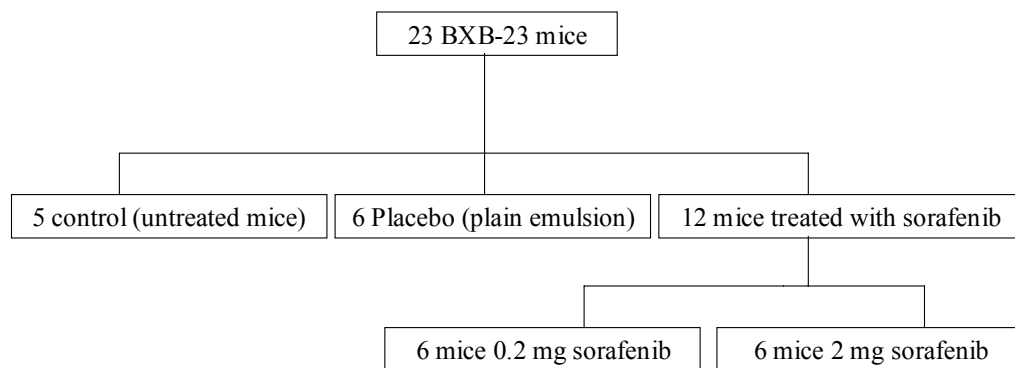


Figure 5: Treatment schedule of sorafenib p.o. using two doses for treatment of lung adenoma of BXB-23 mice.

In the present experiment, in order to assess the sorafenib effect on the lung adenoma after p.o. treatment, the lung sections of transgenic BXB-23 mice after one month treatment were examined for the tumor percent (tumor area), number of foci adenoma/mm² (tumor content), proliferation and apoptosis.

2.4.1 Histological examination of hematoxylin and eosin stained BXB-23 lung tissues after the treatment period

Previous studies showed that the antitumor effect after treatment can be evaluated by several parameters such as lung weight, number of tumors and median tumor size on the lung surface as explained by Koshkina et al. [69, 70]. Another research group [31] used lung histology, number of adenoma foci per mm², proliferation, apoptosis and differentiation as parameters for antitumor effect evaluation.

The purpose of this chapter focuses on the effect of sorafenib emulsion treatment p.o. on the lung morphology. This parameter was studied to see if sorafenib improved the lung morphology by reducing the thickness of the alveolar walls, which indicates proliferation reduction. The effect of the oral sorafenib emulsion treatment was also examined on tumor area of lung adenoma foci, which was expressed as tumor percent. Furthermore, the effect of sorafenib emulsion oral treatment on the tumor number (adenoma foci number/mm²) was determined. The lung weight was elucidated to show if sorafenib treatment had an effect on the lung weight as a result of tumor content reduction and tumor shrinkage. Lung weights were used in this experiment to approximate the tumor content of the lungs. The paraffin embedded lung tissues were stained by hematoxylin and eosin (H&E) to define the lung morphology and to be able to count the cells and adenoma foci. Hematoxylin (blue) stains the nucleus and eosin (red) stains the cytoplasm.

2.4.1.1 Effect of oral sorafenib treatment on the lung morphology

The lung tissues from all mice of the placebo group (animals which received plain emulsion p.o.), control group (untreated mice) and the group treated with sorafenib emulsion 0.2 and 2 mg were stained with H&E in order to define the lung morphology. Figure 6 illustrates all stained lung tissues from these groups.

Histologically, the adenoma foci are defined with large nucleus, composed of cuboid epithelia comparable to alveolar type II cells and the tumor cells show a glandular proliferation, lining the alveolar walls in lepidic fashion [71]. The adenoma foci are surrounded with alveolar spaces and alveolar walls.

After one month p.o. treatment every second day with sorafenib emulsion, the treatment with 2 mg sorafenib did not only reduce adenomas but also improved the overall lung structure as revealed by thin alveolar walls. In contrast, treatment with 0.2 mg sorafenib showed no detectable effect in comparison to placebo treated animals and control animals (Figure 6).

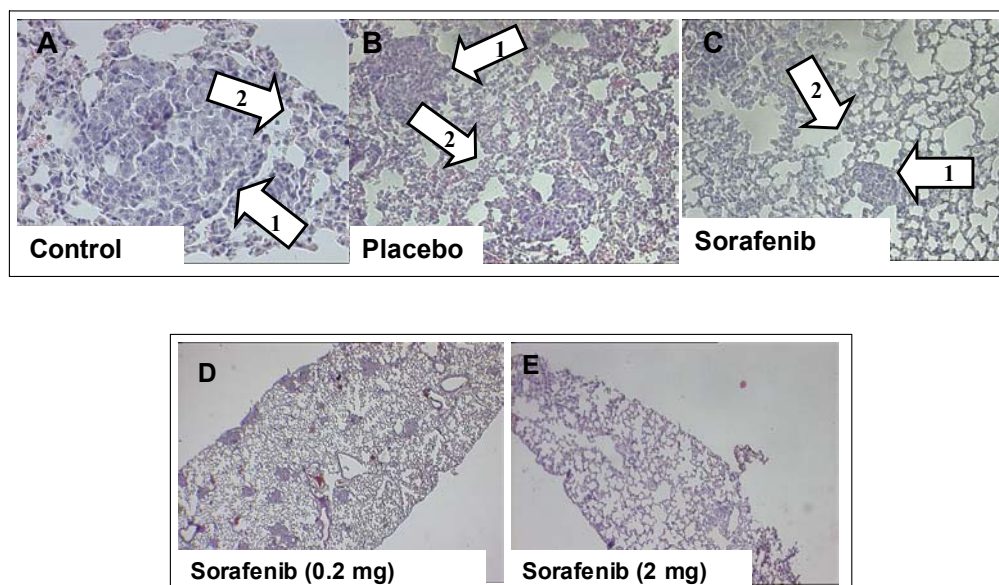


Figure 6: Pharmacological effect of oral administration of two different doses of sorafenib on the lung adenoma and morphology of the lung.

(A, B, C) One month p.o. treatment with 2 mg sorafenib reduced adenomas and improved the lung structure (hematoxylin and eosin staining, scale bar corresponds to 60 μm at 40 \times magnification). (D, E) Treatment with 2 mg sorafenib, but not 0.2 mg reduced lung adenomas and improved the overall lung structure with thin alveolar walls in comparison with 0.2 mg sorafenib and placebo treated animals (4 \times magnification). Placebo (the mice treated with plain emulsion) and control (untreated mice). Arrows represent adenoma foci (1) and alveolar walls (2).

The overview of the H&E stained lung sections of 0.2 and 2 mg treatment with sorafenib are shown in Figure 6 D and E, respectively. This overview revealed the differences in the overall appearance and morphology between the lung sections of BXB-23 mice treated with 2 mg sorafenib emulsion and the other which were treated with 0.2 mg. The structure of the lung was improved and the thickness of the alveolar walls was reduced in case of the H&E stained lung tissues after 2 mg sorafenib. This indicated also the reduction of the proliferation because in BXB-23 lung sections the tumor cells show a glandular proliferation lining the alveolar walls. The improvement of the overall lung structure resulting in thin alveolar walls was earlier used as a suitable parameter for evaluating the antitumor effect [31].

2.4.1.2 Effect on the tumor area and foci number/mm²

The next aim was to determine if sorafenib p.o. had an effect on the tumor size and tumor number. Therefore, the lung sections of animals treated with 2 mg sorafenib were further analyzed. The tumor area of the orally treated animals and placebo group (mice administered plain emulsion) was expressed as tumor percent and calculated by dividing the tumor area of the adenoma foci by the total area of the high power field. For this purpose H&E stained lung tissues were used. The tumor percent in 3 different sections of every mouse was determined and averaged. The number of adenoma foci was calculated by counting the adenoma foci and dividing the number by the total area of the high power field and then calculating the number of foci per mm² area.

In the present study, the tumor percent was significantly reduced after treatment with 2 mg sorafenib p.o. in comparison to the placebo treated animals (Figure 7 A). The reduction in the tumor percent of the animals treated with 2 mg was from 11.9 ± 2.77 % to 8.5 ± 1.5 % compared to the placebo group (Figure 7 A). This translates into a 29 % inhibition of the tumor area as compared with the placebo group.

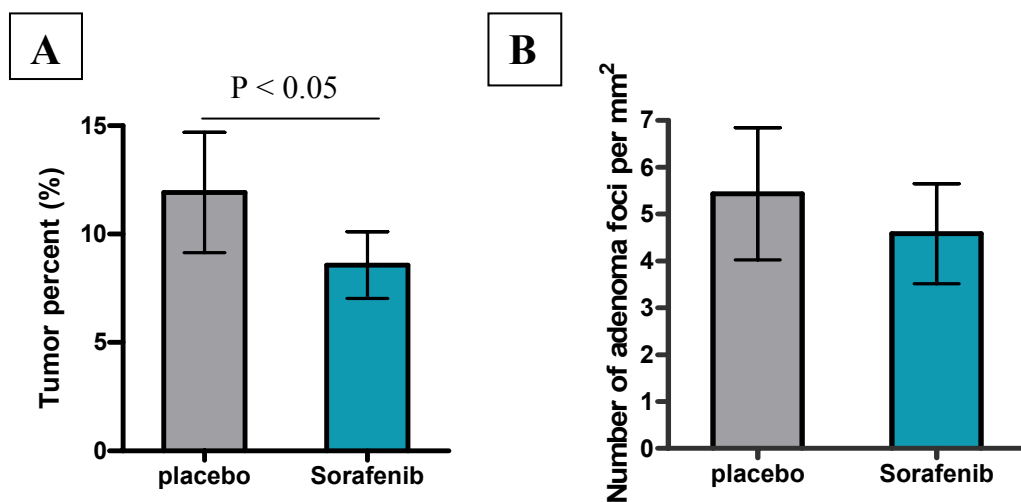


Figure 7: Sorafenib (2 mg) reduced the lung adenomas area (tumor percent %) but had no significant influence on the number of adenoma foci per mm².

(A) The lung adenomas area was reduced, expressed as tumor percent (%) after oral treatment with 2 mg sorafenib for one month. (B) Sorafenib did not change the number of foci per mm². The data (mean ± SD) was statistically analyzed using t test (Graph Pad Prism) and a P-value of < 0.05 was regarded as an indication of statistical significance (n = 6).

In contrast, treatment with 2 mg sorafenib p.o. did not change the total number of the tumor adenoma foci of 4.6 ± 2 per mm^2 in comparison with the placebo group which revealed 5.4 ± 1.4 adenoma foci per mm^2 (Figure 7 B). This indicated that the treatment of BXB-23 mice orally every second day with 2 mg sorafenib per mouse had an effect on the adenoma foci by reducing the area of the single foci but did not influence the total tumor content (adenoma foci/ mm^2). It can be concluded that sorafenib was successfully released and absorbed from the emulsion and exhibited antitumor effect on the lung adenoma of BXB-23 mice.

In a previous study [29] sorafenib showed potent and dose-dependant inhibition of tumor growth in three human tumor xenograft models (colon, pancreatic and ovarian). The anti-tumor activity was observed at 10 mg/kg (45 %), 30 mg/kg (64 %), 100 mg/kg (68 %) doses of sorafenib. Similar results were achieved with pancreatic (MiaPaCa-2) and ovarian (SK-OV-3) xenograft models. On the last day of dosing every day for 14 consecutive days, colon (HCT 116) tumors were significantly reduced in sorafenib treated animals compared to control animals.

In addition, Wilhelm et al. [20] found that the antitumor activity of sorafenib in human xenografts produced a dose-dependent tumor growth inhibition. Mice bearing 75 to 150 mg tumors were treated orally with sorafenib at dose levels of 7.5 to 60 mg/kg, administrated daily for 9 days. In the human colon tumor models (HT-29, Colo-205 and DLD-1) and in the non small cell lung cancer (NSCLC) A549 model, complete tumor stasis was observed during treatment with 30 to 60 mg/kg sorafenib after calculating the mean tumor weight. Tumor growth was inhibited in another NSCLC model (NCI-H460), but complete stasis during treatment was not achieved at doses up to 60 mg/kg. The breast tumor model (MDA-MB-231) was the most sensitive to sorafenib. Only after 9 days of the treatment with dose of 30 mg/kg, the mean size of these tumors was reduced by 42 % [20].

In the present study the antitumor activity of sorafenib was achieved at 80 mg/kg on lung adenoma of BXB-23 mice model. The effect was a reduction in the tumor size (29 %) in comparison to the placebo group after oral treatment every second day for one month. Although the result of the present investigation was not comparable with the previous published results because the tumor model used in the present study was different and the treatment period was not the same, the present sorafenib treatment p.o. showed its antitumor activity on lung adenoma in BXB-23 mice model.

2.4.1.3 Effect on the lung weight

Since lung weights determination has been described as a parameter to evaluate the antitumor effect of treatment [31, 69], in this chapter the effect of 2 mg sorafenib treatment p.o. on the weight of the lung was examined as a factor which indicated the effect of sorafenib treatment on the tumor content of the lung.

No remarkable effect on the lung weight was observed (Figure 8). There was no significant difference between the lung weights of the sorafenib treated animals 0.19 ± 0.02 g and placebo 0.18 ± 0.03 g or control animals 0.2 ± 0.03 g.

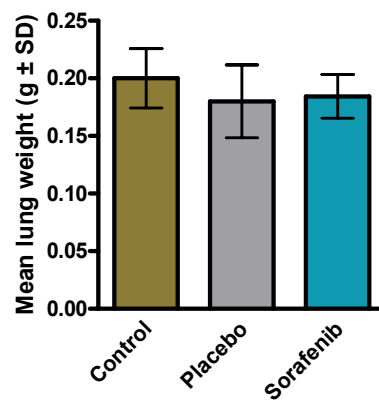


Figure 8: Sorafenib treatment (2 mg) every second day for one month had no effect on the lung weight (g). In comparison with the lung weight of the placebo group (n = 6) and untreated animals control (n = 4) there was no significant effect of 2 mg sorafenib oral treatment (n = 6) on the reduction of the lung weight.

It was expected to achieve a reduction in the lung weights of the sorafenib treated animals because in the present study 2 mg sorafenib oral treatment resulted in a reduction of approximately 29 % in the tumor area (see 2.4.1.2). On contrary, no significant reduction in the lung weights of the treated animals in comparison with placebo and control groups was observed. Additionally, no significant effect was detected on the adenoma foci number after 2 mg sorafenib treatment.

Koshkina et al. [69] and Kramer et al. [31] found a significant correlation between the lung weights and the number of tumors so they used lung weights to approximate the tumor content of lungs.

Another earlier study [70] explained that depending on the treatment frequency, lung weights reduction may be either attributed to the tumor size reduction alone or related to the reduction in tumor size along with tumor number.

In the present study, lung weight was not affected by tumor size nor foci number after sorafenib oral treatment. Probably, the determination of lung weights in the present case was not sensitive enough to predict the antitumor activity.

2.4.2 Effect of sorafenib (2 mg) peroral treatment on proliferation and apoptosis

The adenoma foci were further analyzed for proliferation and apoptosis in order to assess the effect of sorafenib treatment p.o. on tumor cell growth and survival on molecular level. For this purpose proliferation (PCNA) and apoptosis (caspase-3) were examined.

2.4.2.1 Effect of sorafenib treatment on proliferation

The degree of proliferation is one of the major marking indicators for the evaluation of rate, duration and molecular characteristics of tumor progression [31, 72]. A good marker for proliferating cells is the 36 kDa Proliferating Cell Nuclear Antigen (PCNA) protein. It is synthesized in early G1 and S phases of the cell cycle. Immunohistochemistry detection of Proliferating Cellular Nuclear Antigen (PCNA) serves as an important prognostic factor, because of its unique expression [73, 74]. PCNA detection is useful in the evaluation of tumor induction and development measured as growth alterations when compared to healthy or untreated tissues and cells as described earlier [31, 72, 75].

In the present study the immunohistochemical detection of PCNA using the paraffin embedded lung tissues of animals treated with 2 mg sorafenib every second day for one month and the placebo animals were examined. The percentage of PCNA brown stained positive cells was calculated by dividing the number of PCNA positive cells by the whole cell number of the adenoma foci.

There was a clear reduction in the percent of PCNA positive cells of the 2 mg sorafenib treated animals (Figure 9 A, B). Figure 9 B shows the adenoma foci and the nucleus after staining with hematoxylin, the brown cells indicate the positive staining of the proliferating cells. The percent of adenoma proliferating cells in animals treated with 2 mg sorafenib

was statistically significantly ($P < 0.05$) reduced from $28 \pm 1.4 \%$ to $21.5 \pm 1.5 \%$ in comparison to the placebo animal group (Figure 9 A).

This reduction of the percentage of proliferating cells can be the reason for the improvement of the lung structure in the treated mice group as discussed before (2.4.1.1). When the cells stop to proliferate that may affect the thickness of the alveolar walls because the histology of BXB-23 mice lung sections reveals that the tumor cells are surrounded by alveolar walls, which are lined with a glandular proliferation in lepidic fashion [71].

The present observation was consistent with the finding of Kramer et al. [31] that after intraperitoneal (i.p.) treatment of BXB-23 mice with CI-1040 (MEK inhibitor) the lung structure was improved and the proliferation rate of lung cells was decreased as well.

It was expected to achieve proliferation reduction in the present study because *in vitro* experiments with NIH 3T3 cells showed that sorafenib inhibited the activation of two downstream Raf effector kinases (MEK and ERK) in tumor cells and inhibited cellular proliferation [29]. Sorafenib hindered tumor cell proliferation at a dose that inhibited Raf activity. Moreover, sorafenib exhibited complete tumor stasis in other tumor models (human colon and non small cell lung cancer (NSCLC)) when given orally at 30 to 60 mg/kg [20]. This was confirmed with the present study as sorafenib treatment p.o. for BXB-23 mice revealed a reduction of the proliferation.

2.4.2.2 Effect of sorafenib treatment on apoptosis

Apoptosis mediated by anticancer drugs may involve activation of cell death inducing ligand/receptor systems such as cleavage of caspase and the increase of apoptosis correlated with an activation of the caspase-3 pathway [31]. By studying the molecular events in apoptosis systems, it is now clear that cleavage of protein substrates by caspase is an important cascade that is unique to apoptotic cells [76, 77]. Caspase-3 is necessary for DNA fragmentation, the cleavage of a large number of proteins, nuclear collapse during apoptosis and for apoptosis-associated chromatin margination [78].

In the present study the apoptotic cells were detected by immunohistochemistry for activated caspase-3. Lung tissues from six BXB-23 mice treated every second day orally for one month with 2 mg sorafenib emulsion and lung tissues from six animals as placebo were immunohistochemically stained for activated caspase. The percent of active

caspase-3 positive cells was calculated through dividing the number of caspase-3 positive cells by the whole cell number in the adenoma foci.

No statistically significant difference between the 2 mg sorafenib treated animals (2.75 ± 0.5 %) and their placebo (3.08 ± 0.35 %) was detected after one month treatment (Figure 9 C).

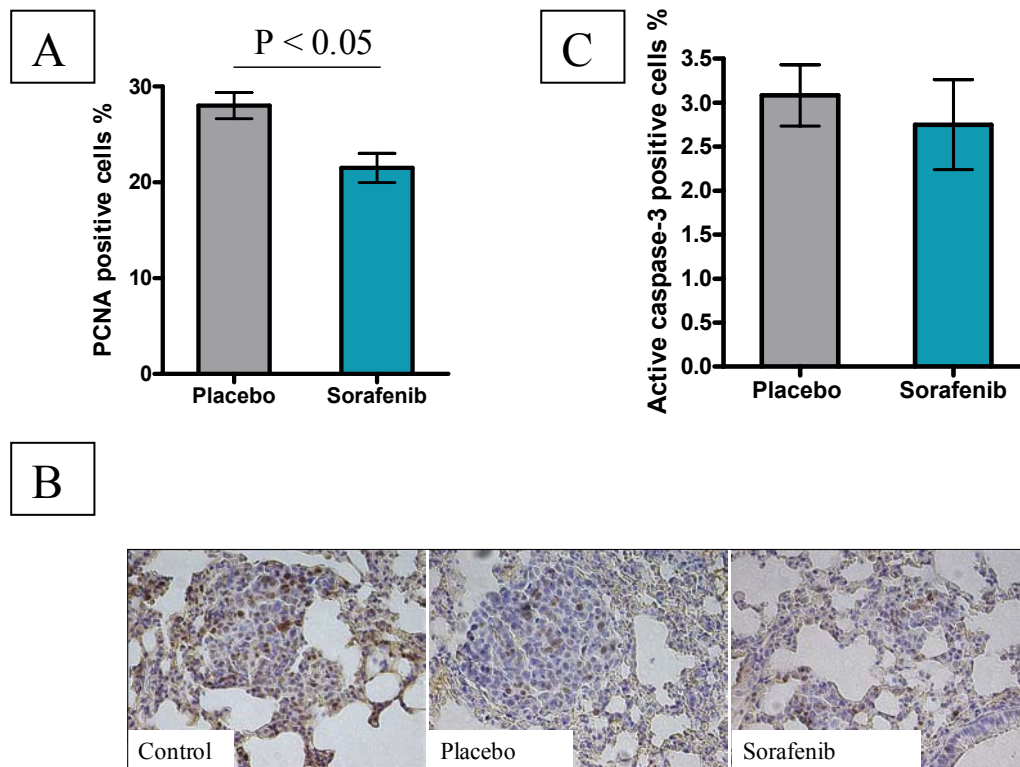


Figure 9: Sorafenib (2 mg) every second day for one month reduced proliferation in lung adenoma but did not influence apoptosis.

(A and B) 2 mg sorafenib treatment ($n = 6$) reduced the PCNA brown positive cells in lung adenomas in comparison with the placebo treated animals ($n = 6$). The data (mean \pm SD) was statistically analyzed using t test (Graph Pad Prism). (C) The 2 mg sorafenib treatment ($n = 6$) did not activate the caspase-3 mediated apoptotic pathway in lung adenomas. Magnification $40\times$ is indicated (scale bar $60\ \mu\text{m}$). Control (untreated mice), Placebo (mice received plain emulsion).

In the present study it was expected to achieve an apoptotic effect on lung adenoma after sorafenib p.o. treatment because sorafenib was previously [24] found to induce apoptosis in many human cancer lines such as renal carcinoma, colon carcinoma (HT-29), breast carcinoma (MDA-MB-231), hepatocellular carcinoma (HCC) and non small cell lung cancer (NSCLC) A549. Furthermore, sorafenib induced apoptosis of leukaemia cells [28]. In addition, sorafenib mediated apoptosis through an MEK/ERK and caspase-independent

mechanism in human melanoma cell lines [79]. Moreover, it was recently explained that sorafenib promotes apoptosis in tumor vasculature [80]. Unfortunately, in the present investigation sorafenib p.o. treatment did not induce apoptosis of adenoma foci cells which could be attributed to the insufficient sorafenib concentration in the lung to induce apoptosis. Another possible explanation may be that the determination of activated caspase-3 was not the suitable assay or was not sensitive enough for apoptosis detection.

2.4.3 Sorafenib concentration in mice serum after oral treatment

Measuring the mice serum concentration of sorafenib after 2 mg oral treatment for one month was important in order to know if sorafenib was completely eliminated or if there was still some concentration present in the blood 24 h after the end of the treatment period. The determined sorafenib concentration in mice serum was lower than the low limit of quantitation (LOQ). The LOQ was measured in the validation of the newly developed HPLC method as 80 ng/ml. This result was not surprising because it was explained before in the present pharmacokinetic experiment (2.3) that sorafenib was rapidly eliminated and its concentration in blood was 96 ng/ml 24 h after single oral administration of 2 mg. Thus, sorafenib was also rapidly eliminated after multiple doses as occurred after single dose administration.

2.5 Conclusion about sorafenib oral treatment

It can be concluded from the results obtained with oral sorafenib treatment every second day for one month with 2 and 0.2 mg sorafenib emulsion that only 2 mg sorafenib in emulsion preparation showed tumor area and proliferation reduction in three months old BXB-23 mice lung adenoma.

It was expected in the present study to achieve antitumor effect after 2 mg sorafenib p.o. treatment on all parameters tested to evaluate this effect. Although sorafenib concentration was not determined in the lung tissues, the concentration level of sorafenib in mice serum 2 hours after oral administration of 2 mg sorafenib was 3800 nM as determined in the present pharmacokinetic experiment (2.3), which was higher than the previously published IC_{50} [20, 31].

The IC₅₀ value for C-Raf inhibition by sorafenib was 16 nM as determined by Kramer et al. [31] using ELISA assay. The activity of sorafenib was measured by detecting phospho-ERK which depends on Raf and MEK activity.

Wilhelm et al. [20] described a biochemical assay in which varying concentrations of sorafenib were tested for their capacity to inhibit MEK-1 phosphorylation by the catalytic domains of Raf-1. They found that sorafenib potently inhibited Raf-1 with an IC₅₀ value of 6 nM.

The results of the present investigation raise the question why the present treatment affected the tumor area and proliferation but had no influence on the number of adenomas or apoptosis.

One explanation could be that the sorafenib concentration in blood was probably not sufficient at the tumor bed to affect all parameters used in antitumor activity evaluation. This low concentration may be related either to the rapid elimination of sorafenib or connected to the distribution of sorafenib in other organs. It was explained before that sorafenib displayed a terminal half life in mice of between 3.2 and 4.2 h after its oral administration at various doses [13, 29]. The short $t_{1/2}$ of sorafenib in mice reveals rapid elimination of the drug. Moreover, sorafenib is metabolized by two pathways CYP3A4 and UGT1A9, and approximately 50 % of an orally administered dose is recovered as unchanged [39].

In the present study, sorafenib was eliminated more rapidly after multiple doses and it was completely eliminated 24 h after the end of treatment period (2.4.3).

The other reason for such non homogenous effect obtained after sorafenib p.o. treatment might be the distribution of the drug in other organs, which leads to dilution of sorafenib concentration and influences its level at the site of action (the lung and the tumor). Subsequently its therapeutic effects will be affected as the concentration of sorafenib at the active site must be adequate.

In addition, the weak effect of sorafenib treatment p.o. on the lung adenoma in the present study could be attributed to the difficulty of Raf kinases inhibition due to multiple feedback mechanisms [81]. It was already discussed previously by Hall Jackson et al. [82] that inhibitors targeting the kinase activity of Raf may be counterbalanced by reactivation. Thus, Raf suppresses its own activation by a novel feedback loop.

In the present case, the effect of sorafenib as Raf inhibitor on the lung adenoma could be reduced because its inhibition activity of Raf was probably counterbalanced by

reactivation. This reduction subsequently affected sorafenib antitumor activity on the lung adenoma. Kramer et al. [31] showed in their study that administration of sorafenib (100 mg/kg) daily for 21 days intraperitoneally for treatment of lung adenomas of BXB-23 did not influence adenomas. They attributed their observation to the feedback reactivation mechanism.

As a conclusion sorafenib exhibited antitumor activity on lung adenoma when administered orally to BXB-23 mice. Thus, sorafenib worked as antineoplastic agent in this mice strain after oral treatment. The next issue was to investigate if the targeting of sorafenib directly to the BXB-23 mice lung will improve its efficacy.

2.6 Targeting the lung

Ideally, the drug should be placed directly at the site of action to maximize the effect and minimize side effects relating to unwanted responses at sites other than the target tissues.

Drug targeting means selective delivery of the drug to target cell or site using a carrier system. The aim of the targeted therapies is to increase the efficacy and to reduce the toxicity of the drug.

There are several types of drug targeting [83]:

a) First-order targeting

This implies delivery to discrete organs or tissues and involves the use of biologically active agents which are potent and selective to a particular site in the body.

b) Second-order targeting

This describes targeting to a specific cell type within a tissue or organ. It involves the preparation of pharmacologically inert forms of active drugs which are activated by a chemical or enzymatic reaction when reach the active site (prodrug approach).

c) Third-order targeting

This represents delivery to a specific intracellular compartment in the target cells utilizing a biologically inert macromolecular carrier system which delivers the drug directly to a specific site in the body (drug-carrier approach).

Previous investigations [84-86] revealed that the delivery of certain drugs to the respiratory tract in liposome formulation may have advantages of non-invasive administration, such as high pulmonary concentrations, reduced toxicity and reduced dosage requirement compared to oral and parenteral administration.

Many reports have previously described intratracheal administration of liposome-encapsulated drugs such as atropine [87], gentamycin [88], α -Tocopherol [89] and glutathione [53] into the lungs of rodents and rabbits. This approach achieves three therapeutically desirable goals in cases of lung diseases: (i) direct targeting of the drug where it is most needed, (ii) prolonging residence time of the drug through its release from liposomes and (iii) the possibility of increasing drug regimens with minimal toxicity.

In a previous study [53] the intratracheal delivery of glutathione (GSH), in liposome-encapsulated form was chosen. This study had been designed to determine the extent and time-course of pulmonary tissue uptake of administrated ^{14}C -labelled liposomes containing [^3H]GSH. This study showed that the residence time of the drug in the rat lung was prolonged and the liposomes delivered to the lung showed specific pulmonary recovery patterns.

Encapsulation of cytosine arabinoside (Ara-C), vinblastine, actinomycin D or daunomycin within liposomes caused an enhanced retention of these drugs in the bloodstream and in the tissues after pulmonary instillation by affecting their pharmacokinetic behaviour [90, 91].

In the present investigation it was elucidated whether a further improvement and increase of the effect of sorafenib in a lung adenoma model might be achieved. For this purpose targeting of sorafenib directly to the lung to increase its effect was considered. The other question was to find a suitable formulation and route of delivery, which was able to target the drug to the site of action. The drug was incorporated in a liposome formulation as another carrier system for lipophilic drugs. The intratracheal instillation was chosen as the suitable route to deliver the drug to the lung.

2.7 Liposomes as carrier system for sorafenib

2.7.1 Advantages of liposomes

In the present study liposomes were used as the second carrier system for the lipophilic drug sorafenib. Liposomes are considered as a versatile drug carrier technology with considerable potential for improved solubilization of lipophilic drugs [92].

Several reasons suggested the choice of liposomes as carrier system for sorafenib:

- Liposomes are biocompatible and biodegradable because of their bilayer structure. Lipids are similar to those of the biological membranes, so no toxicity after liposome

systemic administration was shown even at chronic aerolized [93]. Liposomes have limited intrinsic toxicity with no antigenic or pyrogenic reactions [94].

- Liposomes can be prepared from phospholipids, which are endogenous to the respiratory tract as a component of pulmonary surfactant. For this reason liposomes are considered as suitable drug carrier system for pulmonary drug delivery [93].
- Liposome encapsulation could alter the pharmacokinetics of materials. This was achieved by increasing the local concentrations of the loaded materials, whilst the levels at sites distant from the site of action were decreased [95]. Consequently, a greater fraction of the dose reached the target site with prolongation of their residence time [96-98].
- Liposomes can also alter the pharmacokinetics and pharmacodynamics of encapsulated drugs by enhancing drug uptake and delaying rapid drug clearance [99].
- The most important reason which related to the present study was that cancer cells must consume large amounts of fat to preserve rapid growth. Therefore, liposome encapsulated drugs are recognized as a potential source of nutrition [100]. Accordingly, the tumor cells will engulf the liposome entrapped drug with subsequent drug release and finally the drug has the possibility to destroy the tumor cells. In addition, accumulation of liposomes at tumor sites is due to their ability to negotiate their way through pores in the capillary endothelium [100]. The antitumor activity of liposomal anticancer drug formulations is dependent on drug release rates which can achieve therapeutic concentrations at the tumor site [101].
- Liposomes can be modified with specific molecules including specific antibodies against tumor surface antigens or by the adjustment of their size and composition to enable organ-selective drug delivery [102].
- Usage of liposomes controls the retention of incorporated drugs in the presence of biological fluids. Also liposomes control vesicle residence in the systemic circulation or other compartments in the body and hence enable vesicle uptake by the target cells [94].

2.7.2 Liposome structure

Liposomes are microscopic vesicles composed of membrane-like phospholipid bilayers surrounding an aqueous medium. The lipid vesicles are formed spontaneously when phospholipids are hydrated in aqueous medium. Liposomes are considered as vesicles carrier system because of their entrapping ability. Liposomes are unique due to their ability

to enclose both hydrophilic and hydrophobic molecules (Figure 10). The bilayer membrane entraps hydrophobic molecules whereas hydrophilic molecules can be encapsulated in the internal aqueous region [100].

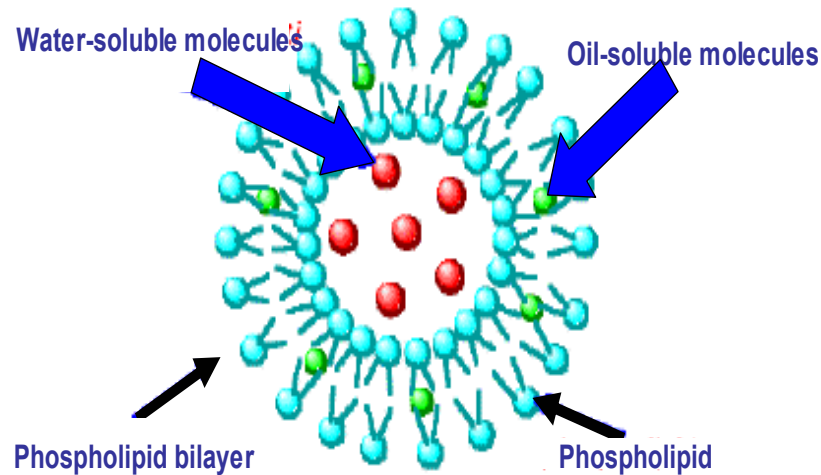


Figure 10: Liposome structure

The liposome contains a lipid membrane that encapsulates an internal aqueous cavity used to entrap water soluble therapeutic agents. Alternatively, lipid soluble therapeutic agents can be carried within the phospholipid bilayer (Modified after Jamil et al. [100]).

Liposomes are classified into three groups [100, 103]:

- Multilamellar vesicles (MLVs) are generally heterogeneous in nature and may have several compartments. They are easy to prepare and can vary in size from 0.5 to 5 μm .
- Small unilamellar vesicles (SUVs) range in size from 20 to 50 nm. They have a spherical shape and are homogenous in size.
- Large unilamellar vesicles (LUVs) are larger (200-1000 nm) giving them greater space for encapsulation of aqueous medium. They are utilized for hydrophilic drugs.

2.7.3 Interaction of liposomes with cell surfaces

Liposomes interact with the cell surface via two main mechanisms: adsorption and endocytosis. Liposomes can be directly adsorbed to a cell surface (non-specifically) or by specific interaction with a cell-surface receptor. For specificity, liposomes can be modified

with protein, antibody or carbohydrate moieties or with other polymers. The liposome content transfers by diffusion through the lipids of the liposome and the cell membrane.

In contrast, during endocytosis the liposomes are internalized actively by the target cell. The adsorbed or bound vesicle can be engulfed by the cell into the endosome and after fusion with lysozymes, lytic agents (enzymes, protons-lower pH) digest the liposome [104]. The entire liposomal contents are made available to the cell. The lysosomes distinguish the liposome and are used by the cell to digest or breakdown most complex organic molecules.

In addition, there are two other mechanisms of liposome interaction with the cell surface [100]: fusion of the cell with the vesicles and lipid exchange. Lipid exchange takes place due to the low aqueous solubility of the lipids, therefore the liposome and cell membrane can exchange lipid molecules. This exchange is higher for liposomes in a liquid crystalline phase and for lipids with shorter hydrocarbon chains. Another type of interaction is fusion of the liposome with the cell membrane. Thus, the lipid portion of the vesicle becomes part of the cell wall and then diffuses or endocytoses into the cell [104].

2.7.4 Lyophilization as a sorafenib liposome preparation method

Finding a suitable preparation method to entrap drugs in the liposome is important in drug targeting [105]. So the first step in the present study was to find a suitable procedure to prepare liposomes. A lyophilization method was chosen in which the final liposome product is freeze dried to evaporate the organic solvent in which the lipid and the drug were dissolved (see experimental procedures 3.5.2). The final dry lipid film was reconstituted with PBS immediately prior to administration. This type of procedure increases the stability of the liposome and increases the shelf-life of the finished product by preserving it in a relatively more stable dry state [106-108]. Freeze-drying affords protection against many of the processes causing liposome instability in aqueous dispersions.

In the present preparation, the lyophilization of sorafenib liposome was performed according to Waldrep and Koshkina [70, 106] with some modifications of the solvents used. Sorafenib and dilauroylphosphatidylcholine (DLPC) (ratio 1:7.5) were dissolved in *t*-butanol. The respective solution was frozen using liquid nitrogen and lyophilized overnight. Subsequently, the dried lipid film was hydrated with pre-warmed PBS pH (7.4)

containing maltose at a ratio lipid:maltose 1:1 by weight to get a final drug concentration of 10 mg/ml. The mixture was incubated for 30 min in a water bath at a temperature above the lipid melting temperature (T_m) at 37 °C with intermittent vortexing to produce multilamellar vesicular (MLV) liposomes. The liposomal suspension was maintained for another hour in a water bath at 37 °C to anneal the liposome structure. Subsequently, the suspension was sonicated for 10 min using a bath sonicator to obtain small multilamellar vesicles (SMLV) then the liposomal suspension was freeze-dried.

The lipid chosen for the liposome preparation was dilauroylphosphatidylcholine (DLPC) which is a neutral lipid which has a low transition temperature and can encapsulate large amounts of the drug [93]. Darwis et al. [93] used various lipids in the preparation of beclomethasone dipropionate (BDP) liposomes and they found that DLPC which has a low transition temperature (T_m) incorporated high amounts of BDP as compared to those lipids with a high transition temperature. The phase transition temperature is defined as the temperature required to induce a change in the lipid physical state from the ordered gel phase to the disordered liquid crystalline phase.

Darwis and Kellaway [93] explained that the ability of the bilayer structure of the liposomes to incorporate BDP is inversely proportional to the T_m of the phospholipids. The lipids with high T_m produce more solid and rigid liposomes, resulting in their inability to encapsulate BDP.

DLPC was found to be a suitable lipid used for inhalation [69, 70, 106, 109]. The reasons which made the DLPC phospholipid suitable for inhalation in the liposome preparation were firstly that this kind of lipid is endogenous to the respiratory tract as a component of pulmonary surfactant [93]. Additionally, Knight et al. [109] evaluated the safety and tolerability of the phospholipids used in the preparation of the 9-nitrocamptothecin liposomes prepared with DLPC. Rats exposed to 1 h of continuous aerosol for 28 consecutive days showed no adverse effect of the phospholipids [110]. Phase I/II studies in humans with DLPC aerosols have also demonstrated its safety and tolerability [111].

Multilamellar liposomes were characterized as a desirable delivery system for hydrophobic drugs [112]. Thus, it appeared also appropriate for sorafenib as a highly lipophilic drug to use multilamellar liposomes as carrier system for its delivery. In the present preparation method, sorafenib liposomes formed in phosphate buffered saline (PBS) have shown an important loss of viscosity compared to liposome prepared in distilled water. Boulmedarat

et al. [113] also observed that liposomes in buffer solution had a lower viscosity as in distilled water. This chosen procedure in the present study yielded a creamy white homogenous suspension with moderate viscosity according to visual observation.

The suspension was sonicated for 10 min in order to decrease the particle size and also to prevent the aggregation of the particles.

Some aggregation of the particles was initially observed in the present study after reconstitution of the lyophilized powder. This aggregation could be due to the nature of liposome bilayers which depends on hydrogen bonding between water molecules and the polar head groups of the constituent phospholipid for stability [114]. Therefore, water loss during drying produced changes in its bilayer behaviour and loss of integrity and hence bilayer fracture, fusion and vesicle aggregation. Consequently, loss of the entrapped material and change in liposome size distribution might be occurred.

Such changes may be minimized by the inclusion of cryoprotectants, usually disaccharide sugars, within the formulation. Trehalose and similar sugars are useful in protecting liposomes through their action on two stabilizing mechanisms, which takes place during freeze-drying [114]. In order to overcome the aggregation and fusion problems of the particles in the present investigation after reconstitution of the lyophilized powder during the second freeze drying and rehydration step, the incorporation of maltose (disaccharide) in PBS used for reconstitution of the lyophilized liposomal powder in a ratio of 1:1 lipid:maltose was important.

2.7.5 Characterization of the sorafenib liposome

2.7.5.1 Liposome size determination

The liposome particle size and its distribution can be determined using several methods. Among these methods are coulter particle size analyser [53, 115, 116]. Other research groups [112, 117, 118] used dynamic light scattering or laser light scattering technique [119] for particle size determination. In a previous study [120] the size distribution was measured using a photon correlation spectrophotometer. Another research group [121] utilized flow cytometry for liposome size distribution.

In the present investigation the vesicles' size distribution was determined for free and sorafenib loaded liposomes using coulter counter LS 230 particle size analyser. The mean particle size of empty and sorafenib loaded liposome was 7.6 ± 0.6 and 8.6 ± 0.3 μm ,

respectively. So no difference in the mean particle size of the loaded and empty liposomes was observed. It was concluded that incorporation of sorafenib in the liposome suspension did not affect the mean particle size of the liposome preparation.

In the present measurement, a relatively narrow range of size distribution of multilamellar vesicles (MLVs) was noticed, which laid between 3.2 μm -12.75 μm in case of plain liposome and laid between 3.9 μm -13.85 μm in case of the loaded one.

In case of plain liposomes 50 % of the particles were smaller than 6.8 μm and in case of loaded liposomes 50 % were smaller than 7.7 μm . 90 % of the particles of the plain liposome were smaller than 12.75 μm , whereas 90 % of the loaded liposome particles were smaller than 13.85 μm (Figure 11). It was concluded that the incorporation of sorafenib in the liposome preparation did not affect the particle size distribution.

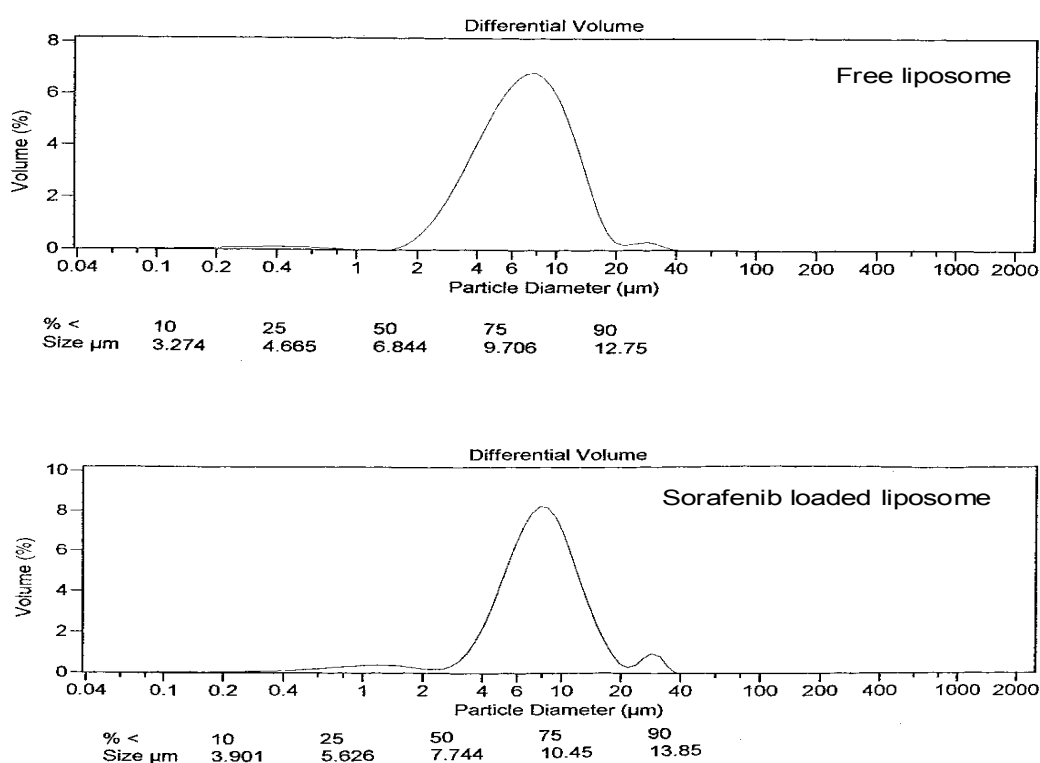


Figure 11: Representative chromatograms of sorafenib loaded and non-drug containing liposome suspensions illustrate particle size distribution of free and sorafenib loaded liposome as obtained by coulter counter analysis ($n = 3$).

For microscopical evaluation of liposomal suspensions either an optic microscope [122] or a transmission electron microscope [123] can be employed. In the present investigation

liposome suspensions were examined under the light microscope. The particles of the non-drug containing and sorafenib loaded liposomal dispersion were round in shape with multilayers. There was no difference in the vesicles' shape between the non-drug containing and sorafenib loaded liposomes on the microscopic examination.

Since the preparation of empty liposomes was successful showing good particle morphology and resulting in suitable homogenous particle size distribution, it was important that incorporation of sorafenib in this liposome formulation does not influence these properties.

2.7.5.2 The entrapment efficiency of sorafenib liposome

There are different ways to determine the encapsulation efficiency of liposomes. HPLC technique was the common method used for drug concentration determination. In some studies, the amount of the drug was determined only in the lipid portion either after centrifugation of liposome suspension [109] or after drug extraction from the loaded liposome suspension [124]. Other research groups [120, 125] determined the drug content in the lipid pellets and the non-encapsulated drug in the supernatant. The trapping efficiency was expressed as percent. The non-encapsulated drug concentration in the supernatant was less than 0.1 %. Others determined the encapsulation efficiency by calculating the free drug in the supernatant after centrifugation of the liposomal dispersion. The encapsulation efficiency was expressed either as mg of drug entrapped per mM of lipid (mg/mM) [126] or as percent of the difference between the amount of the drug added in the preparation and the free drug in the supernatant divided by the total amount of the drug added [122, 127].

In the present experiment the amount of the free sorafenib was determined in the supernatant after centrifugation of a certain volume of the sorafenib liposome suspension. After extraction of the supernatant (see experimental procedures 3.3.2), the amount of sorafenib was measured by HPLC. The difference between the total drug amount in the preparation and the drug content in the suspension supernatant was calculated.

Encapsulation efficiency was expressed as percent of the drug encapsulated in the liposome. The percent encapsulation efficiency (% EE) was calculated as follows [122, 127]:

$$\% EE = \frac{TotalS - FreeS}{TotalS} \times 100$$

Where TotalS and FreeS are total concentration of sorafenib added for the preparation of liposomes and total concentration dissolved in the upper aqueous phase after centrifugation of the liposomal suspension, respectively.

Analysis of the supernatant fraction of the centrifuged suspension revealed that $98 \pm 0.5 \%$ ($n = 3$) of sorafenib was retained by the lipid of the liposome. This indicated that the encapsulation efficiency of sorafenib loaded liposomes was high. This high EE might be attributed to the lipid used (DLPC) in liposome preparation (see 2.7.4).

Another reason for the high encapsulation efficiency of sorafenib loaded liposome in the present study was probably the highly lipophilic nature of sorafenib and its presumably pronounced affinity to phospholipid bilayers enhanced the loading efficiency in liposomes. The sorafenib concentration achieved in the liposome formulation was 20 mg/ml in the present study. This high encapsulation efficiency and loading capacity enabled the incorporation of the required amount of sorafenib for administration to mice in a small volume of 50 μ l. This was suitable for intratracheal administration.

2.7.5.3 Stability of sorafenib liposomal dispersion

Previous studies [112, 126, 128] investigated the effects of storage conditions such as different time periods and different temperatures on the stability of drug loaded liposome suspensions. To assess the effects of such storage conditions on the stability of sorafenib liposome suspension in the present study the empty and sorafenib loaded liposome preparations were stored for one month at 4 °C and 25 °C followed by visual and microscopic observation.

In the present stability experiment the microscopic observation of the free and sorafenib liposomes stored at 4 °C did not show any significant change in vesicles' shape and did not show aggregation of the particles after storage for one month. There was also no change in particle size observed. On the other hand, microscopic observation of the liposomal dispersion which was stored at 25 °C showed no change in the particle shape and size after 15 days, but showed pronounced crystal formation after one month storage. These crystals were possibly attributed to degradation of the liposome preparation and crystals of

sorafenib being no longer encapsulated in the liposome. This meant that sorafenib loaded liposome preparations were not stable when stored at 25 °C for one month.

Moreover, the EE was determined at the end of 15 and 30 days from the date of preparation by HPLC method (see experimental procedures 3.3). The percentages of sorafenib retained in the loaded liposomes were 98 and 97.4 % after 15 days storage at 4 and 25 °C, respectively. After storage for one month, 97.6 % and 89 % of sorafenib retention was observed in liposomes stored at 4 and 25 °C, respectively, (Table 5). Encapsulation efficiency of 89 % obtained after storage for one month at 25 °C is consistent with the crystals observed under the microscope as described above. Thus, sorafenib exhibited good retaining properties in the liposome when stored at 4 °C for one month. Conversely, the sorafenib liposomal suspension stored at 25 °C was only stable for 15 days.

Table 5

Encapsulation efficiency percent (% EE \pm SEM) after storage of 15 and 30 days at different temperatures (initial EE was 98 %), (n = 3)

Storage periods	4 °C	25 °C
After 15 days	98.0 \pm 0.66 %	97.4 \pm 0.35 %
After 30 days	97.6 \pm 0.40 %	89.0 \pm 1.30 %

Empty liposomal dispersions stored at different temperatures were treated in a way similar to that of sorafenib loaded liposomes. Their supernatants showed no peak at the retention time corresponding to that of sorafenib when evaluated by HPLC. Chromatograms for empty liposomes, initial and after one month storage at 25 °C were similar. Thus, no interfering peak at the same retention time as that of sorafenib and the internal standard was found in the extract of the supernatant of the empty liposome. This meant that the amount of sorafenib found in the supernatant of the loaded liposome could be calculated accurately to assess the encapsulation efficiency.

To summarize, the formulation composed of DLPC with a drug/DPLC ratio of 1:7.5 (w/w) gave good incorporation efficiency for sorafenib and a good stability of the reconstituted liposomes for one month at 4 °C.

2.7.5.4 Release test of sorafenib from liposome suspension by dialysis

A widely used technique in the release studies is an *in vitro* dialysis technique [112, 118, 122, 126, 129]. *In vitro* release studies are often performed to predict how a delivery system might work in ideal situations. This could give some indication of its *in vivo* performance and release characteristics.

In the present investigation the release of sorafenib was initially studied by a regular dialysis method. The regular dialysis experiment was performed according to Ugwu et al. [118] and Shabbits et al. [129] to check whether sorafenib was released from the liposomes. Since the maximum solubility of sorafenib in PBS at room temperature was 0.41 µg/ml, only a small volume of the sorafenib loaded suspension was used that incorporated a drug amount less than the maximum solubility of sorafenib in PBS. This sorafenib amount was soluble in the whole volume of given a 100 % release of sorafenib. Therefore, 30 µl of the sorafenib loaded liposome suspension were transferred into a dialysis bag and placed in a temperature controlled beaker containing 1L of PBS at 37 °C under constant stirring (see experimental procedures 3.5.3.4). At various time intervals, samples were withdrawn from the medium and assayed by HPLC.

For control, sorafenib solution was used to compare sorafenib release from the liposome suspension because sorafenib solution should reveal a 100 % release.

The *in vitro* release profile of sorafenib is shown in Figure 12, which illustrates that the amount of sorafenib released in 24 h from the 30 µl sorafenib liposomal suspension (0.3 mg sorafenib) was 65 % as compared with 97 % release from sorafenib solution (0.3 mg sorafenib) after 24 h.

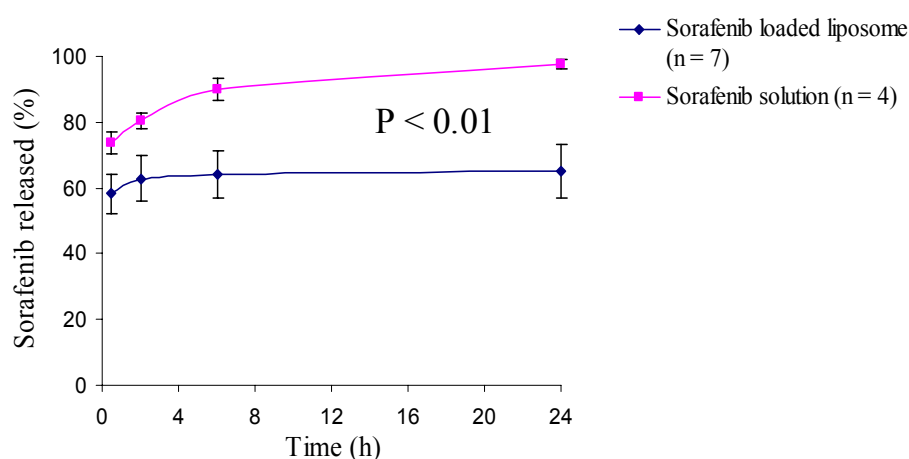


Figure 12: Cumulative release of sorafenib from solution and loaded liposome suspension into phosphate buffer, pH 7.4 at 37 °C. Means \pm SEM (n = 7) for sorafenib loaded liposome and means \pm SEM (n = 4) for sorafenib solution are presented. The data was analyzed statistically using t test (Graph Pad Prism), P-value < 0.01.

It was noticed that the free drug in the control solution diffused freely across the membrane and in fewer than 6 hours of dialysis nearly 90 % of the free drug had crossed the membrane. It was expected to achieve 100 % release of sorafenib in solution from the dialysis bag immediately after the beginning of the dialysis experiment. In contrast, there was a delay in the release of sorafenib. This delay in release probably was attributed to the adsorption of sorafenib to the dialysis membrane, which related to the lipophilicity nature of sorafenib.

However, less than 70 % of drug was released from liposomal formulation after 24 hours of dialysis. The initial rapid release of sorafenib from the liposomal suspension was expected because the present liposome formulation was not designed as a sustained release formulation. Furthermore, the rapid initial burst of the drug from liposome formulation could be due to the release of sorafenib accumulated on the particle surface.

In the present study a significant prolongation of sorafenib release was achieved with the liposomal suspension ($P < 0.01$) in comparison with the respective control solution (Figure 12). This significant difference was calculated by comparing the mean values \pm SEM of the sorafenib solution and the sorafenib loaded liposome. Approximately 59 % of sorafenib was released fast from liposome after 0.5 h of dialysis and the subsequent release appeared to be constant. After 2 h the encapsulated sorafenib was released as a result of the

difference in the concentration of the drug inside the liposome and in the dialysis bag. The difference in the release behaviour of sorafenib from the solution and liposome preparation perhaps was due to the intercalation of sorafenib (hydrophobic molecule) within the bilayer membrane of the liposome preparation, which subsequently lead to incomplete release of sorafenib from the liposome after 24 h in comparison with its solution. 35 % of sorafenib remained encapsulated in liposome after 24 h of dialysis.

The results of the present investigation suggested that sorafenib was associated with liposome in accordance to the previous *in vitro* release studies [118, 129]. Zhigaltsev et al. [117] did also a comparative study of the loading and retention properties of three very closely related lipophilic vinca alkaloids (vincristine, vinorelbine and vinblastine) in liposomal formulations. They found that the differences in loading and retention can be related to the lipophilicity of the drugs tested. Sorafenib retention in the liposome preparation 24 h after the present dialysis assay also corroborates with high entrapment efficiency data previously reported in determination of the encapsulation efficiency 2.7.5.2. Another possible explanation of why the release of sorafenib from the liposome was not 100 % after 24 h could be the affinity of sorafenib as a lipophilic compound to the dialysis membrane. The dialysis membrane could retain sorafenib inside and/or adsorbed it outside the dialysis tube and did not allow it to further diffuse into the release medium. The release of sorafenib from the liposome preparation was also affected by several parameters such as particle size and liposome degradation rate.

It can be concluded that the *in vitro* release of sorafenib encapsulated in liposome was driven by the concentration gradient and limited by two barriers, the phospholipids bi-layer and the dialysis membrane. The present dialysis assay indicated that sorafenib was released from the liposome preparation.

2.7.5.5 Release of sorafenib from the liposomal suspension in cell culture

It was known that sorafenib inhibits Raf-1 kinase mediated ERK phosphorylation in cell culture assays. Wilhelm et al. [20] found that sorafenib inhibited ERK phosphorylation in serum activated NIH3T3 cells (mouse fibroblast) in a concentration dependent manner. Other research groups [28, 32] demonstrated that exposure of other types of cells to sorafenib was also associated with a decrease in ERK phosphorylation.

There were two objectives for the present experiment. The first objective was to determine whether sorafenib was released from the liposome preparation in cell culture as an alternative confirmation of sorafenib release (see 2.7.5.4). The other point was to examine if the released sorafenib was able to inhibit Raf-1 mediated activation of ERK in a cellular mechanistic assay as the inhibition of ERK phosphorylation is an indication of the sorafenib effect as Raf-1 inhibitor.

In the present investigation the release of sorafenib from liposome preparation was studied using NIH3T3 cells and its pharmacological effect on the cell proliferation by phospho-ERK inhibition was determined by Western blot analysis (see experimental procedures 3.5.3.5.1). The cells were incubated 2 hours with different concentrations of sorafenib loaded liposome preparation. The same sorafenib concentrations in DMSO solution were utilized for comparison. Non-drug containing liposomes were also used and served as placebo samples. The cell lysates were analyzed by Western blot assay for the detection of phospho-ERK protein using antibody directed against phospho-ERK. ERK2 antibody was used as loading control (Figure 13 A lower panel). The protein band intensity was densitometrically quantitated. The percent inhibition was calculated in comparison to placebo. Western blot analysis revealed a concentration dependent inhibition of p-ERK by sorafenib both from the liposomes and the solution (Figure 13 A, B).

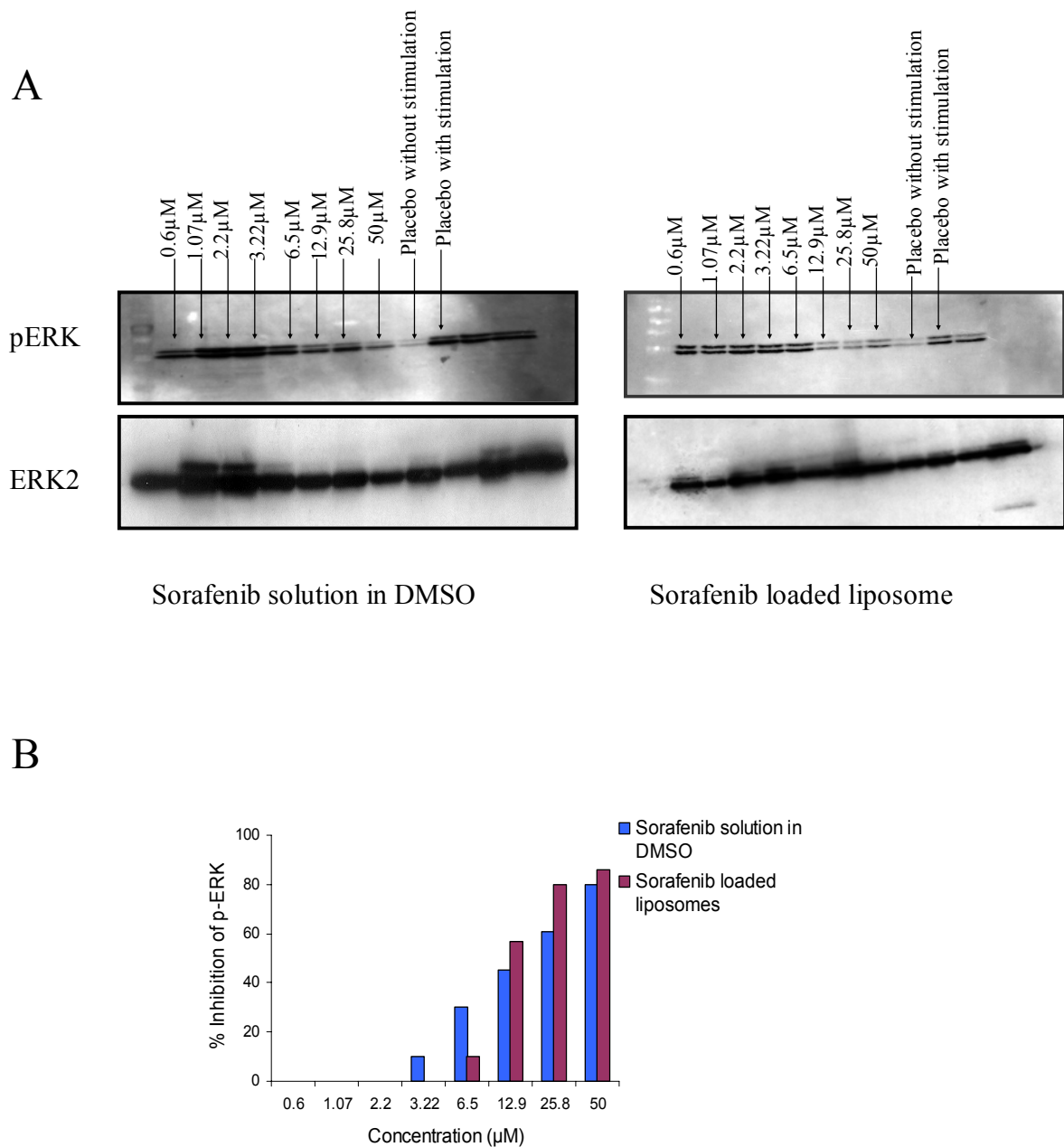


Figure 13: Western blot analysis of phospho-ERK in NIH 3T3 cell lysate.

A) Western blot analysis was conducted in NIH3T3 mouse fibroblast cells, 20 μg of total protein from cell lysates were run on SDS-PAGE and phospho-ERK (p-ERK) protein was probed with anti-phospho-ERK rabbit polyclonal antibody and visualized by chemiluminescence (top panel). ERK2 was used as a loading control to control for equal loading and transfer of proteins (lower panel). The sorafenib loaded liposomes showed inhibition of p-ERK in a concentration dependant manner. The placebo samples (free liposomes) are represented in the top panel with and without serum stimulation.

B) Sorafenib inhibition of ERK phosphorylation was conducted in serum activated NIH3T3 cells in a concentration dependent manner after 2 hours incubation. The results were expressed as % of inhibition, which was determined densitometrically measuring the intensity of the Western blot bands and dividing the measured band intensity of the sorafenib liposome cell lysate by the placebo cell lysate. Sorafenib was successfully released from the liposomes causing a pronounced inhibition at 12.9, 25.8 and 50 μM in comparison with sorafenib in DMSO solution ($n = 2$).

In case of the loaded liposomes, the drug was successfully released and exerted 10 % inhibition of ERK phosphorylation at 6.5 μM whereas the same concentration of sorafenib in DMSO solution showed a 30 % inhibition. In addition, at 12.9, 25.8 and 50 μM concentrations of sorafenib loaded liposome the percent inhibition was 60, 80 and 85 %, respectively.

It was noticed in the present experiment that the effect of sorafenib in the solution was initially more pronounced at 3.22 μM and 6.5 μM sorafenib concentrations, which resulted in 10 and 30 % p-ERK inhibition, respectively. In contrast, the p-ERK inhibition was 0 and 10 % at the same sorafenib concentrations in the liposomes, respectively. This pronounced effect was not surprising because it was obvious from the previous dialysis assay (2.7.5.4) that the release of sorafenib in the solution was more rapid than its release from the liposome preparation.

But by further dissection of the p-ERK inhibition percent results, it was found that the percent of p-ERK inhibition was higher at sorafenib concentration from 12.9 to 50 μM in case of sorafenib liposomes compared to sorafenib solution. The effect of sorafenib on p-ERK inhibition was probably not only depending on the release of sorafenib from both liposome and solution, which was studied previously (see 2.7.5.4), but also depending on the interaction of sorafenib loaded liposome with the cells and cellular uptake of sorafenib. So the sorafenib activity on p-ERK inhibition exerted by liposomal formulation may be attributed to the fusional interaction between membrane phospholipids of liposomes and the cells.

The results of the present investigation indicated that sorafenib was successfully released from the liposome suspension in cell culture and exhibited activity on cell proliferation, which was determined indirectly by calculating the percentage of phospho-ERK inhibition. The present *in vitro* release study of sorafenib in the cell culture confirmed the previous results of the *in vitro* release of sorafenib using the dialysis method which was reported earlier in 2.7.5.4. This result was important because it indicated that sorafenib liposome preparation can be used for further *in vivo* experiments as it showed a good release property *in vitro* and also the sorafenib released exerted a pharmacological effect on phospho-ERK inhibition.

2.8 Treatment of BXB-23 mice intratracheally with sorafenib liposomes

2.8.1 Advantages and disadvantages of intratracheal instillation

To design an appropriate inhalation exposure system, special experience and equipments are required. Such requirements are not available at many institutions and are expensive. Even when such facilities are available, other issues may make inhalation exposures unpractical e.g. the limited amount of test material or the test material may be highly toxic. Furthermore, the use of intratracheal instillation is more efficient for mice than inhalation technique. In rodents, after inhalation some material deposited in the trachea and upper bronchi will be transported upward and swallowed. A large fraction will be deposited in the nasopharynx. Consequently, the dose actually deposited in the lung can not be precisely determined. As a result of these restrictions, the direct instillation of test material into the lungs via the trachea has been utilized in several studies as an alternative exposure procedure to inhalation. Therefore, intratracheal instillation is widely used for research purposes [130].

Instillation has many advantages over inhalation, as discussed previously [131]. For example, instillation assures delivery of actual dose to the lung of each animal. Moreover, instillation reduces hazards to laboratory workers including highly toxic, carcinogenic, or radioactive materials [132]. Employing instillation is simpler than inhalation exposure procedures and not expensive. Intratracheal instillation allows the delivery of a range of doses to the lung within a short time [133].

Intratracheal instillation proves the concept of the suitability of inhaled administration of the drug in the research area. An intratracheal instillation dose can be used for extrapolating the inhalation dose. Instillation procedure can be used as an alternative method for inhalation technique due to its simplicity and requirement of only microliters of a compound to generate a useful and reliable dose-response [133].

Some issues related to the intubation method are required when using intratracheal instillation to avoid pulmonary toxicity such as the vehicle, the volume of the delivered material, the dose and the anesthetic agent. Intratracheal instillation is commonly accomplished using a short-acting anesthetic and transoral intubation of the trachea followed by instillation of the test agent dissolved or suspended in physiologic saline. The volume of vehicle is commonly 1-2 ml/kg body weight [130].

There are also some disadvantages of intratracheal instillation:

A. To achieve delivery reproducibility, experience and appropriate training for the individual performing the procedure are required. Even with such training, it is difficult to compare interlaboratory results due to results variability [134, 135].

B. It exist a possibility of tracheal injury due to needle insertion that is rarely specifically considered [136].

C. After intratracheal instillation, probably some of the injected material could be either coughed up or quickly cleared from the trachea that may be attributed to either rapid recovery from anesthesia or the use of a large instillation volume [134, 137].

D. Some studies [138-142] indicated that using intratracheal instillation leads to exaggeration of adverse pulmonary responses to particles. Such exaggeration may be due to high dose rate, high lung load and/or vehicle effects. Reduction of response exaggeration after instillation can be achieved by using of low doses.

2.8.2 The difference between intratracheal instillation and inhalation

The main differences between the intratracheal instillation and inhalation methods are the dose rate and distribution of materials. Inhalation leads to deposition within the upper respiratory tract but instillation bypasses this portion of the respiratory tract [131]. No wastage of valuable test compound occurs by using intratracheal instillation technique as only milligram quantities of drug per animal are required [133].

The other difference is related to the intrapulmonary distribution of particles. Inhalation leads to a nearly homogenous distribution of particles throughout the lungs, while instillation, in general, results in less homogeneity of dose distribution in the alveolar region and can lead to a local high dose of the drug. Such differences in dose distribution can influence effective doses to certain cells and tissues, clearance pathways, and the degree and site of systemic absorption [130]. One of the major respiratory tract clearance pathways includes particle uptake and removal via pulmonary macrophages. Pritchard et al. [135] reported that inhalation resulted in a deposition of few ingested particles within the macrophages while with intratracheal instillation macrophages comprised a large number of particles.

Moreover, the distribution of particles among macrophages was more homogenous with inhalation than with instillation. Therefore, the route of exposure affected the particle

distribution in the macrophages and could influence clearance pathways and clearance kinetics.

The database on pulmonary toxicity of various materials [130] indicates that quantitatively similar results for variety of biologic endpoints, such as pulmonary inflammation, fibrosis, susceptibility to infection and allergic sensitization was achieved after using instillation and inhalation routes [130].

2.8.3 Delivery of liposomes via intratracheal instillation

Most investigations using liposomes as drug-delivery systems have relied on parenteral routes of administration. In order to accomplish targeted delivery to the lung, the direct instillation of liposomes into the airways has the advantage of overcoming systemic dilution and removal by other tissues and organs [53].

Direct administration of liposomes into the bronchi and alveoli has been investigated for the delivery of antitumor drugs to the pulmonary system [53, 69, 70, 90, 109, 143]. Organ-selective targeting of anti-cancer agents was suggested to increase their growth inhibitory activity and reduce their side effects. For this reason in the present investigation the intratracheal instillation (Figure 14) was chosen as a route for delivery of sorafenib liposome formulation.

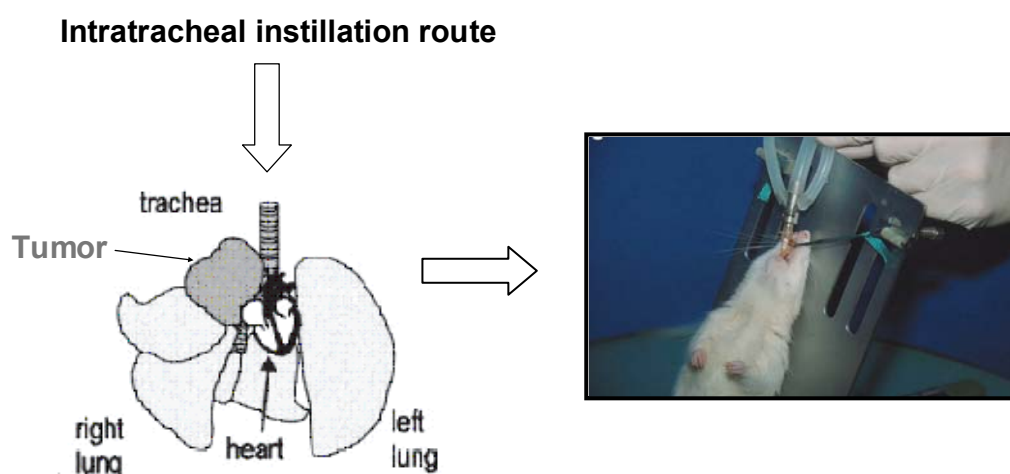


Figure 14: Demonstration of intratracheal instillation route as direct delivery of drug to the lung (modified after Kastl et al. [144]).

Local delivery can offer a number of advantages for pulmonary targeting. It is possible to give much higher local concentrations directly to the site of the tumor [69, 102, 109]. The long residence time of the drug in the lung following intratracheal administration suggests that this approach may require infrequent dosing to achieve the desired clinical effect. Such infrequent dosing is important for liquid dose instillation applications nature via an endotracheal tube.

2.9 Pharmacokinetics of sorafenib after intratracheal administration

The next step in the present investigation was to assess the pharmacokinetic behaviour of sorafenib encapsulated in the conventional liposome preparation using wild type mice (B6D2F1) after intratracheal instillation (IT) administration.

50 wild type mice weighing between 20 and 30 g were used in this study. The animals were divided into 5 groups and instilled with a single dose of sorafenib (1 mg). Each group was sacrificed at different time points 2, 24, 48, 72 and 168 hours after instillation. Blood samples and lungs were collected to determine the sorafenib concentration. Sorafenib was extracted from serum and quantified by the newly developed HPLC method (see 3.3). Likewise, sorafenib concentration was determined in the frozen lung tissues by HPLC (3.6.4).

In spite of mortality observed in the different groups following anesthesia and/or infection, the number of animals was sufficient to maintain a minimal number of three animals in each group (see experimental section 3.6.2). Mean serum and lung sorafenib levels following intratracheal administration are plotted in Figure 15.

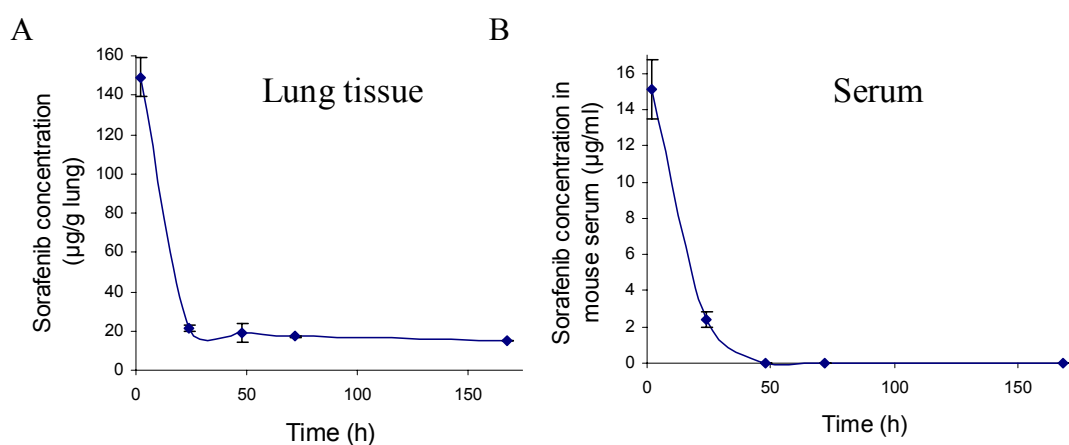


Figure 15: Lung and serum sorafenib concentration/time curves based on the total sorafenib levels measured by HPLC. The sorafenib mean concentration in lung tissues (A) and mouse serum (B) post-intratracheal administration at different time points 2, 24, 48, 72 and 168 h after a single dose (1 mg) of sorafenib loaded in liposome suspension. Symbols represent the mean and standard deviation of 3-4 mice.

Significant levels (C_{\max} 149 $\mu\text{g/g}$ lung) of sorafenib were measured in the lung tissue 2 hours after instillation of liposome-encapsulated sorafenib. Subsequently concentrations declined and remained nearly constant over 168 hours period of study (Figure 15).

A similar time course was observed in serum samples, but without reaching correspondingly high systemic level of sorafenib (C_{\max} 15 $\mu\text{g/ml}$).

Lung concentrations remained detectable for at least one week following intratracheal administration of the sorafenib loaded liposomes. In contrast, serum sorafenib concentrations remained low after intratracheal administration. This may be an indication that sorafenib liposomal formulation reduced systemic absorption and toxicity, as sorafenib was absorbed by the lung into the systemic circulation in small amounts. In the present investigation a question arose as to why the total amount of sorafenib determined in the lung tissues (0.04 mg) was much lower than the administered dose (1 mg) even as early as 2 h after instillation (Figure 15).

It was expected to achieve higher levels of sorafenib in the lung tissues after sorafenib loaded liposome instillation. The unexpected low concentration of sorafenib in the lung tissue may be attributed to its rapid elimination. This rapid elimination depends on the physicochemical properties such as ionization and lipophilicity of sorafenib or it can be related to other factors following the instillation.

After intratracheal administration, the rate and extent of lung uptake can also affect the pharmacokinetic behaviour of the drug [53].

In addition, the low sorafenib concentration in the lung tissues can be related to the intratracheal instillation technique itself. It is possible that after intratracheal instillation, some liposomes were removed by mucociliary clearance and transported to pharyngeal and nasal passage [116, 145]. Since the bronchopulmonary tree have different characteristics, the drug release from liposomes can be affected by the distribution of formulation achieved during administration and later altered by mucociliary transport and other mechanisms. Animal studies [53, 116] have used instillation of liquid formulations to achieve accurate dosimetry. The spreading of the instilled dose within the lung could be complicated by the presence of components, which affected the spreading process [119].

Moreover some of the instilled material could be either quickly cleared from the trachea or coughed up, especially if the recovery from anesthesia is too rapid [134, 137].

In the present investigation although the sorafenib loaded liposome was not a sustained release preparation, sorafenib concentrations in the lung tissue were still detectable 20 µg/g up to one week after single dose (1 mg) instillation. The sorafenib concentration in the lung tissue was also higher than its concentration in serum. These findings perhaps were attributed to the use of a liposome as carrier system for sorafenib delivery to the lung, which served as a means of altering the pharmacokinetics of sorafenib, prolonging its residence time within the airways. Previous studies [69, 70, 145] demonstrated that drugs delivered directly to the respiratory tract in liposomal formulation remained at the site of initial application resulting in high pulmonary drug concentrations. Another reason could be due to the use of the intratracheal instillation route, which leads to direct deposition of the drug formulation in the site of action (the lung). The results indicate that the sorafenib preparation can be further used for *in vivo* administration in order to treat BXB-23 mice lung adenoma. The sorafenib concentration in the lung tissue was high enough to expect pharmacological effects.

2.10 Antitumor effects of liposomal sorafenib

The purpose of this study was to investigate if the intratracheal instillation of sorafenib loaded liposome suspension affected the lung adenomas. The *in vivo* activity of the

liposomal preparation of sorafenib administered by intratracheal instillation was performed in BXB-23 mice. The treatment plan for the present experiment is shown in Table 6.

Table 6: Schedule of the intratracheal instillation experiment of the sorafenib loaded liposomal suspension to treat lung tumor adenoma in four months old BXB-23 mice

Item	Description
Drug dose	1 mg sorafenib loaded in liposome suspension per mouse
Instilled volume	50 μ l
Intubation frequency	Three times per week
Handling period	Three weeks. A group of mice (n = 5-8) was sacrificed every week. Another group of mice (n = 8) was handled with free liposome and served as placebo group. Five animals were considered as control (untreated animals).
Recovery groups	Group of mice (n = 5) was stayed two months alive after the end of the treatment period (three weeks) without further treatment. Another group of mice (n = 5) was considered as a recovery placebo. Five untreated mice served as a recovery control group.

In the present experiment the antitumor effect of sorafenib treatment was evaluated by the following parameters: tumor percent (tumor area), number of adenoma foci/mm², ratios of the lung weight/body weight, proliferation and apoptosis.

2.10.1 Histological examination of the lung sections

Examination of lung histology has been used before as a parameter for antitumor effect evaluation [31]. To our knowledge, this is the first study demonstrating the effectiveness of

sorafenib intratracheally instilled treatment for local therapy of lung tumors in mice. Thus, it was important in the present study to examine the lung structure after direct administration of sorafenib into the lung.

Lung tissues of all treated groups, placebo and control groups were examined after H&E staining under the light microscope. Enlargement of the alveoli area was observed in a few lung sections and the alveolar walls were to some extent destructed (Figure 16). This observed structure could be defined as emphysema.

Pulmonary emphysema is a chronic lung condition in which alveoli, or air sacs, may be destroyed, narrowed, collapsed, stretched and/or over-inflated causing decrease in respiratory function and breathlessness. Emphysema is a result of infection or irritation of the bronchial tubes and has been defined as the permanent enlargement of air-spaces distal to terminal bronchiole caused by destruction of alveolar walls and without significant fibrosis [146].

In the present investigation the presence of emphysema in the mice lung sections after the intratracheal administration may be attributed to the intratracheal technique (Figure 16).

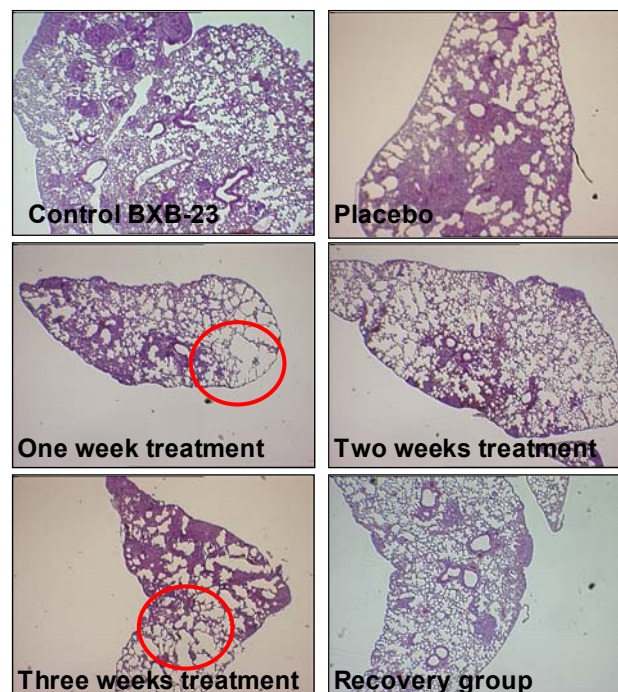


Figure 16 Representative lung sections of BXB-23 mice after intratracheal sorafenib treatment (Red circles indicate emphysema), original magnification 4 ×.

Also the intratracheal intubation may lead to an injury effect of the trachea and the lung during needle insertion and hence, irritation and inflammation can be observed [136].

In the present investigation after intratracheal instillation it was noticed that the lungs were also enlarged in size. Increase of the static pressure in the dependent portions of the lung resulted in distention of these particular alveoli and hence lung growth as described earlier by Muensterer et al. [147]. The examination of the H&E stained lung sections in the present study after intratracheal instillation showed some oedema and spreading diffusion of the adenoma foci (Figure 17). The adenoma foci appeared to be connected together and form a big area. These effects may be either attributed to the soft spongy nature of the lung tissues or related to the intratracheal instillation technique which created pressure that caused some changes in the lung morphology. The spreading diffusion of the adenoma foci could be seen in the lung sections of sorafenib treated groups (Figure 17 A, B and C) and also in the placebo group (Figure 16). In contrast this spreading had disappeared in the lung sections of the recovery group (Figure 17 D) and could not be detected in the control group (Figure 16). Therefore, in the present histological study it was obvious that the intratracheal technique could be the main cause of the observed changes in the lung morphology (Figure 17).

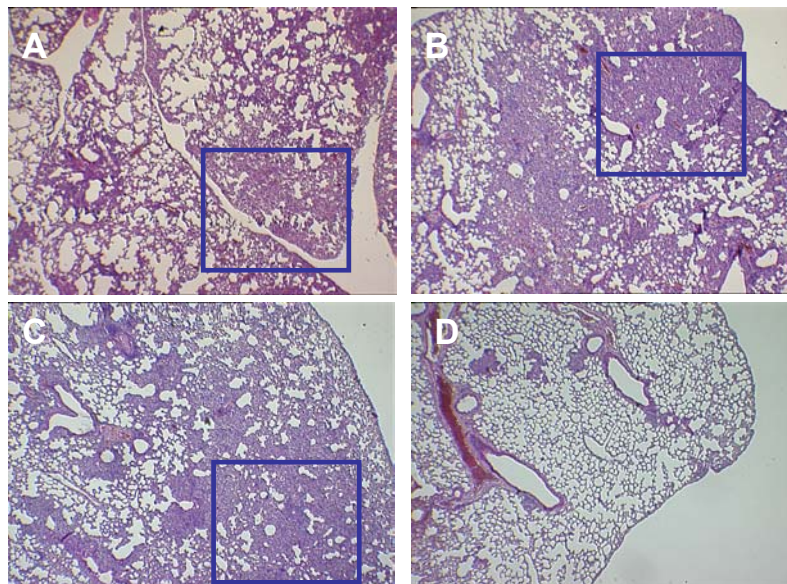


Figure 17: Representative H&E stained lung tissues after sorafenib liposome suspension intratracheally showing disappearance of the abnormal lung structure in the recovery group compared with other treatment groups. (A) Lung section of one week treated mice, (B) lung section of two weeks treated mice, (C) lung section of three weeks treated mice and (D) lung section of the recovery group (magnification 4 ×). Blue squares represent the abnormal lung structure.

In case of the lung tissue of the recovery group the lung morphology was normal BXB-23 lung tissue structure showing different separated adenoma foci. The abnormal lung structure in case of the other three sorafenib treated groups of intratracheally treated mice was visualized. Thus, direct instillation of sorafenib into the lung of BXB-23 mice had an effect on the lung morphology which abolished to some extent the evaluation of antitumor effect due to difficulty in distinguishing the separated foci and subsequently counting the cells.

2.10.2 Effect of intratracheal instillation sorafenib treatment on the tumor area

The objective of this evaluation was to determine the effect of sorafenib liposome instillation on the tumor area which was expressed as tumor percent and calculated by dividing the tumor area of the adenoma foci by the total area in the high power field. For this purpose the H&E stained lung tissues were used. The tumor percent was determined in 3 different sections for every mouse and averaged. The tumor area for all mice groups was measured by calculating the tumor percent and the results are shown in Figure 18.

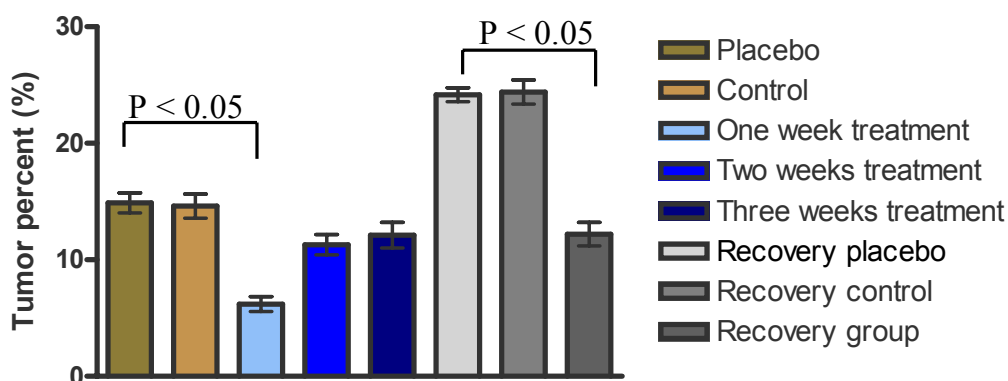


Figure 18: Determination of tumor area of lung adenoma foci of BXB-23 mice (n = 5-8) after treatment with 1 mg sorafenib incorporated in liposome suspension. The data was statistically analyzed using one way ANOVA test (Graph Pad Prism) followed by Tukey test, P-value was regarded as an indication of statistical significance. The data represent the mean \pm SEM.

It was a remarkable statistically significant reduction of the tumor percent from 15 % to 5 % after one week treatment as compared with the placebo and control groups. After further instillation of sorafenib liposome into the lung for another two weeks no significant reduction in the tumor area was achieved (11.2 % and 12 %, respectively). On the other hand there was a significant reduction in the tumor area of the adenoma foci from 24 % to 12 % in the recovery group in comparison with the recovery placebo and recovery control animals. Thus, sorafenib demonstrated antitumor effect two months later after the end of the treatment period, which could be due to the presence of high sorafenib concentration in the lung tissues after direct instillation of multiple doses. This finding was not surprising because recently two studies [29, 30] suggested that the growth of HCT 116 (colon) tumors was discontinued when monitored for 14 days after sorafenib administration. Animals continued to show significant reduction in tumor size compared to control animals after administration of 10, 30 and 100 mg/kg sorafenib. These recent results showed that the anti-tumor activity of sorafenib was maintained after discontinuance of sorafenib dosing.

In the present study an elevation in the percent of the lung tumor area of the recovery control and recovery placebo groups from 15 % to 24 % was noticed as compared with the placebo and control groups (Figure 18). This elevation may be related to the progression of the age of the animals as recovery placebo and recovery control groups stayed two months longer. It can be concluded that a significant reduction of the tumor area after one week treatment with 1 mg sorafenib three times per week was obtained but further treatment for two and three weeks did not achieve any progress in the antitumor activity of sorafenib.

2.10.3 Effect on the number of foci/mm²

The number of tumor foci/mm² for all groups of animals was determined by counting the number of foci in the H&E stained lung tissues under the light microscope per mm² (Figure 19).

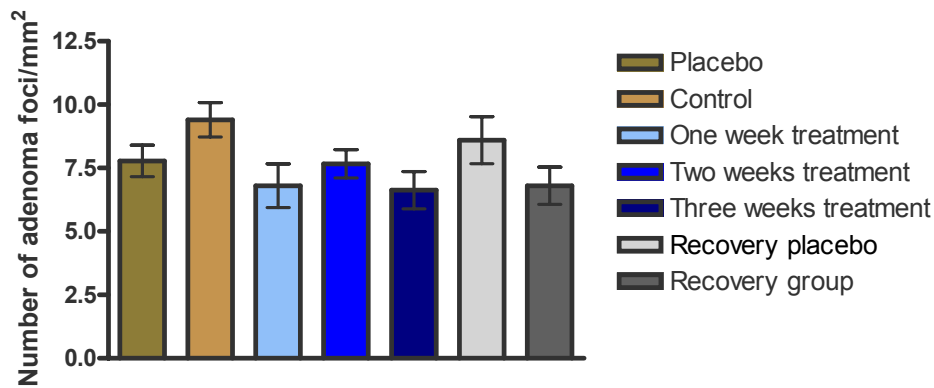


Figure 19: Determination of number of adenoma foci/mm² after instillation of 1 mg sorafenib intratracheally and the data represent the mean \pm SEM (n =5-8).

No statistical difference in counts of tumor foci was detected between all three treated animal groups. The number of adenoma foci in the one week, two weeks and three weeks treated group was 6.8, 7.7 and 6.6 per mm², respectively and 7.7 per mm² for the placebo group and 9.4 per mm² for the control group. In addition, no significant reduction in the foci number of the recovery group (6.8 per mm²) in comparison with recovery placebo (8.5 per mm²) was detected.

It can be concluded that one week treatment with 1 mg sorafenib liposome three times per week had a reducing effect on the tumor area of the single adenoma foci, but did not influence the whole foci number. In contrast, further treatment for two and three weeks with sorafenib liposome did not affect either the tumor area or the foci number.

2.10.4 Effect on the ratio of lung weight to body weight (mg/g)

Determination of the ratio between lung weight and body weight was utilized before as a parameter to assess the antitumor effect of drugs [31]. Reduction of this ratio is considered as another indication of tumor number reduction. Therefore, measurement of this ratio in the present study was important to assess if sorafenib treatment intratracheally had an effect on tumor content. The ratios of lung weights (mg) to body weights (g) were obtained from all groups of mice (all treated groups, placebo group, control group and the recovery group). The results of the calculation are shown in Figure 20.

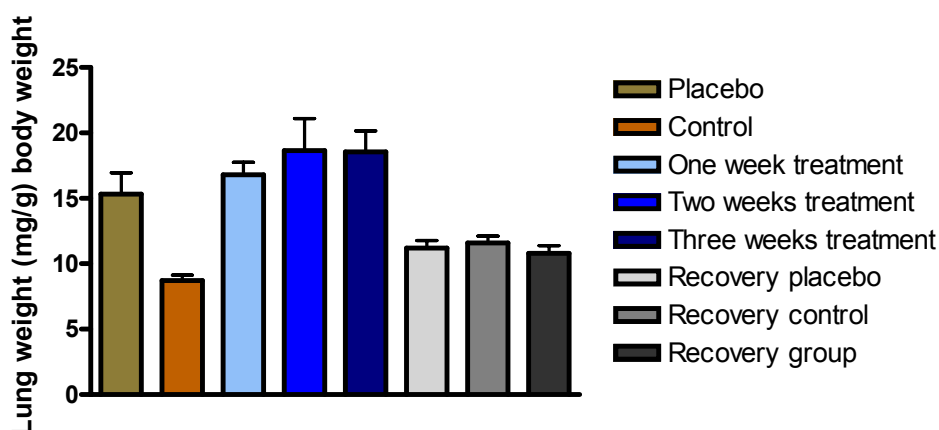


Figure 20: Ratios of the lung weight (mg) to body weight (g) obtained from mice (n = 5-8) after sorafenib intratracheal treatment, placebo, control and recovery group.

A pronounced elevation in this ratio of the three sorafenib treated animal groups was detected of 16.8, 18.7 and 18.5 mg/g, respectively compared to the control group 8.7 mg/g. A remarkable elevation in the ratio of placebo group 15.3 mg/g was also obtained. In contrast, no significant increase of this ratio in the recovery group (10.8 mg/g) was observed as compared with the recovery placebo (11.2 mg/g) and recovery control (11.6 mg/g) groups. This elevation may be attributed to the intubation technique itself and/or to the volume of sorafenib suspension instilled which led to oedema formation in the lung tissues. A decrease in this ratio was observed in the recovery group and its placebo after cease of intratracheal intubation which caused the increase of those ratios in case of the treated groups and their placebo.

It can be concluded that the elevation in the ratio between lung weight and body weight, which was probably due to the presence of oedema, hindered the ability to investigate the effect of sorafenib instillation on lung weight and consequently on the tumor content.

2.10.5 Immunohistochemistry for lungs of BXB-23 mice after intratracheal administration of sorafenib liposome

2.10.5.1 Effect on proliferation (PCNA assay)

Measuring the proliferation degree is important for the evaluation of rate, duration and molecular characteristics of tumor progression as discussed before in 2.4.2.1.

Lung sections from 4 months old mice after intratracheal administration of 1 mg sorafenib three times per week for three weeks were used in this experiment. Immunohistochemistry staining was performed using antibody against PCNA (Proliferating Cellular Nuclear Antigen) to assess the effect of sorafenib treatment on tumor cell growth. This immunohistochemical detection was done on the paraffin embedded lung tissues from all groups of BXB-23 mice at the end of this experiment and the nucleus was identified by hematoxylin staining (see experimental procedures 3.4.3.1). The lung sections were examined under the microscope. The representative lung sections of the treated groups and the placebo group are shown in Figure 21. The single adenoma focus appears large with high magnification surrounded by alveolar region. Hematoxylin staining identified the nucleus and the brown positive cells indicated the positive proliferating cells stained immunohistochemically for PCNA detection (Figure 21).

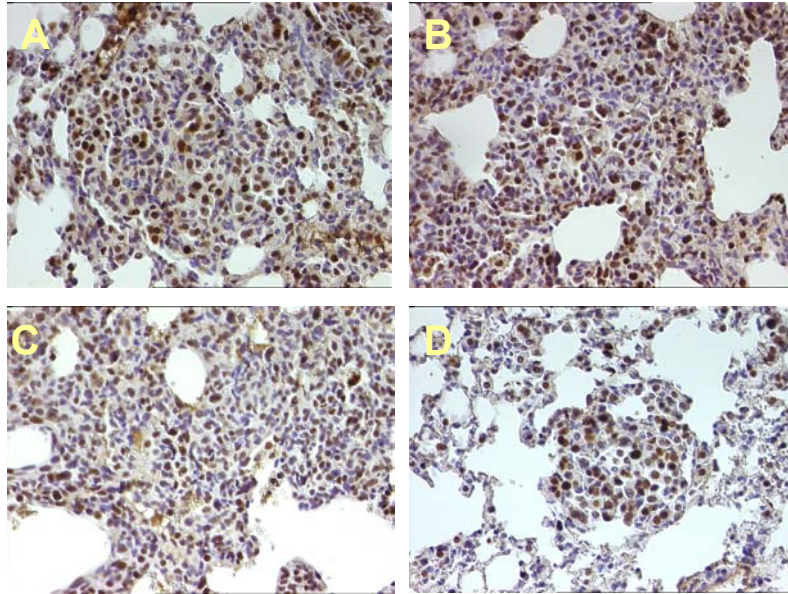


Figure 21: Representative lung tissues after PCNA immunohistochemistry after intratracheal instillation of sorafenib liposome (magnification 40 \times). (A) Placebo, (B) One week treatment, (C) Two weeks treatment and (D) Three weeks treatment.

Furthermore, the number of brown positive PCNA cells was counted and the percent was calculated by dividing the number of positive cells by the number of the whole cells in the adenoma foci (Figure 22). The percent was calculated in three different lung sections for every mouse.

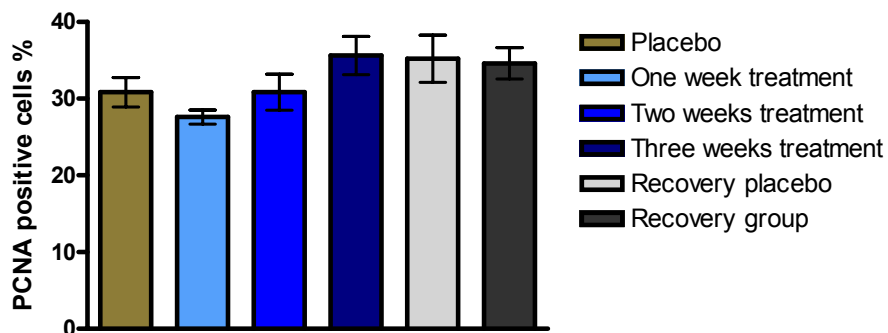


Figure 22: Percent of PCNA (Proliferating Cellular Nuclear Antigen) positive cells. No significant reduction of PCNA positive cells was detected in the all treated mice groups in comparison with their placebo groups. The data represent the mean \pm SEM (n = 5-8).

After the intratracheal administration of sorafenib liposome, no significant reduction in the percent of PCNA positive cells (27.6, 30.8 and 35.6 %) was detected for the three sorafenib treated groups of animals in comparison with 30.8 % for the placebo group (Figure 22). No remarkable difference in PCNA positive cells percent between the recovery group (34.6 %) and the recovery placebo (35.2 %) was achieved. The results of the present experiment indicated that 1 mg sorafenib instillation treatment did not influence the proliferation of the tumor cells.

Since sorafenib p.o. treatment, which was discussed before in 2.4, achieved a reduction of the proliferation, it was expected to observe a proliferation reduction also after direct sorafenib liposome instillation especially as the pharmacokinetic experiment (2.9) showed high sorafenib concentrations in the lung tissues. Surprisingly, no effect on the proliferation after sorafenib liposome instillation experiment was acquired. This result could be either related to the specific mechanisms developed by the tumor cells during sorafenib treatment or may be attributed to the physiology of the tumor tissue such as its poor vasculature. Additionally, the abnormal lung structure attained after sorafenib instillation, which was described earlier in 2.10.1, abolished to some extent the accurate counting of proliferating positive cells.

2.10.5.2 Effect on apoptosis (caspase-3 assay)

The induction of apoptosis is correlated with an activation of the caspase-3 pathway as explained before in 2.4.2.2.

In the present assay, the caspase-3 immunohistochemistry staining on the paraffin embedded lung tissues of all mice groups after sorafenib liposome instillation treatment was examined to investigate the effect of sorafenib treatment on tumor cell survival. The positive activated caspase-3 cells were counted in the tumor foci area and then divided by the whole number of cells in the foci to get the percent of activated caspase-3 positive cells. The results were analysed statistically using one way ANOVA (Figure 23).

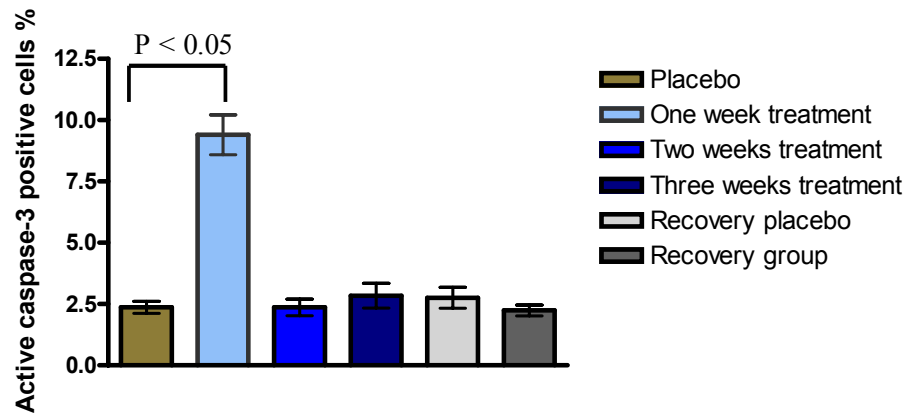


Figure 23: Percent of positive caspase-3 cells after intratracheal instillation of sorafenib liposome. The data was statistically analyzed using one way ANOVA test (Graph Pad Prism) followed by Tukey test. A P-value < 0.05 was regarded as an indication of statistical significance. The data represent the mean \pm SEM (n = 5-8).

The percent of positive caspase-3 cells was increased after one week sorafenib instillation treatment. A significant difference between the percent of activated positive caspase-3 cells of one week treated group (9.4 ± 1.8 %) and the placebo group (2.3 ± 0.7 %) was achieved. No remarkable difference in the percent of positive cells (2.3 and 2.6 %) for two and three weeks treated groups, respectively, in comparison to the placebo group (2.3 %) was obtained. In addition, no significant difference between the recovery mice group (2.2 %) and the recovery placebo group (2.6 %) was attained.

The representative pictures of all treated groups, recovery group and placebo showing the positive caspase-3 positive brown cells in the tumor foci are shown (Figure 24).

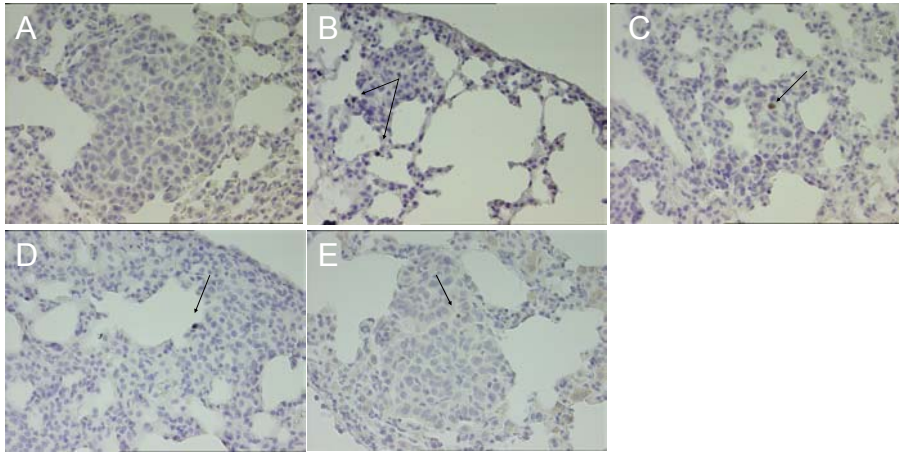


Figure 24: Representative pictures of activated positive caspase-3 cells after intratracheal instillation of sorafenib. (A) Placebo, (B) One week treatment, (C) Two weeks treatment, (D) Three weeks treatment; and (E) Recovery group (magnification 40 ×). Black arrows show the brown positive apoptotic cells in the adenoma foci.

Adenoma foci were examined under the microscope for lung sections obtained from all treated animal groups and the placebo group. Hematoxylin identified the nucleus of the adenoma foci cells and the brown staining show the positive activated caspase-3 cells which were stained immunohistochemically (see experimental procedures 3.4.3.2).

It can be concluded that sorafenib exhibited an antitumor effect on apoptosis only after one week instillation treatment since many cells died after this treatment period. No apoptosis induction was achieved with further sorafenib intratracheal treatment for two and three weeks.

Several previous studies showed that sorafenib exhibits apoptosis induction in many human cancer lines [24, 28, 79], so it was also supposed in the present investigation to achieve an increase in the number of apoptotic cells. In the present study, the sorafenib apoptotic effect was obtained only after one week instillation treatment while prolongation of the treatment period for two and three weeks showed no increase in the number of apoptotic cells. This might be due to the development of a resistance by the adenoma foci cells to the prolonged sorafenib treatment.

2.10.6 Determination of sorafenib concentration in the lung tissues and blood samples after intratracheal treatment

In order to elucidate the presence of sorafenib in lung tissues and serum samples at the end of the treatment period, the sorafenib concentration in serum and lung tissue samples for each group of animals treated intratracheally with 1 mg sorafenib loaded in liposome suspension was measured by HPLC (see experimental procedures 3.3 and 3.6.4). The mice in each group were sacrificed 24 h after the last dose and subsequently the sorafenib concentration was determined in lung tissues and serum samples. The sorafenib concentration in the lung tissues was very low (below 10 $\mu\text{g/g}$ lung) after one and two weeks treatment. Likewise, sorafenib concentration in the blood was below the low limit of quantitation (LOQ). On the contrary, the sorafenib concentration was high in the lung tissues after three weeks treatment (144.9 $\mu\text{g/g}$ lung) and a detectable sorafenib concentration (0.41 $\mu\text{g/ml}$ serum) was measured in the blood samples. In addition, no peak of sorafenib was detected by HPLC for the recovery group in lung tissues and serum samples as well.

Although in the pharmacokinetic experiment (see 2.9) the sorafenib concentration in the lung tissue was detectable one week after single dose of sorafenib (1 mg), after instillation of multiple doses of sorafenib (1 mg) the drug was completely eliminated after one week treatment. In contrast, the sorafenib concentration detected in the lung tissue after three weeks treatment was high (144.9 $\mu\text{g/g}$ lung), which is consistent with the found sorafenib concentration 2 h after sorafenib single dose instillation. In addition, low sorafenib concentration (0.41 $\mu\text{g/ml}$ serum) was measured in the blood samples after instillation of multiple doses for three weeks. This is also consistent with the presence of a low sorafenib concentration in the blood 2 h after single dose instillation (see 2.9).

In comparison with the pharmacokinetic experiment (see 2.9), the results of the present experiment were unexpected as sorafenib concentration could not be detected after one week and two weeks treatment. In contrast, high sorafenib concentration was found in the lung tissues after three weeks treatment with traces of the drug in serum samples (Table 7).

Table 7: Sorafenib concentration in the lung tissues and blood samples collected after intratracheal instillation treatment with 1 mg sorafenib three times weekly

Animal groups	Sorafenib concentration in the lung tissues ($\mu\text{g/g}$ lung)	Sorafenib concentration in serum ($\mu\text{g/ml}$)
One week	Below 10 $\mu\text{g/g}$	Below 0.08 $\mu\text{g/ml}$ (LOQ)
Two weeks	Below 10 $\mu\text{g/g}$	Below 0.08 $\mu\text{g/ml}$ (LOQ)
Three weeks	144.9 ± 37.2 $\mu\text{g/g}$	0.41 ± 0.31 $\mu\text{g/ml}$
Recovery group	No peak found	No peak found

One explanation could be that sorafenib was more rapidly eliminated after administration of multiple doses than after a single dose. Another explanation could be the behaviour of the diseased lung which might be different from the healthy lung used in the pharmacokinetic experiment including drug uptake by the cells and passage of the drug across the diseased tissue. Therefore, the lung tumor might reduce the quantity of sorafenib detected in the lung.

According to the multidrug resistance mechanisms, the drug is removed from the cell and the drug concentration can be still detected in the lung tissues and blood as well. Therefore, the high sorafenib concentration in the lung tissues without antitumor effect after three weeks treatment may be attributed to a multidrug resistance mechanism developed by the adenoma foci cells. Moreover, the high sorafenib concentration in the lung tissues after three weeks treatment might be the reason for the tumor area reduction in case of the recovery group as explained before in 2.10.2. In addition, the effect of sorafenib on the tumor area in case of the recovery group was weaker than that after one week treatment, which could be due to the slow downregulation of the multidrug resistance and complete elimination of the drug.

As conclusion of the intratracheal instillation of sorafenib liposomes, positive results were attained only after one week treatment. Further treatment for two and three weeks revealed no additional antitumor activity. These results suggested a multidrug resistance phenomenon which was subsequently elucidated in more details.

2.10.7 Evaluation of multidrug resistance induction by sorafenib

2.10.7.1 Multidrug resistance phenomena

The multidrug resistance phenotype is a major problem encountered during chemotherapy and characterized by the overexpression of P-glycoprotein (P-gp). P-gp is a member of the ATP binding cassette (ABC) transporter superfamily coded in humans by the multidrug resistance (MDR1) gene [148]. It is a glycosylated 140-170 kDa protein containing 12 transmembrane domains and two cytoplasmically located ATP-binding sites as illustrated in Figure 25 [149, 150].

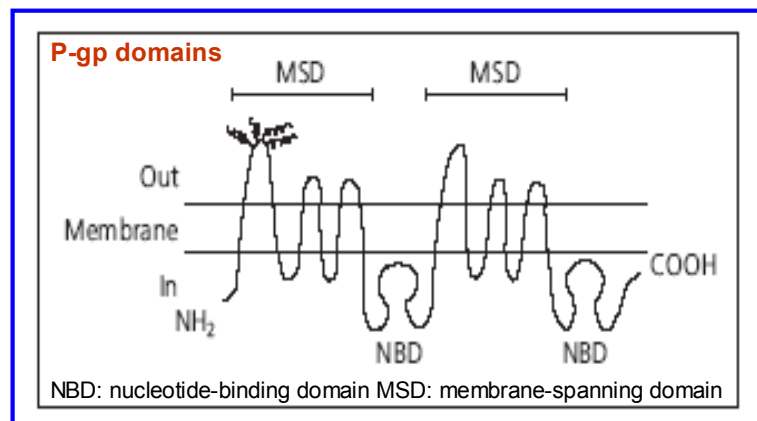


Figure 25: Schematic model of P-glycoprotein domains (modified after Nielsen [150]).

P-glycoprotein and multidrug resistance related proteins (MRP) are members of the ATP binding cassette superfamily of transporters. These proteins actively pump a wide range of substrates out of the cell as they are located on the cellular membrane. Two isoforms have been described in rodents and are coded by *mdr1a* and *mdr1b* genes. In addition, MDR3 in humans and *mdr2* in rodents are expressed predominantly in the liver. These isoforms do not confer multidrug resistance and seem to be included in the transport of phospholipids into the bile [151-153].

A high expression of these proteins in tumor cells is responsible for the failure of therapies. They are also widely distributed in normal tissues. P-glycoprotein is mainly expressed in the intestine, kidney, adrenal glands and liver [153].

The existence of these proteins in normal tissues plays an important physiological role. In particular, their location in the liver, kidney, intestine, blood brain barrier and placenta offers a secretory function and a role in detoxification process. Therefore, they protect normal tissues from endogenous and exogenous toxic substances [153].

The multidrug resistance mechanism was described as follows (Figure 26) [154, 155]:

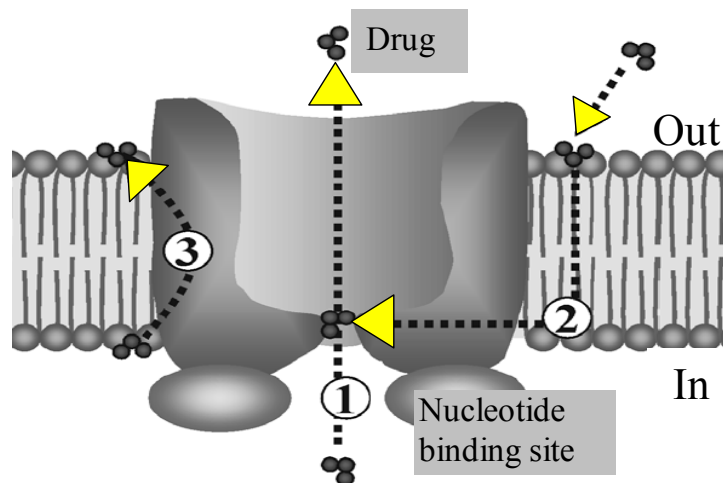


Figure 26: Modified hypothetical model of multidrug resistance mechanism [154, 155].

- 1) A drug molecule can move directly to the aqueous phase outside the cell.
- 2) A lipid soluble molecule dissolves in the cytosol of the plasma membrane and diffuses into the membrane and then binds to the site of the multidrug resistance (MDR) protein. The P-gp transporter sucks up and ejects drugs penetrating a cell's plasma membrane. This mechanism is powered by adenosine triphosphate (ATP) hydrolysis.
- 3) By using the energy of the ATP hydrolysis, the ATP binding sites on the P-gp molecule extend into the cell, where it is believed to provide energy necessary to transport the drugs back across the membrane and out of the cell.

2.10.7.2 Immunohistochemistry detection of MDR expression in lungs of BXB-23 mice after intratracheal administration of sorafenib liposome

The expression of the multidrug resistance associated protein was examined in lung tissue sections using monoclonal antibody that specifically detects this protein in an immunohistochemical technique. The mAb C219 recognizes all isoforms of P-gp [156, 157]. The paraffin embedded lung tissues of all treated animal groups (one, two and three weeks animal groups), the placebo group, recovery group and the recovery placebo were used for this purpose. Mouse kidney tissues were used as a positive control because it was described earlier [153] that P-glycoprotein is mainly expressed in the kidney. The MDR expression in lung tissues of all sorafenib treated groups, the placebo and control groups after intratracheal instillation of 1 mg sorafenib loaded in liposome suspension are illustrated in Figure 27.

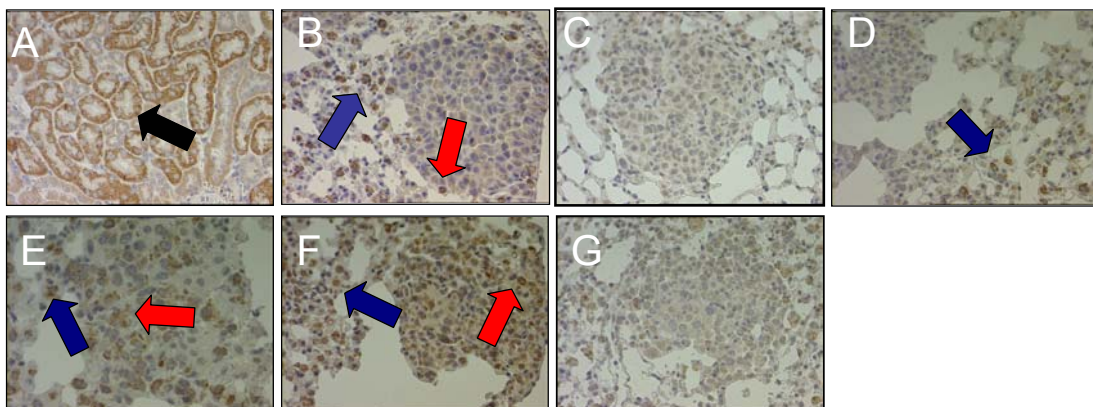


Figure 27: Expression of multidrug resistance (MDR) related protein as detected by C219 (anti-MDR1 P-gp) in paraffin sections of (A) Positive control (black arrow), (B) Placebo lung tissue, (C) Control lung tissue, (D) One week treated lung tissue, (E) Two weeks treated lung tissue, (F) Three weeks treated lung tissue and (G) Recovery group. The blue arrows show MDR expression in the normal tissue and the red arrows show MDR expression in the tumor area (Magnification 40 ×).

A positive expression of the MDR related protein was detected by immunohistochemistry assay and reveals a brown color on the tissue sections. The tissues were furthermore stained with hematoxylin to identify the nucleus. MDR expression in the tumor area (adenoma foci) and also in the normal tissues was observed (Figure 27). The

immunohistochemistry staining revealed that there was a higher expression of MDR in the tumor foci of two and three weeks sorafenib treated lung tissues in comparison to the placebo and the control lung tissues. On the other hand the MDR expression was reduced in the tumor foci of the recovery group (Figure 27 G).

The positive MDR cells in the tumor foci of all treated groups were counted and the percent of these cells in relation to the whole cells in the tumor area was calculated. The percent of MDR of all treated groups with the placebo group was compared. The MDR expression percent of positive cells is represented in Figure 28.

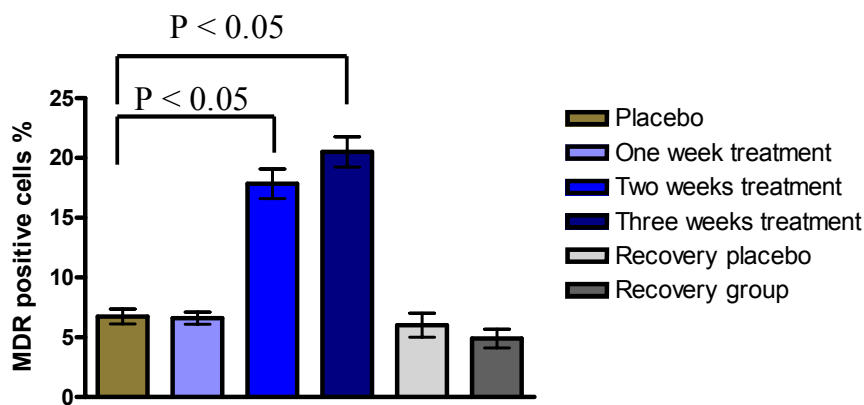


Figure 28: Percent of MDR positive cells for all treated animal groups, the placebo group, recovery group and its recovery placebo group. The data was statistically analyzed using one way ANOVA test (Graph Pad Prism) followed by Tukey test, P-value was regarded as an indication of statistical significance. A significant difference between the percent of MDR positive cells of the two and three weeks sorafenib treated animals compared to placebo group was detected. The data represent the mean \pm SEM (n = 5-8).

There was a significant difference between the percent of MDR positive cells of the two and three weeks sorafenib treated animals compared to placebo group (Figure 28). The percent of positive cells after two and three weeks sorafenib treatment was $17.8 \pm 3.0\%$ and $20.5 \pm 3.5\%$, respectively but in case of the placebo group the percent was $6.7 \pm 1.9\%$. In contrast there was no significant difference in the MDR positive cells percent between animals treated for one week ($6.6 \pm 1.1\%$) and placebo group ($6.7 \pm 1.9\%$). No significant

difference between the recovery group (4.8 ± 1.9 %) and the recovery placebo (6 ± 2.2 %) was noticed.

Two previous studies [158, 159] suggested that the presence of more than 10 % positive cells should be considered as positive MDR expression. In the present study the MDR expression percent calculated after two and three weeks treatment period was more than 10 %. Such positive MDR expression was believed to be due to the resistance developed by the adenoma foci cells during sorafenib treatment by the intratracheal route.

Surprisingly, in the present investigation after sorafenib targeting to the lung of the transgenic mice (BXB-23) using the intratracheal instillation three times per week for three weeks the only detected effect of the sorafenib treatment was after one week and this effect was only a reduction in the tumor area (67 %) and elevation of the apoptotic cells.

These findings can be now explained by the multidrug resistance phenomena. After the immunohistochemical detection of MDR for the sorafenib treated groups in comparison with the placebo and control groups, the positive MDR expression was increased with prolongation of the sorafenib treatment period. The positive MDR cells were more numerous after three weeks treatment than after two and one week treatment. This indicated that the tumor cells in the adenoma foci developed resistance against sorafenib treatment and this resistance affected the pharmacological effect of sorafenib on the lung adenomas.

It is well known that resistance phenomena increase the problem of tumor treatments. Thus, a lack of tumor size reduction or a clinical relapse after an initial positive response to antitumor treatment is related to the occurrence of multidrug resistance (MDR) [160]. The resistance mechanism of the tumor tissues can have different origins. The poor vasculature and unsuitable physicochemical conditions of the tumor cells can lead to the development of resistance. In addition tumor cells can create specific mechanisms resulting in resistance [161]. Furthermore, in solid tumors adequate delivery of therapeutic agents to tumor cells is a prerequisite for the effectiveness of cancer therapy. Therefore, inadequate delivery could lead to residual tumor cells, which in turn could result in regrowth of tumors with a possible development of resistant cells [162]. In addition tumor blood supply plays a pivotal role in the delivery of therapeutic agents to solid tumors [163, 164].

To our knowledge, this is the first study demonstrating the effectiveness of sorafenib intratracheally instilled treatment for local therapy of lung tumors in mice. However, although we did not observe pronounced effects on the tumor growth in this animal model

(BXB-23), we believe that the effectiveness of this treatment may be further improved with a combination therapy, using agents that have different mechanisms of action on cancer cells such as doxorubicin [46, 165, 166].

On the other hand, MDR reversing agents such as the calcium channel blockers verapamil [161] and the immunosuppressant cyclosporin A [167, 168] could be used. Inhibiting the P-gp overexpression and increasing the intracellular accumulation of the anticancer drugs are two mechanisms by which these drugs influence MDR [169, 170]. Shen et al. [171] explained that tamoxifen can reverse the MDR of colorectal carcinoma in nude mice.

Many attempts have been investigated to overcome drug resistance using strategies which consider the problem of the drug biodistribution either at the cellular level or at the tissue level [161, 172]. Vauthier et al. [173] discussed that the use of nanoparticles can overcome MDR phenomena via increasing the intracellular concentration of the drug using endocytosis such as in case of doxorubicin [174].

Finally, the present studies 2.1.1 and 2.9 revealed that sorafenib exhibited antitumor effect when given orally in an emulsion and when loaded in liposome using the intratracheal route in BXB-23 mice model for lung adenoma treatment. Regardless of MDR development by the adenoma foci cells after two and three weeks sorafenib instillation, targeting of sorafenib directly to the lung was successfully achieved using a convenient route. Although the administered dose of sorafenib which was instilled directly to the lung (1 mg) was lower than that given orally (2 mg), sorafenib exhibited antitumor activity on adenoma foci after one week treatment. Such antitumor effect was tumor area reduction (67 %) and induction of apoptosis. In contrast, the effect obtained after sorafenib p.o. treatment was only 29 % tumor area reduction with concomitant reduction of the proliferation. Additionally, a high sorafenib concentration was achieved in the lung tissues compared to its blood concentration after sorafenib instillation. Also, the sorafenib concentration was high in the blood after instillation as compared to that after p.o. treatment.

In the present investigation the next aim was to design another dosage form for sorafenib in order to improve its effect for tumor treatment trying to overcome the multidrug resistance phenomena developed by the tumor cells. Among the new drug delivery systems are the polymeric microspheres which have been considered as promising carriers for anticancer drugs such as cisplatin [175], 5-fluorouracil [176] and camptothecin [177].

Therefore, it was interesting to use this carrier system which is favourable for lipophilic drugs.

2.11 Microspheres as carrier system for sorafenib

One of the most popular areas of research is the usage of polymeric microspheres for delivery of chemotherapeutic agents because of the possibilities of enhancing controlled release activity and also localizing the drug delivery [178, 179].

Poly (lactic-co-glycolic acid) (PLGA) is a synthetic biodegradable and biocompatible polymer that has been widely used in drug delivery research (microparticulate formulations) [178, 180]. PLGA microspheres have been used as a controlled delivery system of many proteins and others such as cytokines, hormones, enzymes, vaccines and chemotherapeutic agents [181].

Poly (L-lactic-acid) (PLA) and its copolymer with glycolic acid (PLGA) have been widely used for controlled drug delivery systems. The lactide/glycolide polymers chains are hydrolyzed into natural metabolites (lactic and glycolic acids), which are removed from the body by the citric acid cycle. Depending on PLGA composition and its molecular weight, a wide range of degradation rates from months to years can be attained [182].

The goal of the current investigation was to design a microsphere drug system with a drug controlled delivery (delivery of drug at a controlled rate for an extended time), based on the biodegradable polymer PLGA. The active substance was sorafenib, a hydrophobic molecule. The second objective was to determine the physicochemical characteristics (i.e. encapsulation efficiency, *in vitro* release, size distribution) of the developed microspheres.

2.11.1 Microspheres preparation

Emulsion-solvent-evaporation technique was the widely used method for microspheres preparation [175, 177, 178, 183-187]. Recently [188, 189], a new method, emulsion-diffusion-evaporation was reported using ethyl acetate as an organic solvent.

The aim of the present study was to use this emulsion-diffusion-evaporation method to prepare sorafenib loaded microspheres. The method was adapted with suitable modifications to obtain sorafenib microspheres. Briefly, the microspheres were prepared as follows: PLGA was dissolved alone or dispersed with sorafenib in dichloromethane. The

organic solvent was then added to an aqueous stabilizer solution of polyvinyl alcohol (PVA) under stirring. The resulted o/w emulsion was stirred 3 h before homogenizing for 10 min. To this emulsion water was added under stirring resulting in precipitation of the microspheres. Stirring was continued overnight on a water bath to remove the organic solvent.

Polyvinyl alcohol (PVA) served as stabilizer to prevent coalescence and formation of agglomerates during and after the emulsification process. The adsorption of the stabilizer at the interface between the dispersed and the continuous phase prevents this coalescence by lowering the interfacial tension and the energy of the system [188]. Dichloromethane was used in the present preparation as an organic solvent because it yielded stable microspheres preparation with good reproducibility. Additionally, Lee et al. [185], Herrmann and Bodmeier [184] found that utilizing dichloromethane as an organic solvent led to high encapsulation efficiency of the microspheres preparation as compared with ethyl acetate. Because of the low solubility of sorafenib in dichloromethane, the drug was finely dispersed in the polymer solution under stirring.

The dispersion of the solvent due to stirring led to formation of irregular-sized globules in equilibrium with continuous phase. The size of globules was reduced after homogenization process. The addition of water destabilized the equilibrium to force the organic solvent to diffuse to the continuous phase. Consequently, the particles precipitated resulting in production of small microspheres. Overnight stirring at 30 °C assured the complete evaporation of the organic phase (see experimental procedures 3.7.2). The advantage of this method was the reproducibility.

2.11.2 Microspheres characterization

2.11.2.1 Particle size and size distribution determination

There are several techniques to determine the microspheres particle size and their distribution such as laser diffraction method [190-192] and laser [178, 193] or dynamic [185] light scattering analyzer. Optical microscopy was used [175, 194, 195] for particle size distribution visualisation and determination. A coulter counter size analyser was utilized for the assessment of the particle size and its distribution [176, 181, 196, 197].

In the present investigation a coulter counter was used for the determination of particle size distribution as the other techniques described above were not available. The size

distribution for plain and sorafenib loaded microspheres is shown in Figure 29. The mean particle size for plain and sorafenib loaded microspheres was $1.3 \pm 0.2 \mu\text{m}$ and $1.7 \pm 0.2 \mu\text{m}$, respectively. The size distribution was nearly the same for the plain and loaded microspheres as in case of the plain microspheres 90 % was smaller than $2.1 \mu\text{m}$ and for the sorafenib loaded ones 90 % was smaller than $2.9 \mu\text{m}$. For both microspheres the range of size distribution was narrow $0.7\text{-}2.1 \mu\text{m}$ for plain and $0.63\text{-}2.9 \mu\text{m}$ for the loaded microspheres.

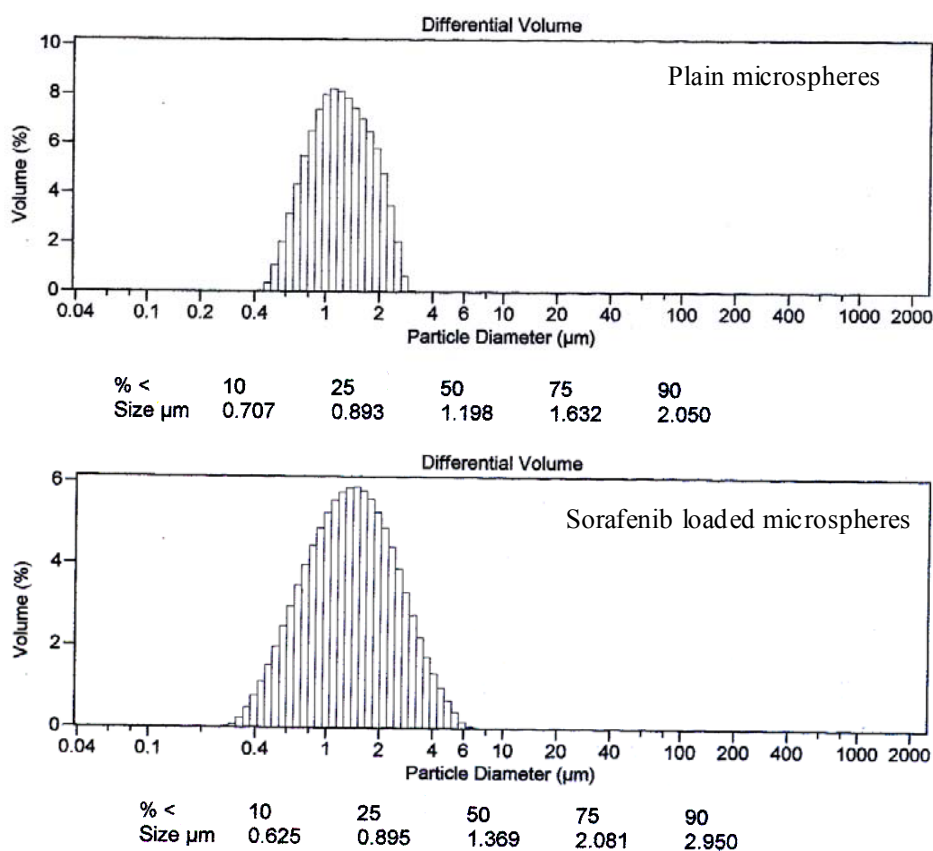


Figure 29: Particle size distribution of plain and sorafenib loaded microspheres as determined by coulter counter.

Thus, particle size and size distribution of the plain and sorafenib loaded microspheres revealed that the incorporation of sorafenib into the microspheres did not have a significant effect on the particle size of the preparation.

2.11.2.2 Morphology of microspheres

A widely used technique to visualize the microspheres' morphology is the electron scanning microscopy (SEM) [176, 178, 181, 185-187, 192, 193]. In the present study the morphology of the plain and sorafenib loaded microspheres was examined using this technique (Figure 30).

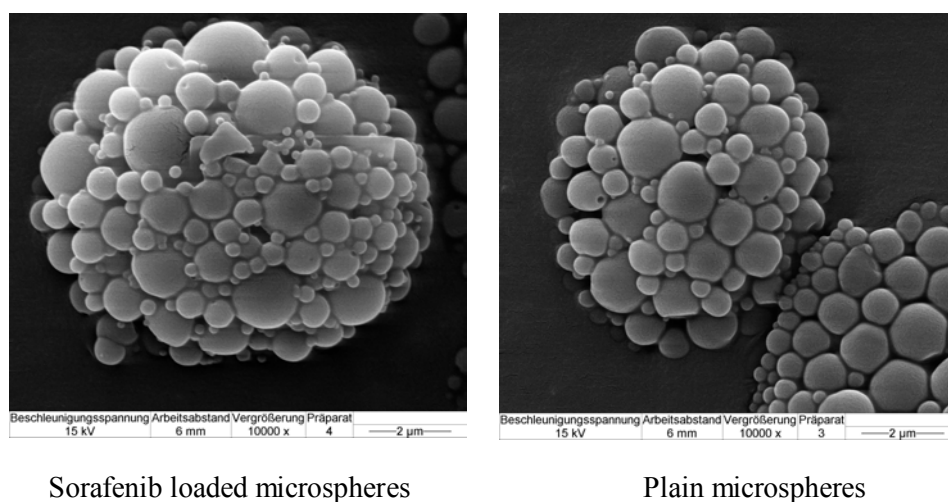


Figure 30: Scanning electron microscope (SEM) photograph of plain and sorafenib microspheres.

Scanning electron microscopy showed that the microspheres were spherical in shape and had a relatively smooth surface as shown in Figure 30. The spherical particles revealed many pores in case of both the plain and sorafenib loaded microspheres. These pores are the result of solvent evaporation as described earlier [175]. The morphology of the plain and sorafenib loaded microspheres was a normal morphology which characterized the microspheres preparation as described before [177, 178, 181, 184-186, 196]. The size range of the microspheres was found to be consistent with that deduced from the coulter counter (2.11.2.1). This indicated that loading of sorafenib in the microsphere preparation did not significantly influence the microspheres morphology. Since the preparation of the plain microspheres was successful showing good particle morphology and resulting in suitable homogenous particle size distribution (2.11.2.1), it was important that

incorporation of sorafenib in this microspheres formulation does not influence these properties.

2.11.2.3 Yield and encapsulation efficiency of sorafenib microspheres

Determination of the encapsulation efficiency was achieved by calculating the actual drug content incorporated in the microspheres (direct method). The measurement of the actual drug content in the microspheres was performed by dissolving a specific amount of the microspheres powder in an organic solvent and then the drug content was assayed by spectrometry or HPLC. The encapsulation efficiency was calculated from the ratio of the drug content of the microspheres and the amount of the drug used for the microspheres preparation [175, 176, 178, 186, 187, 190-193].

In the present study it was difficult to determine the sorafenib content by dissolving the microspheres in an organic solvent because the microspheres components obstructed the accurate determination of the actual sorafenib content with HPLC due to the presence of interfering peaks. In order to overcome this problem, free sorafenib was determined in the supernatant which was obtained during the preparation process and the washing step (indirect method) [182]. Sorafenib was extracted from the supernatant by liquid-liquid extraction and its content was measured using HPLC as discussed in 3.3. The percent encapsulation efficiency (% EE) was calculated as follows according to Huo et al. [198].

$$\% EE = \frac{TotalA - FreeS}{TotalA} \times 100$$

TotalA is the total amount of sorafenib added in the microspheres preparation and FreeS is the sorafenib content calculated in the whole supernatant volume after centrifugation and washing of the microspheres.

The percent encapsulation efficiency was determined for 6 batches and the mean percent was 98.5 ± 1.5 %. This high encapsulation efficiency of sorafenib may be attributed to its high partition coefficient, and hence its retention in the organic phase as the microspheres solidify [179, 186]. In the same vein, Gupte and Ciftci [178] found that the hydrophobic

paclitaxel had a high encapsulation efficiency (90 %) when incorporated into microspheres. Another research group [199] discussed that the encapsulation efficiency was highly dependent on the lipophilicity of the drugs, reaching the maximum for the lipophilic drugs. In addition, Hombreiro-Perez et al. [186] reported that more than 83 % encapsulation efficiency was achieved with nifedipine as compared to 51-59 % with propranolol HCl. They explained that by the lipophilicity of nifedipine ($\log P = 2.97$) and hence its higher affinity to the organic phase than the aqueous phase. Therefore, drug loss into the external PVA solution was rather low. Accordingly, the high lipophilicity of sorafenib ($\log P = 5.16$) probably led to the observed high encapsulation efficiency.

Also, the high encapsulation efficiency of sorafenib in the present investigation can be attributed to the preparation method (o/w) used. The encapsulation efficiency obtained with o/w method was higher than those achieved with the w/o/w method as described earlier [186]. This might be explained by the lower volume of the outer PVA phase (water phase) which was used in the case of o/w method compared to the w/o/w method, resulting in less drug loss into this phase [186].

Lee et al. [185] found that the highly hydrophobic cyclosporine A had a high encapsulation efficiency. They discussed that in general, a more lipophilic solvent or solvent mixture was convenient in preventing drug loss to the external aqueous phase. High encapsulation efficiency was achieved when microspheres were prepared using methylene chloride rather than ethyl acetate, regardless of the type of preparation method.

In the present study methylene chloride was used as an organic solvent so the high encapsulation efficiency could be additionally due to the utilization of this organic solvent in the preparation procedure. Due to the low solubility of sorafenib in methylene chloride, the drug was dispersed in the polymer solution with the aid of stirring, followed by emulsification of the dispersion into the external aqueous phase. Such dispersion process could be another parameter which increased the encapsulation efficiency as described earlier [184]. In the present study the initial loading of sorafenib was 10 % (w/w). The yield for sorafenib microspheres was 86 %.

2.11.2.4 *In vitro* release study of sorafenib from the microspheres

There are different methods used to study the *in vitro* release of drugs from microspheres. For example, in previous studies [175, 176, 185] a dialysis method was used. Other

research groups [178, 181, 183, 186, 187, 193, 200] determined the *in vitro* drug release by incubating the microspheres preparation in phosphate buffered saline under shaking conditions. At different time points, samples were withdrawn and the drug concentration was determined by HPLC analysis.

In the present assay the incubating method was used. Sorafenib loaded microspheres were incubated under shaking in phosphate buffered saline containing tween 80 (0.01 %). Using dialysis bags was omitted due to adsorption of the lipophilic drugs to cellulose of the dialysis bag [177].

At predetermined time intervals 1 ml was withdrawn to determine the sorafenib amount released. Sorafenib concentration was assayed using a HPLC method (see experimental procedures 3.7.3.4). The *in vitro* release study for sorafenib solution (250 μg in methanol) was done in phosphate buffer containing 0.01 % tween 80 and the procedure was continued as described above. The *in vitro* release profile for sorafenib microspheres is shown in Figure 31.

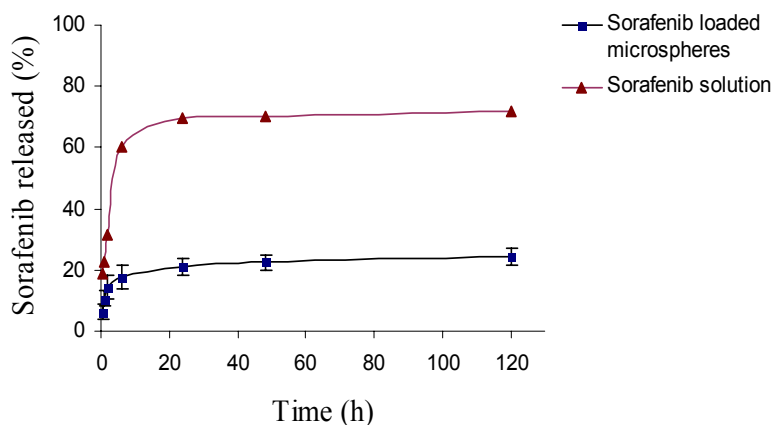


Figure 31: *In vitro* release profile of sorafenib loaded microspheres prepared by emulsion-diffusion-evaporation method using PLGA 50:50 compared with sorafenib solution. Each value represents the mean \pm SEM (n = 3).

There was an initial release of 6 % from sorafenib microspheres after 30 min. This initial release of the drug could be explained by the release of some drug that was poorly entrapped in the polymer matrix and loosely bound on the surface of the microspheres

[201]. This loosely bound drug could be released by diffusion through the aqueous pores on the surface of the microspheres immediately after their exposure to water [202, 203]. The low solubility of sorafenib in dichloromethane might be attributed to the easy exclusion of the drug from the polymer matrix during particles formation and hence the drug would be accumulated on the particle surface. This explanation was described before by Lin et al. [193] in the *in vitro* release study of doxorubicin. This initial release of sorafenib from the microspheres was later followed by nearly constant release of the drug from the microspheres for 5 days. The release of sorafenib from the microspheres was slow which was most probably attributed to the much lower solubility of sorafenib in the release medium resulting in low concentration gradients, the driving forces of diffusion. The slow and continuous release of sorafenib from the microspheres may be additionally attributed to the diffusion of the drug localized in the PLGA core of the microspheres. Hombreiro-Perez et al. [186] found that the slow release behaviour of the lipophilic nifedipine was probably related to its much lower solubility in the released medium.

In the present assay sorafenib solution was used as a control because sorafenib solution should reveal a 100 % release. In case of sorafenib solution the release was higher than that from microspheres as only 22.6 % sorafenib was released after 5 days from the microspheres and on contrary 72 % sorafenib was released in solution after 5 days. This indicated that the microspheres preparation provided a slow and constant release of sorafenib over 5 days. The incomplete release of sorafenib in solution may be explained by the low solubility of sorafenib in the release medium (PBS). Also this incomplete release could be related to the precipitation of the insoluble drug during the processing of the samples prior to HPLC analysis.

There are several parameters which affect the *in vitro* release of the therapeutic agent from the microspheres.

The release of the entrapped therapeutic agents from nano- and microparticles can be altered by modifying different formulation parameters [204, 205] including polymer molecular weight, composition, formulation methods, particle size and the type of emulsifier used. The release of the entrapped therapeutic agent occurs during the early phases mainly through diffusion in the matrix whereas the release is mediated through both diffusion of the therapeutic agent and degradation of the polymer matrix itself during the later phases [204]. Therefore, the *in vitro* release of the therapeutic agent from PLGA matrices depends mainly on degradation rate of the polymer matrix [206].

Sorafenib release profile was different in case of microspheres as that of liposomes formulation. Such difference could be related to the method used in the *in vitro* release study as the dialysis method was utilized in case of the liposome formulation whereas incubation method was used in case of microspheres. The release of sorafenib from the liposomal suspension was rapid as approximately 70 % of sorafenib was released after 24 h. In contrast, the sorafenib release from microspheres was slow followed by constant and continuous release which was mainly dependent on the PLGA composition used and its degradation rate.

Although the sorafenib release from the microspheres was slow, the preparation can be further applied *in vivo*.

The whole data of the present investigation indicated that the biodegradable microspheres based on PLGA 50:50 containing the lipophilic drug sorafenib were successfully prepared with oil-in-water (o/w) emulsion-diffusion evaporation technique. The system was characterized physicochemically and performed a good microspheres yield, high encapsulation efficiency, homogenous particle size distribution and constant slow release of sorafenib. It can be concluded that the sorafenib microsphere preparation can be further used *in vivo* as a carrier system for sorafenib.

2.12 Gene delivery and cationic vectors

In order to treat a variety of pulmonary dysfunctions such as cystic fibrosis, alpha-1 antitrypsin deficiency, pulmonary hypertension, asthma and lung cancer, delivery of the therapeutic genes to the lung was considered as an attractive strategy [207]. Different delivery routes such as intratracheal instillation, aerosol and intravenous injection have been employed with varying degrees of efficiency. Significant levels of transgene expression in the lungs have been achieved by using both viral [208] and non-viral vectors [209].

There are several types of vectors used in gene delivery as discussed before by Gautam et al. [207].

1. Viral vectors

Viruses are ideal carriers for gene delivery according to their molecular biology. One of their advantages for gene delivery is the high transduction efficiency. In clinical gene

therapy protocols, viruses are the most widely used vectors. They are classified into three groups:

A. Retroviruses

In stem cell gene therapy they are useful for *ex vivo* gene transfer and also for *in vivo* applications such as treatment of cancer and HIV. The retrovirus is an RNA virus consisting of two copies of a single stranded RNA genome [210]. For long-term gene expression, retroviruses are able to integrate into the host genome and stably transduce the cells. The generation of retro- and adenoviral vectors includes the replacement of viral genes or elements required for replication in the host cell, with the desired therapeutic gene [5].

B. Adenoviruses (DNA viruses)

Adenoviral vectors are the most extensively utilized viral vectors for gene therapy [211]. Using adenoviruses for pulmonary gene therapy is restricted because the receptors for adenovirus are located at the basolateral surfaces, making it difficult to target the apical surface of the epithelium through the airways.

C. Adeno-Associated Virus (AAV)

It is a non-pathogenic single stranded DNA virus. AAV vectors have generated a lot of interest in pulmonary gene therapy, especially due to their potential use in cystic fibrosis gene therapy [212].

2. Non-viral vectors

Undesirable and occasionally toxic immune response to the viral vectors reduces their use for systemic gene delivery [213]. These undesired effects can be prevented by using non-viral vectors. Lack of immunogenicity, commercial availability and low cost are the major advantages of non-viral vectors over viral vectors [214]. However, the low transfection efficiency of non-viral vectors *in vivo* as compared with the viral vectors is a major limitation. Cationic liposomes and cationic polymers are two of the most important non-viral vectors employed for gene delivery [215, 216]. Both agents bind to DNA by electrostatic interactions protecting the DNA from nucleases and reduce its dimensions.

Subsequently, hydrophobic collapse leads to particle formation in the nanometer range [217].

A. Cationic liposomes

The cationic liposomes interact with the plasma membrane lipid structure by fusion and deliver the gene into the cell. Most cationic liposomes consist of a hydrophobic lipid group capable of interacting with the anionic DNA [218-223].

B. Cationic polymers

The cationic polymers possess a high charge density and buffering capacity, which assist their compactness with the DNA and hence protecting it from degradation by nucleases in the low pH endosomal/lysosomal compartment. There are three different types of cationic polymers commonly used for the delivery of genes to cells and tissues. **Dendrimers** are a class of polymers where the amine group is repeatedly substituted at its amino termini resulting in a branched structure. **Polyaminoacids** are another class of polymers used for efficient transfection of cells both *in vitro* and *in vivo*. Poly-L-lysine (PLL) is the most widely used polymer of this group [224, 225]. These polyaminoacids, especially the higher molecular weight polymers (>25 kDa), have been shown to be quite toxic.

Polyethylenimines (PEIs) are another class of cationic polymers which have been widely employed for gene therapy [226, 227]. Both linear and branched PEI forms have different molecular weights. Administration of PEI intravenously or by intranasal instillation revealed the highest transfection efficiency in the lungs. Additionally, PEI can be used to deliver DNA aerosol for pulmonary gene therapy [209, 228]. The buffering capacity of PEI in the endosomes appears to play a decisive role in protecting the DNA and carrying it to the nucleus. In contrast, the cationic liposomes dissociate from the DNA in the endosomes [209, 229].

2.12.1 Polyethylenimine (PEI) as a cationic polymer for gene delivery

The ability of polyethylenimine (PEI) to facilitate the escape of DNA from endosomes was studied by Kichler et al. [230]. After endocytosis of the cationic complexes, acidic

endosome buffering through PEI that stimulates a massive proton accumulation followed by passive chloride influx with subsequent increase of the osmotic pressure and finally endosome lysis followed by the release of endocytosed material [231]. Kichler et al. [230] concluded that the transfection efficiency of PEI depends on its ability to capture the protons which are transferred into the endosomes during their acidification. This mechanism is based on the chemical structure of the polymer. Polyethylenimine is the organic macromolecule with the highest cationic-charge potential, every third atom being amino nitrogen that can be protonated (Figure 32). According to the pK profile, PEIs show a substantial buffer capacity over almost the entire pH range [232]. The PEI mechanism of action is illustrated in Figure 33.

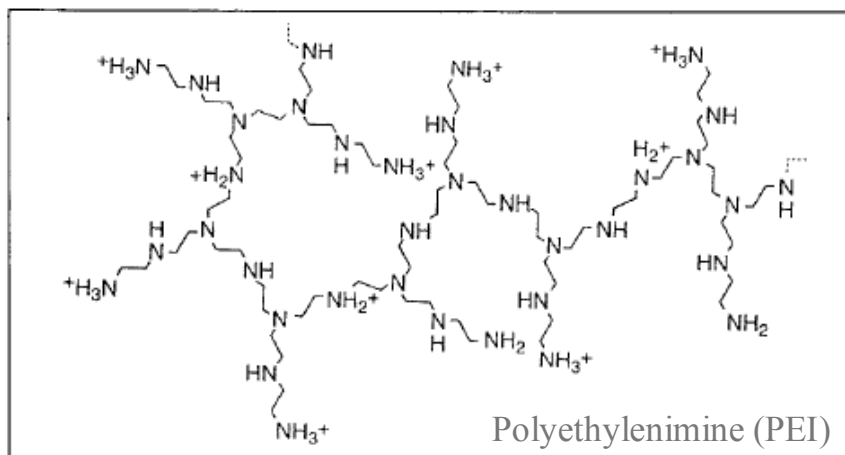


Figure 32: Structure of polyethylenimine (PEI) modified after Kichler et al. [230].

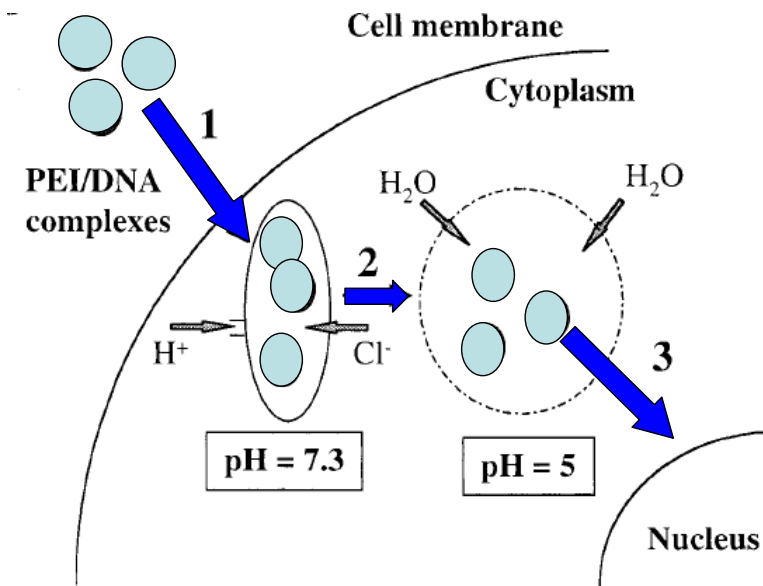


Figure 33: Polyethylenimine (PEI) mechanism of action (modified after Kichler et al. [230]).

- (1) The proton sponge effect after endocytosis of the cationic complexes
- (2) Acidic endosome buffering
- (3) Increase of osmotic pressure and subsequent lysis

A number of PEI molecules have been described in detail with varying molecular size or structure, initially branched PEI with an average molecular weight of 800 kDa (PEI800) and 25 kDa (PEI25) [231, 233]. In addition, a linear form with an average molecular weight of 22 kDa (PEI22) showed a high transfection activity *in vitro* and *in vivo* [231, 234-236]. Intravenously delivered PEI22/DNA complexes produced in salt-free buffer revealed a high gene expression in the lung and lower gene expression in other organs (spleen, kidney, liver and heart) [236]. These small complexes crossed rapidly the endothelial cells of the lung capillary bed. Furthermore, gene expression was mainly found in alveolar cells and pneumocytes [236-238]. In contrast, branched PEI (25 and 800 kDa) are generally less efficient and often toxic, particularly at high polycation nitrogen to DNA phosphate ratios (N/P), as compared to linear PEI22 [216, 234, 236]. For efficient gene delivery *in vivo*, the use of L-PEI/DNA complexes is recommended due to their high transfection capacity and the lack of toxicity [237].

2.13 *In vivo* application of transfection complex of a reporter gene using different vectors and different routes in tumor bearing BXB-23 mice

The success of lung gene therapy is largely dependent on the development of a vector or vehicle that can efficiently deliver a gene to the lung. Thereby, polyethylenimine (PEI) was employed for gene delivery in the present study due to its previously discussed advantages (see 2.12.1). The objective of the present investigation was to use polyethylenimine as a cationic vector targeting the lung adenoma in BXB-23 transgenic mice. In order to elucidate the gene expression using this kind of cationic polymer, reporter genes like green fluorescent protein (GFP) [239] or LacZ (β -galactosidase) [240] were utilized in the present study as well. The intravenous and intratracheal routes were chosen as administration routes.

Previous studies showed that in drug targeting strategy, the delivery of drugs to the lung via the blood stream was performed [236-238, 241]. For the treatment of lung diseases such as lung cancer and cystic fibrosis, drug targeting constructs can be applied via the blood stream using cationic vectors such as liposome and polyethylenimine. For prophylactic and curative gene therapies in humans, intravenous administration is the suggested delivery route.

Thus, the genes cross the capillary barrier and reach target tissues without being degraded [237, 241].

Different routes of administration were shown to result in different deposition of the DNA. The transfection after intravenous administration is generally limited to the alveolar region comprising endothelial cells and pneumocytes [234, 236-238]. In comparison, intratracheal administration of the same formulation predominantly showed gene expression in the bronchial cells [240] with lower expression in the alveolar region [234]. This route proved to be useful in case of cystic fibrosis [242], in which bronchial cells must be targeted [243]. Additionally, gene delivery by instillation demonstrated to be appropriate in different disease models of endobronchial pulmonary cancer as explained by Blezinger et al. and Zou et al. [244, 245].

2.13.1 Examination of GFP (Green Fluorescent Protein) reporter gene expression after systemic application via tail vein using PEI as a cationic vector

In the present experiment green fluorescent protein (GFP) was used as a reporter gene [239, 246]. Thus, 50 μg GFP was complexed with polyethylenimine and the complex was injected via tail vein in the BXB-23 mice (Figure 34). A group of mice ($n = 4$) was anesthetized and then scarified 24 h after the intravenous injection. Another mice group ($n = 4$) was anesthetized and then scarified 48 h after the injection and four mice were anesthetized and then scarified 24 h after twice injection with 15 min interval. Additionally, a group of mice was considered as placebo which was injected with buffer and another group served as control (untreated mice).

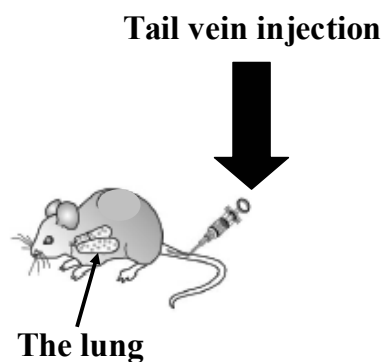


Figure 34: Demonstration of intravenous injection for mice via tail vein injection (modified after Akerman et al. [247]).

The lung tissues were examined under fluorescence microscope for the GFP expression. Unfortunately, examination of GFP expression in the lung tissues after the injection was difficult. The difficulty was to distinguish the actual GFP-derived fluorescence expression from tissue autofluorescence which was due to the presence of blood traces and impurities. The control and placebo lung sections showed also green fluorescence. Kishimoto et al. [248] explained that this problem of tissue autofluorescence can be solved by using a special kind of double excitation and emission filter which can distinguish

between actual GFP-derived fluorescence and autofluorescence through wavelength filtration. In the present case it was not possible to have this kind of filter, for this reason LacZ was used as an alternative reporter gene.

2.13.2 Examination of LacZ (β -galactosidase) expression in lung tissues using PEI as a cationic vector

Since GFP did not efficiently work in the present study as a reporter gene (see 2.13.1), LacZ (β -galactosidase) was utilized. The objective of the present investigation was to study the ability of the linear PEI/DNA complex to target the lung of the transgenic mice model BXB-23 and to assess its transfection efficiency in the adenoma foci cells when delivered intravenously and intratracheally.

2.13.2.1 Examination of LacZ expression after intravenous injection

The PEI22/DNA complexes prepared in HEPES buffered glucose (HBG) efficiently delivered the reporter gene to various tissues, with the highest gene expression in the lungs [236, 238]. The PEI22/DNA complexes produced in $0.5 \times$ HEPES buffered saline (HBS) were less active than the HBG-generated complexes (100-fold reduction). The complexes prepared in salt-free conditions (HBG) remained small over an extended period [249]. Wightman et al. [249] found that mice showed 100-fold higher gene expression in the lung with linear PEI22/DNA complexes formulated in salt-free HBG as compared to that in HBS. It was previously described [234-238, 249] that the application of linear PEI22/DNA complexes via the tail vein led to rapid crossing of the complexes from the blood into the lung tissue resulting in high lung gene expression.

Zou et al. [238] explained that when the amount of DNA was increased from 20 μ g to 50 μ g, the detected amount of the reporter gene was increased by 50-100 folds in the lung after 24 h. Moreover, the increasing of the N/P ratio (4 to 10) led to high levels of transfection in all organs [238].

According to the suitability of using PEI/DNA HBG complexes in gene delivery as discussed above, this system was also employed in the present study. Five BXB-23 mice were injected slowly into the tail vein with the PEI22/DNA complex (250 μ l/mouse) containing 50 μ g LacZ DNA at N/P ratio of 10. A group of mice (n = 4) served as a

placebo group injected with 250 μ l HEPES buffered glucose (HBG). The mice were anesthetized 24 h after injection then were sacrificed and the lungs were perfused. After perfusion, the lungs were dissected and the β -galactosidase reaction continued for 48 h by immersion in the X-gal staining solution in PBS at 30 °C (see experimental procedures 3.8.4.5). The frozen lung tissues were examined under the microscope for LacZ (β -galactosidase) expression 24 h after PEI/LacZ complex injection using X-gal staining (see experimental procedures 3.8.4.5) to reveal the blue β -galactosidase (LacZ) expression and subsequently stained with eosin which identifies the cytoplasm with red colour (Figure 35).

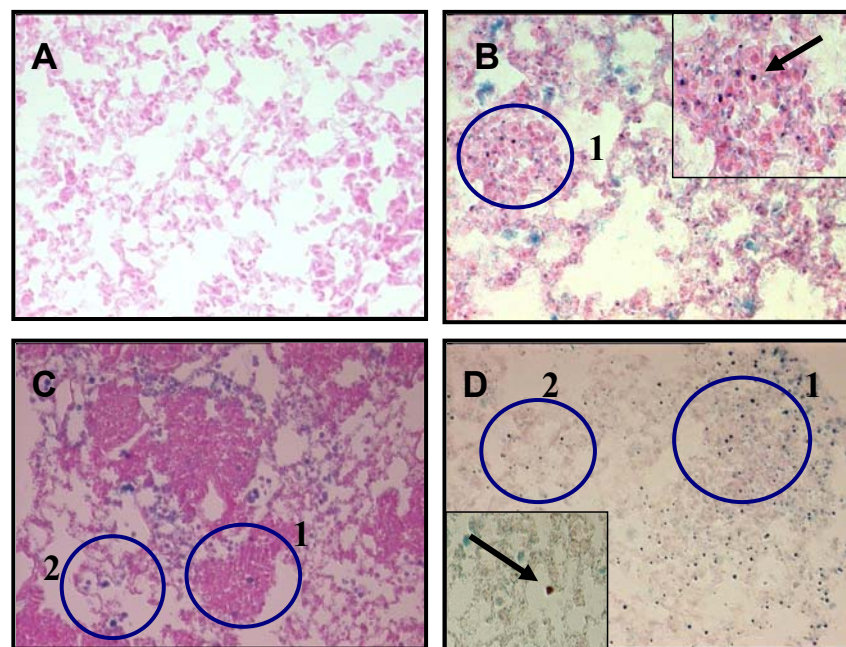


Figure 35: Expression of β -galactosidase in the lung tissues of BXB-23 mice. 50 μ g of pSV40- β gal was injected into the tail vein after its complexation with 22 kDa PEI at an N/P of 10, which was prepared in 250 μ l 5 % glucose. The animals were anesthetized and then sacrificed 24 h later and the lungs were perfused and stained for β -galactosidase activity (blue staining). (A) Placebo lung tissue received 250 μ l HBG. (B), (C) and (D) represent lung tissues of PEI/LacZ injected mice group. Transgene expression is shown in clusters or points of cells located throughout the respiratory zone of the lung. The blue staining can be detected in the alveolar region and some staining in the adenoma foci including great epithelial cells (type II pneumocytes). Black arrow in (B) demonstrates the expression in the adenoma foci but in (D) demonstrates the expression in the alveoli (Magnification 40 \times). Blue circles represent the adenoma foci (1) and alveolar regions (2).

There was a high β -galactosidase (LacZ) expression in the lung tissues 24 h after PEI22/LacZ complex injection (Figure 35 B, C and D) which was indicated by the presence of blue X-gal staining especially in the alveolar regions which is in agreement with previous studies [236, 250]. No LacZ expression was detected in the placebo group (Figure 35 A). In addition, some LacZ expression in the tumor foci including the great epithelial cells (type II pneumocytes) was achieved.

It was observed before [216, 230, 234-238, 250-252] that injection of PEI/DNA complexes exhibited high gene expression in the healthy lung tissues. In the present investigation the high gene expression was observed in the lung bearing tumor of BXB-23 mice model with some LacZ expression occurred in the adenoma foci. This indicated that PEI worked as a cationic vector for gene delivery to the lung of BXB-23 mice model and can be further employed for gene therapy to treat the lung adenoma. In contrast, no LacZ expression was detected in the invaded (tumor bearing) lung as described by Coll et al. [253]. They found that in the invaded lungs no X-gal-positive cells were visible. It was shown that not only tumor cells were difficult to transfect, but also the normal lung cells surrounding these tumor cells became resistant to gene expression [253]. On the other hand, in the normal lungs, an intense staining of the alveoli was detected after X-gal staining of L-PEI/pCMV-LacZ-treated animals.

2.13.2.2 Examination of LacZ expression after intratracheal instillation

The use of polyethylenimine-DNA (PEI/DNA) complexes was considered as a promising strategy for lung-specific gene delivery. These complexes can be employed to deliver genes to the lungs via instillation in the airways [228, 252, 254-258]. The success of gene delivery into the lungs via the intratracheal administration required different factors. Accordingly, utilizing of PEIs with low ratio of positive charges resulted in the highest levels of transfection [234]. As opposed to systemic delivery, intratracheal-injected complexes do not have to interact with the negatively charged blood components. Therefore, less positive complexes are required for high levels of lung transfection [234]. For this reason in the present experiment the N/P ratio used was less than that used before in the intravenous experiment 2.13.2.1.

Five BXB-23 mice were instilled slowly once via the trachea with 150 μ l transfection complex/mouse. This complex contained 50 μ g LacZ DNA, which was the same dose as that delivered intravenously, at N/P ratio of 6. Another mice group (n = 4) was considered as placebo group and instilled with 150 μ l HBG. 24 h after intubation, the mice were anesthetized then scarified and subsequently the lungs were perfused and the frozen lung tissues were stained for β -galactosidase activity and examined for LacZ expression under the microscope (Figure 36).

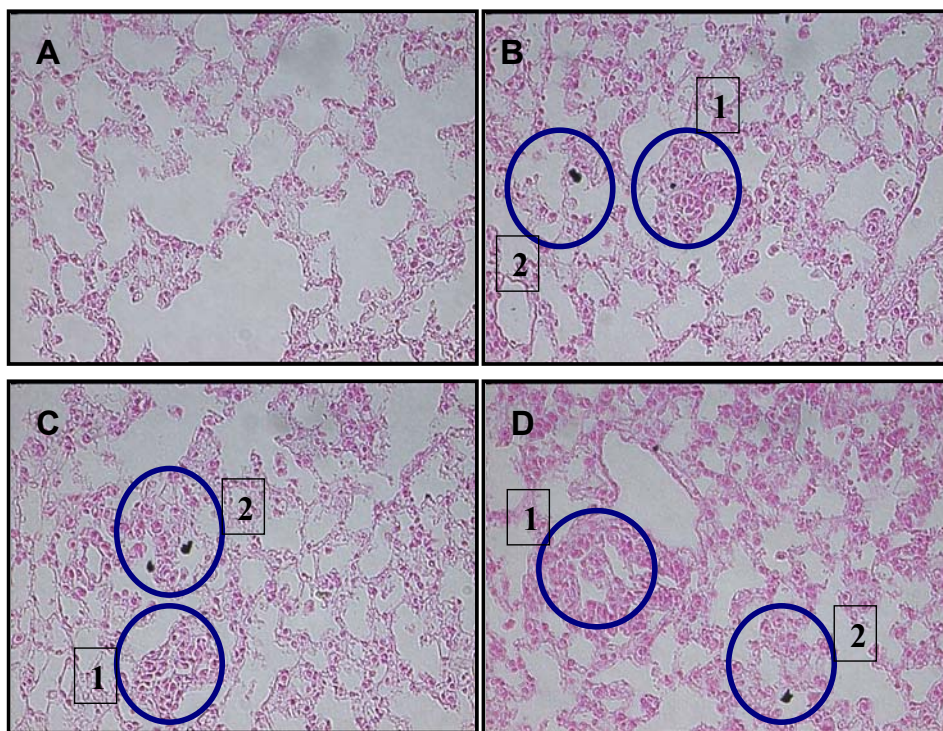


Figure 36: Expression of β -galactosidase in the lung tissues of BXB-23 mice. 50 μ g of pSV40- β gal was instilled intratracheally after complexation with 22 kDa PEI at an N/P of 6 in 150 μ l 5 % glucose. The animals were anesthetized and then scarified 24 h later and the lungs were perfused and stained for β -galactosidase activity. (A) Placebo lung tissue received 150 μ l HBG. (B), (C) and (D) represent lung tissues of PEI/LacZ instilled mice group (n = 5). Transgene expression is shown in clusters of cells located in the respiratory zone of the lung. The blue staining can be observed in the alveolar region and low staining in the adenoma foci. β -galactosidase expression was visualized under a light microscope (Magnification 40 \times). Blue circles represent the adenoma foci (1) and the alveolar regions (2).

LacZ expression was detected 24 h after instillation which was indicated by the presence of blue X-gal staining. This expression was mainly observed in the alveolar regions and very

low expression was found in the adenoma foci (Figure 36 B, C and D). No expression was detected in the lung tissues of the placebo group (Figure 36 A).

It was previously discussed that PEI/DNA gave principally high gene expression in the distal tract of the bronchial tree (alveolar ducts) and the bronchial epithelial after intratracheal instillation [234, 259] in healthy mice lungs. The difference in gene expression between the present case and the previously studied cases [234, 259] could be attributed to the special mice strain used in the present experiment. Although the gene expression in the present study was low in the adenoma foci, PEI exhibited activity for targeting the airways in the lung bearing tumor of BXB-23 mice model. Probably some improvements are required for its delivery in this mice model such as increasing the delivered dose or the dose frequency. Bragonzi et al. [234] suggested that instillation of polyplexes intratracheally could overcome the surfactant barrier which inhibited the lung transfection by cationic lipids. On the contrary the lung transfection in the present study was probably inhibited to some extent by the surfactant barrier that resulted in low transfection. In the present experiment the LacZ expression was low as compared with the previous intravenous experiment 2.13.2.1 in the BXB-23 mice model. It can be concluded that the administration of PEI/LacZ complexes intravenously was more efficient than the instillation route in transfecting the lung bearing tumor of the BXB-23 mice model including the adenoma foci.

2.13.2.3 Examination of LacZ expression after systemic application of two polyplexes

An ideal gene delivery system has to carry out several criteria to access tumor tissue [260]: (1) ligands incorporation which mediate cell specific recognition and internalization into target cells (2) non-specific interactions with the biological compartments such as blood components and non-target cells should be avoided in order to achieve a successful gene delivery.

Polyethylenimine (PEI) transfers efficiently gene to several organs after systemic tail vein injection [236, 238, 250, 253] and after topical administration to the lungs [234, 256, 261, 262] in various animal models *in vivo*. Many studies showed that a positive overall surface charge of the polyplexes was necessary to yield stable complexes and high transfection rates. This positive overall surface charge of the polyplexes makes the use of these

polyplexes limited due to their toxicity and their interaction with blood components. Indeed, interaction of the positively charged polyplexes with their physiological environment such as erythrocytes and plasma proteins affected the gene transfer efficiency [216, 238].

One possibility to conquer these problems was to obscure polyplexes by protective copolymers. Incorporation of polyethylene glycol (PEG) coats the positively charged polyplexes via electrostatic interaction and prolongs their circulation half-life in the blood stream [217, 263, 264].

Moreover, coupling of plasmid containing a therapeutic gene to the receptor specific ligands could achieve targeted gene delivery [265]. Thus, the ligand-DNA complex will bind specifically to cells that express the surface receptors for this ligand. The ligand-DNA complex reaches the endosomal compartment after binding and subsequent receptor-mediated endocytosis. The complex will be subjected to lysosomal degradation if it does not escape the endosome. Therefore, an inducer for endosomal lysis such as polyethylenimine (PEI) has to be included in the complex to achieve efficient gene expression [5].

The epidermal growth factor (EGF) was extensively used as a ligand because its receptors are overexpressed in many human tumors [260, 266, 267] including non-small cell lung cancer (NSCLC) tumor cells [268-273] and hepatocellular carcinoma [274]. In small cell lung cancer (SCLC) cell lines express low levels of EGF receptor [272, 275].

Moreover, Porebska et al. [276] found that the epidermal growth factor (EGF) receptors are overexpressed in colorectal adenocarcinomas and adenomas. EGF receptors were found to be overexpressed also in glioblastoma and lung, liver, breast, head, neck and bladder cancers [277].

The objective of the present investigation was to assess the gene expression in the lung tissues of BXB-23 mice and to examine the transfection of the adenoma foci cells. For this purpose two constructs were utilized. One of them was a polyethylenimine (PEI)-based DNA complex which was shielded by covalent attachment of polyethylene glycol (PEG) and further conjugated with the epidermal growth factor (EGF) as a cell-binding ligand (PEI/PEG/EGF). The other was a polyethylenimine (PEI)-based DNA complex which was only conjugated with the epidermal growth factor (PEI/EGF). LacZ (β -galactosidase) was used in the present experiment in both cases as a reporter gene (see experimental procedures 3.8.6.2).

Four BXB-23 mice were injected slowly into the tail vein once either with PEI/PEG/EGF/DNA complex or PEI/EGF/DNA complex (250 μ l/mouse) which contained 50 μ g LacZ DNA at N/P 6 (see experimental procedures 3.8.6.3). A placebo group (n = 4) was injected with 250 μ l HBG. The mice were anesthetized 24 h after the injection then the mice were scarified, sequentially the lungs were perfused and stained with X-gal solution then embedded in Tissue-tek (OCT) to get the frozen lung tissues (see experimental procedures 3.8.4.5). The frozen lung tissues of BXB-23 mice 24 h after injection showed LacZ expression after X-gal staining (Figure 37).

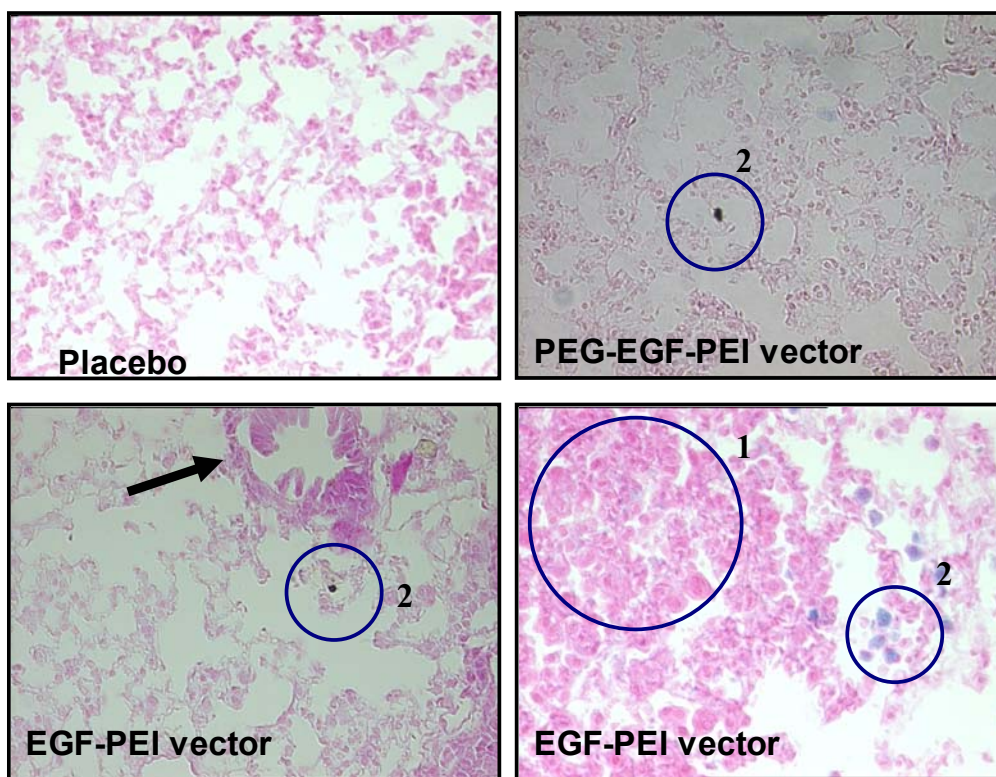


Figure 37: β -galactosidase (LacZ) expression 24 h after single tail vein injection of 50 μ g pSV40- β gal complexed with two polyplexes either PEI/PEG/EGF or PEI/EGF. Placebo mice group was injected with 250 μ l HBG only. After scarification of the mice, the lungs were perfused and stained with X-gal then frozen in OCT. The tissues were counterstained with eosin for the cytoplasm. β -galactosidase expression was visualized under a light microscope (n = 4), (Original magnification 40 \times). Black arrow represents the bronchial epithelium, blue circles represent the adenoma foci (1) and alveolar region (2).

The lung tissues revealed low and heterogeneous clustered LacZ expression in the alveolar region and no expression was detected in the adenoma foci after using of the two

constructs (Figure 37). It can be concluded that the total transfection activity was rather poor using these two polyplexes. The low transfection efficiency in case of using PEI/PEG/EGF polyplex could be due to the PEG shield, which can interfere with the transfection process [278]. Also, Blessing et al. [260] suggested that PEGylated epidermal growth factor containing complexes showed reduced affinity for the lung compared to nonmodified PEI/DNA complexes. The other explanation for the low LacZ expression could be due to the absence of the EGFR in the adenoma foci in the lung tissues of BXB-23 mice. To investigate this possibility it was necessary to examine the epidermal growth factor receptors expression in the adenoma foci.

2.13.2.4 Immunohistochemical detection of EGF receptors in BXB-23 mice lung and adenoma foci

The objective of the present immunohistochemistry study was to examine the EGF receptor (EGFR) expression in the tumor foci of the BXB-23 mice lung. Paraffin-embedded lung sections from BXB-23 mice were deparaffinized (see experimental procedures 3.8.6.4). The slides were incubated with primary anti-EGFR antibody and biotinylated secondary goat anti-rabbit antibody. The slides were examined for expression of EGFR under the light microscope. Some lung tissues were stained in the same manner without incubation with the anti-EGFR antibody and were considered as a negative control to exclude the background effect and determine the anti-EGFR antibody specificity. Hsieh et al. [279] showed that the epidermal growth factor receptors (EGFR) were mainly expressed in the bronchial epithelium. Therefore, the positive control in the present study was the bronchial epithelium of the BXB-23 stained lung tissues. Representative tissue slices are shown in Figure 38.

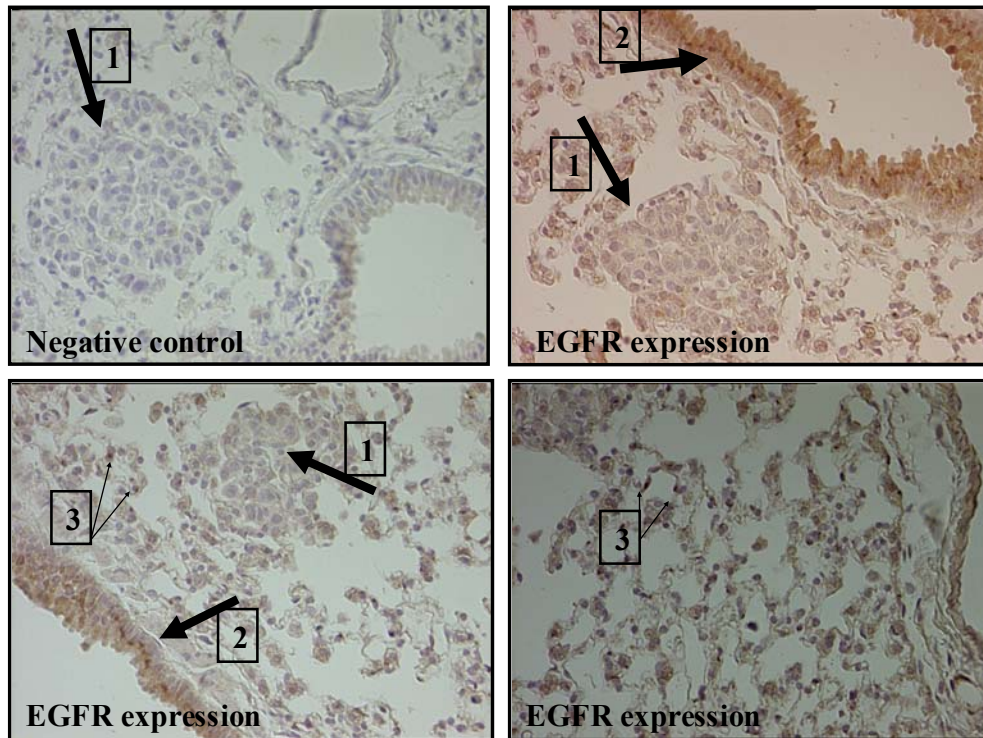


Figure 38: Expression of EGFR in the lung of BXB-23 mice. The EGFR expression was assayed immunohistochemically by using an anti-EGFR antibody. The lung tissues were examined under the light microscope. Negative control section was immunostained in the same manner except the antibody and stained negatively for EGFR. The bronchial epithelium is considered as a positive control which stains positively for EGFR (brown staining) arrows (2). EGFR expression is observed in the alveoli, arrows (3). No EGFR expression can be seen in the adenoma foci, arrows (1), (Original magnification 40 ×).

The immunohistochemistry staining of the lung tissues of BXB-23 mice revealed that no EGFR expression (brown colour) was observed in the adenoma foci and some expression was visualized in the alveoli, which was consistent with the previous results of the LacZ experiment 2.13.2.3. The absence of the EGFR expression in the adenoma foci (Figure 38) could explain the absence of the LacZ expression in the adenoma foci by using PEI/PEG/EGF and PEI/EGF polyplexes (Figure 37). Although the bronchial epithelium of BXB-23 mice showed EGFR expression (Figure 38), LacZ expression was not detected in the bronchial epithelium after tail vein injection of PEI/PEG/EGF and PEI/EGF polyplexes into BXB-23 mice (Figure 37). This result could be explained by targeting of these polyplexes to other organs, which highly express the EGFR. Additionally, the amount of LacZ which was used in the present study could be inadequate to produce an expression in the bronchial epithelium. Therefore, it can be concluded that the use of such constructs

which are based on conjugation of EGF as a ligand was not appropriate to generate gene expression in the adenoma foci of BXB-23 mice model.

3. Experimental procedures

3. Experimental procedures

A. Frequently used chemicals and materials

➤ Reagents used in HPLC method

Acetic acid (Grüssing, Filsum, Germany)

Acetonitrile, HPLC grade (Fisher Scientific, Schwerte, Germany)

Diethyl ether, HPLC quality (Fluka, Taufkirchen, Germany)

Methanol, HPLC grade (Merck)

Sorafenib (BAY 43-9006), provided by Prof. Rapp (Institut für medizinische Strahlenkunde und Zellforschung, Universität Würzburg)

Tolnaftate (Sigma)

➤ Reagents used in immunohistochemistry and histology

Absolute ethanol (Roth, Karlsruhe, Germany)

Biotinylated goat anti-rabbit immunoglobulins (DAKO, Glostrup, Denmark)

Bovine serum albumin (BSA) (Sigma, Steinheim, Germany)

Entellan, rapid mounting agent, combination of several synthetic resins (Merck, Darmstadt, Germany)

Formaldehyde (Roth)

Goat serum (Vector, Burlingame, CA, USA)

Hematoxylin and eosin (Merck)

Hydrogen peroxide, H₂O₂ 30 % (Roth)

Paraffin wax (Merck)

Tissue-tek OCT compound, is a cryostat specimen matrix for cryostat sectioning at temperature of -10 °C and below (Sakura, Zoeterwoude, the Netherlands)

Xylol (Roth)

B. Frequently used devices

Bath sonicator, USR 30 (Merck Eurolab, Germany)

Centrifuge, Biofuge 15 (Heraeus, Hanau, Germany)

Centrifuge, Biofuge A (Heraeus Christ, Osterode am Harz, Germany)

Centrifuge, Labofuge II (Heraeus Christ)
Coulter LS 230 (Coulter electronic GmbH, Krefeld, Germany)
Freeze dryer (Alpha II-12 Christ, Osterode am Harz, Germany)
Light microscope Eclipse TS 100 (Nikon, Düsseldorf, Germany)
Microwave (Siemens, Germany)
Paraffin embedding machine (Leica ASP 200, Bensheim, Germany)
pH meter (Heinse+Ziller, Würzburg, Germany)
Section cutting machine (Leica sections RM 2155)
Shaker Heidolph polymex 1040 (Schwalbach, Germany)
Thermocycler (Bio-med thermocycler 60, Theres, Germany)
Vortex mixer, Bender and Hobein AG (Zürich, Schweiz)
Vortex-Geniez (Scientific industries, Bohemia, USA)

C. Kits

AB complex (Avidin-Biotin, Vectastain[®], ABC Kit, Vector, Burlingame, CA, USA)
Enhanced Chemiluminescence (ECL reagent), western blotting detection reagent
(Amersham Biosciences, Buckinghamshire, England)
Qiagen Plasmid Maxi Kit (Qiagen, Hilden, Germany)

D. Solutions and buffers

➤ **DAB (diaminobenzidine) solution**

1 tablet contains 10 mg of DAB dissolved in 15 ml PBS and filtered, aliquots were kept frozen at -20 °C

3, 3' diaminobenzidine (DAB) (Sigma)

➤ **Blotting buffer**

Glycine 39 mM, Tris 48 mM, 0.037 % SDS and 20 % methanol in millipore water
pH 8.4

Glycine, Tris base and sodium dodecylsulfate (SDS) ultra pure (Roth)

Methanol (Applichem, Darmstadt, Germany)

➤ **Phosphate buffered saline (PBS)**

NaCl (137 mM), KCl (13.4 mM), Na₂HPO₄ (40.9 mM) and KH₂PO₄ (7.4 mM) in millipore water pH 7.4

Sodium chloride (NaCl), Potassium chloride (KCl), Disodium hydrogen phosphate (Na₂HPO₄) and Potassium dihydrogen phosphate (KH₂PO₄) (Roth)

➤ **Sodium citrate buffer 10 mM**

18 ml of 0.1 M citric acid and 82 ml of 0.1 M sodium citrate in 1 liter millipore water pH 6
Citric acid (Roth)

Sodium citrate (Merck)

➤ **SDS-PAGE running buffer**

25 mM Tris base, 250 mM glycine and 0.1 % SDS in millipore water pH 8.3

➤ **X-gal staining solution**

5 mM K₃Fe(CN)₆, 5 mM K₄Fe(CN)₆, 2 mM MgCl₂, 0.02 % Nonidet NP-40, 0.01 % sodium deoxycholate and 1 mg/ml X-gal in PBS. X-gal stock solution (20 mg/ml) in DMF was aliquoted and stored at -20 °C in darkness

Potassium ferrocyanide K₃Fe(CN)₆ and potassium ferricyanide K₄Fe(CN)₆ (Sigma)

Magnesium chloride hexahydrate (MgCl₂) (Roth)

Nonidet NP-40 (Fluka)

Sodium deoxycholate (Roth)

X-gal, 5-Bromo-4-Chloro-3-Indolyl-β-D-Galactopyranosid (Roth)

➤ **TBST buffer (Tris buffered saline plus tween)**

Tris base 50 mM, NaCl 150 mM and 0.05 % Tween 20 in millipore water pH 7.4

Tween 20 (Roth)

➤ **TBS buffer (Tris Buffered Saline)**

Tris base 50 mM and NaCl 150 mM in millipore water pH 7.4

➤ **Blocking buffer**

5 % (w/v) of non-fat dry milk in TBST buffer

Non-fat dried milk (Applichem)

➤ **Stripping buffer**

5 ml of 625 mM Tris-HCL solution, 5 ml of 20 % SDS solution and 0.8 ml of 12.8 M β -mercaptoethanol and complete to 50 ml with distilled water

Tris-HCl (Roth)

β -Mercaptoethanol (Sigma)

➤ **5 \times SDS-loading Buffer (for SDS-PAGE)**

31 mM of Tris-HCl (pH 6.8), 1% SDS, 5 % Glycerol, 2.5 % β -mercaptoethanol and 0.05 % Bromophenolblue in water

Glycerol (Roth)

Bromophenolblue (Sigma)

➤ **OTG lysis buffer (for cell culture)**

1 % N-Octyl- β -, D-thioglucopyranoside, 1M CaCl₂ and 1 tablet complete mini in 10 ml PBS

Complete mini tablets (protease inhibitor cocktail) (Roche, Mannheim, Germany)

N-Octyl- β -, D-thioglucopyranoside OTG (Gerbu biotechnik, Gaiberg, Germany)

➤ **Hepes buffered glucose (HBG)**

20 mM HEPES (pH 7.3). For isomolarity glucose was added to a final concentration of 5 % (w/v), sterile filtration was needed and then it was stored frozen in aliquots

HEPES (Sigma)

Glucose (Sigma, Louis, USA)

➤ **Hepes buffered saline (HBS)**

20 mM HEPES (pH 7.3) and 150 mM NaCl, sterile filtered or autoclaved

➤ **Ketamine anaesthetic solution**

Rompun® 2 % (50 µl), Ketanest® (250 µl) and the volume was completed to 1 ml with millipore water

(S)-ketamin hydrochloride 25 mg/ml (Ketanest® S) (PARK-Davis and Pfizer, Karlsruhe, Germany)

Xylazinhydrochloride (Rompun® 2 %) (Bayer, Leverkusen, Germany)

➤ **Bacterial culture medium LB (Luria-Bertani Broth) medium**

25 gm LB Broth powder to 1 liter distilled water

LB Broth powder (Sigma)

➤ **DNA isolation buffers**

a. P1 Buffer (resuspension buffer)

50 mM Tris-HCL

10 mM EDTA (Sigma)

10 µg/ml RNaseA, pH 8.8

RNaseA (Roche, Mannheim, Germany)

b. P2 Buffer (lysis buffer)

10 % SDS

200 mM NaOH (Sigma)

c. P3 Buffer (Neutralization buffer)

3 M potassium acetate, pH 5.5

Potassium acetate (Sigma)

d. QBT Buffer (Equilibration buffer)

15 % ethanol

0.15 % Triton X-100 (Applichem biochemical)

e. QC Buffer (wash buffer)

2 M NaCl

50 mM MOPS (3-(N-morpholinopropanesulfonic acid) (Sigma), pH 7

15 % ethanol

f. QF buffer (Elution buffer)

1.25 mM NaCl

50 mM Tris-HCl, pH 8.5

15 % ethanol

g. TE buffer (Tris EDTA)

10 mM Tris adjusted to pH 8 with HCl

1 mM EDTA

Hydrochloric acid (Roth)

➤ **1 × Tris-Acetate-EDTA (TAE)**

40 mM Tris-HCl,

40 mM acetic acid (Sigma)

2 mM EDTA, pH 7.8

➤ **10 × DNA gel loading Buffer**

40 % (w/v) sucrose (Applichem)

0.25 % bromphenolblue (Sigma)

0.25 % xylene cyanol (Roth)

➤ **LB (Luria-Bertani) medium for agar plates**

10 g/L Bacto-tryptone (Roth)

10 g/L NaCl (Roth)

5 g yeast extract (Life Technologies, Inc)

15 g Bacto-agar (Roth)

3.1 Preparation of sorafenib (BAY 43-9006) emulsions

3.1.1 Materials and devices

Gum arabic powder (Aldrich, Taufkirchen, Germany)

Olive oil DAB (Fluka)

Water, millipore quality

3.1.2 Preparation of an emulsion containing 2 mg/ml sorafenib

The preparation of the emulsion was performed according to Ph. Helv. VI Band III.

The drug sorafenib (2 mg) was dissolved in 200 mg olive oil by vortexing for 10 min and subsequent sonication for 15 min. Then 100 mg gum arabic was supplemented to the oil phase and mixed well with a pestle before 200 μ l of water was added portionwise under vigorous mixing until a homogenous emulsion was formed. The pH was adjusted to pH 7.0 with 0.1 N NaOH and water was added to reach the final volume of 1 ml (the final oil content was 20 %). The emulsion was sonicated for 15 min with continuous shaking to get the final white homogenous emulsion. The particle size in the emulsion, as determined under the light microscope, was approximately between 4.5–9 μ m.

3.1.3 Preparation of an emulsion containing 20 mg/ml sorafenib

The emulsion was prepared according to 3.1.2 except that 20 mg sorafenib were suspended in 300 mg olive oil before adding 150 mg gum arabic. The final oil content was 30 %. The particle size was also between 4.5–9 μ m.

3.2 Treatment of mice with sorafenib emulsions p.o.

3.2.1 Animals

The wild type mice were of C57Bl6 strain and the transgenic mice were of SP-C-craf BXB-23 strain. All mice, male and female, were 3 months old and their weight was between 20-30 g. The mice were provided by Prof. Rapp and bred in his institute according to Fedorov et al. [72]. The generation of Raf transgenic mice was achieved as described before [71].

3.2.2 Pharmacokinetic experiment

Wild-type mice were tube-fed once with 100 μ l of the low dose emulsion described under 3.1.2 (total dose 0.2 mg/mouse) or the high dose emulsion described under 3.1.3 (total dose 2 mg/mouse). Blood was drawn after 2 h from the tail and after 24 h following sacrifice of the mouse.

The samples were left at room temperature for 10 min and centrifuged at $1880 \times g$ for 5 min. The serum was kept frozen at $-20\text{ }^{\circ}\text{C}$ until analysis. Accordingly, a mouse was fed with 100 μ l plain, drug free emulsions for control.

3.2.3 Pharmacological effect of sorafenib emulsion

a. Transgenic drug treatment group

Six transgenic mice were tube-fed with 100 μ l of the high dose emulsion described under 3.1.3 (total dose 2 mg/mouse) every second day for one month. At the end of the treatment period all the mice were sacrificed and the blood samples were collected, left for 10 min at room temperature and centrifuged at $1880 \times g$ for 5 min. Then the serum samples were stored at $-70\text{ }^{\circ}\text{C}$ until analysis. The lung was isolated and weighed. A part of it was kept in 4 % formaldehyde in PBS. Another part was frozen in liquid nitrogen.

b. Transgenic placebo treatment group

Six transgenic mice were tube-fed with 100 μ l/mouse from the plain emulsion (o/w), containing 30 % olive oil every two days for one month. Further treatment of the animals as described above.

c. Transgenic control group

Five transgenic mice were considered as a control group without any oral administration of drug-containing or plain emulsion.

3.3 HPLC analytics of sorafenib in serum samples

3.3.1 Materials and devices

Mouse serum (Sigma, Taufkirchen, Germany)

Rotating wheel, diameter of 340 mm (self made by in-house technicians)

3.3.2 Samples preparation

To 30 μ l of blank mouse serum, standard calibration or 30 μ l unknown samples 6 μ l of the working internal standard solution tolinaftate was added to obtain a final concentration of 1800 ng/ml. The concentration of the stock solution of tolinaftate in methanol was 3 mg/ml. Sorafenib concentrations in the working standard solutions chosen for the calibration curve were 60, 150, 300, 500, 1000, 1500, 2000 ng/ml by adding 4 μ l from a concentrated stock solution of sorafenib in methanol (1 mg/ml) to the mouse serum. After vortex-mixing, 30 μ l acetonitrile was added to precipitate proteins. Subsequently, all samples were centrifuged at $7833 \times g$ for 10 min (Biofuge A). The supernatant was transferred into glass centrifuge tubes and 1 ml millipore water was added. The mixture was successively extracted twice with each 3 ml diethyl ether.

After every addition of ether the centrifuge tubes were shaken for 20 min at room temperature using rotating wheel (10 rounds/min), centrifuged for 2 min (Labofuge II), at $1000 \times g$. The ether layer was transferred into a 5 ml flask and the collected ether layers from both extractions were evaporated to dryness under a stream of nitrogen at 25 °C. The residue was reconstituted in 60 μ l methanol.

3.3.3 HPLC conditions

The HPLC system consisted of auto sampler (Waters 717 plus), a Binary HPLC pump (Waters1525) and a Waters 2487 Dual λ absorbance detector (Waters, Eschborn, Germany). Data acquisition and analysis was performed using the Breeze[®] software package (Waters). Chromatographic separation was carried out on a reversed phase C18 column (Symmetry[®] C18, 5 μ m, 4.6 \times 150 mm HPLC column). The mobile phase was a linear gradient programme using the following conditions: Solvent A (acetonitrile) and solvent B (millipore water) which contained acetic acid (0.2 %) pH 4.0 (Table 8). The

pump pressure was limited to 4000.0 psi. The temperature of the injector was 10 °C. The temperature of the column was maintained at 25 °C. The detection wave length was set at 254 nm, the injection volume was 20 µl. The column was equilibrated for at least 30 min with the mobile phase at a flow rate 1 ml/min. For subsequent chromatograms, the conditions described in Table 8 from 35 min to 56 min were applied.

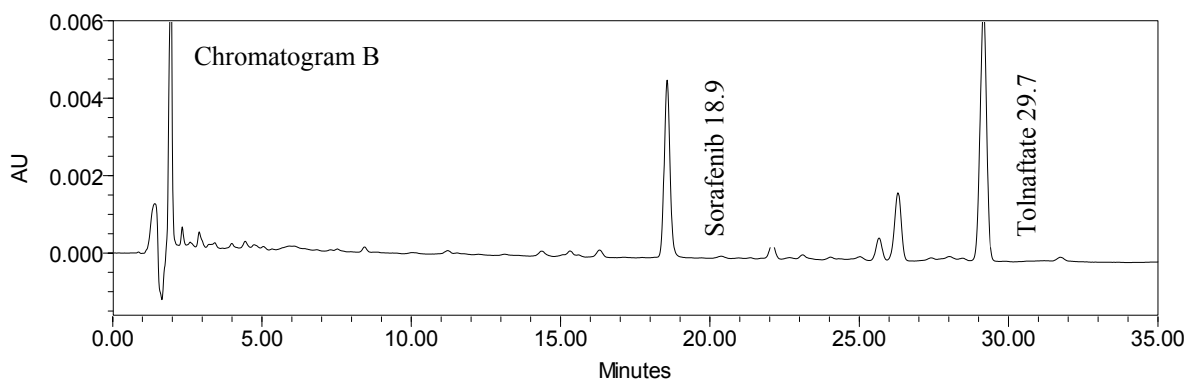
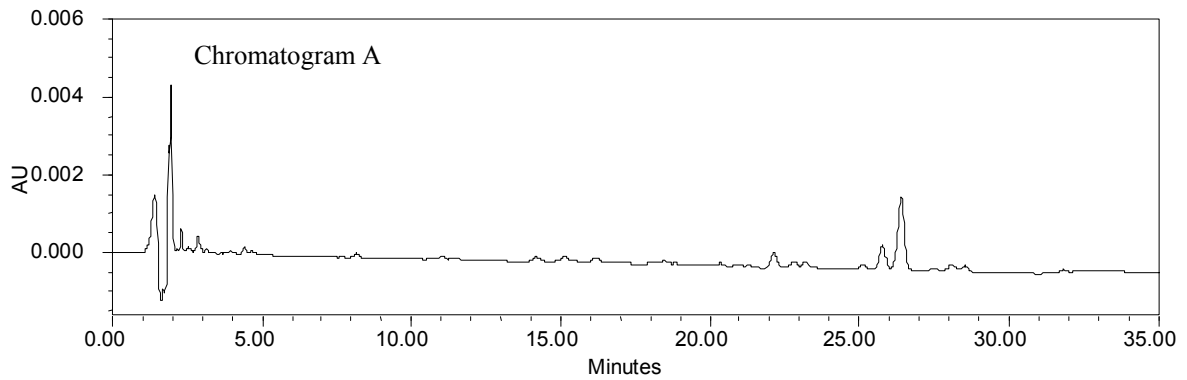
Table 8: Time table of HPLC gradient elution of sorafenib

Time (min)	Solvent A	Solvent B	Comment
0	40	60	Begin of linear gradient
35	71	29	End of chromatogram, return to 40/60
36	40	60	Begin of equilibration
56 = 0	40	60	End of equilibration, begin next chromatogram

3.3.4 Validation of the HPLC method

3.3.4.1 Selectivity

The selectivity of the method was examined by determining if interfering chromatographic peaks were present in blank mouse serum. Under the chromatographic conditions used for the analysis of sorafenib, the retention times for sorafenib and internal standard tolnaftate were 18.9 and 29.7 min, respectively. The total chromatography run time was 35 min. Our HPLC assay was found to be selective and free from other possible interferences. Representative chromatograms of blank mouse serum (chromatogram A) and spiked mouse serum with sorafenib and tolnaftate (chromatogram B) are shown below.



3.3.4.2 Linearity

Calibration standards were set up over the calibration range of 60-2000 ng/ml by adding known amounts of sorafenib to blank mouse serum prior to extraction. The ratios of peak area of sorafenib to that of internal standard and linear least-squares regression were conducted to determine the slope, intercept and correlation coefficient [280]. Calibration curves were linear over the concentration range used. Six calibration curves were constructed on six consecutive days in the range of 60-2000 ng/ml for sorafenib ($n = 7$), Table 9. The linearity of the calibration curve was demonstrated by the correlation coefficient (r^2) obtained for the regression line. The slope, the intercept of the regression line and coefficient of correlation were calculated for the whole data set. Representative results are listed in Table 9.

Table 9: Linearity data for sorafenib, calibration standard response values for a calibration curve range of 60-2000 ng/ml

The calibration curve	Slope	Intercept	R ²
1	0.00053	-0.0024	0.9942
2	0.00044	0.0635	0.9926
3	0.0005	0.0161	0.9902
4	0.00067	0.0081	0.9945
5	0.0004	0.0238	0.9933
6	0.0004	0.0231	0.9984
Mean	0.0005	0.0220	0.9938
SD*	0.0001	0.0225	0.0026

* Standard deviation of the mean

3.3.4.3 Accuracy and precision

Quality control (QC) samples containing sorafenib were prepared from weightings independent of those used for preparing calibration curves. Final concentrations of the QC samples were 100, 600 and 1800 ng/ml.

These samples were prepared on the day of analysis in the same way as calibration standards, see 3.3.2. The performance of the HPLC method was assessed by analysis of 18 quality control samples (six each of low (100 ng/ml), medium (600 ng/ml) and high (1800 ng/ml) concentrations) on a single assay day to determine intra-day accuracy and precision, and 15 quality control samples (five each for low, medium and high concentrations) on each five consecutive days to determine inter-day accuracy and precision [280].

Precision is expressed by relative standard deviation (RSD) in %. Accuracy is expressed in the following equation:

$$\text{Accuracy [\%]} = \frac{\text{calculated amount}}{\text{actual amount}} \times 100$$

The difference between the calculated and the actual concentration and relative standard deviation were not more than 15 % at any QC concentrations [281]. The results of the precision and accuracy for sorafenib are given in Table 10.

Table 10: Precision and accuracy of the method for determination of sorafenib in mouse serum

Concentration (ng/ml)	Mean	SD*	Precision RSD* (%)	Accuracy (%)
Inter-day (n = 6)				
100	94.6	2.79	2.9	94.6
600	692	68.55	9.9	115
1800	1813.8	101.94	5.6	100.7
Intra-day (n = 5)				
100	99.9	11.2	11.2	99.9
600	645.8	36.99	5.7	107.6
1800	1810.2	71.29	3.9	100.5

* Standard deviation of the mean

* Relative standard deviation

3.3.4.4 Sensitivity

The lower limit of quantitation (LOQ) was determined as the minimum concentration which can be accurately and precisely quantified [282]. The LOQ, defined in the presented experiment as the lowest plasma concentration in the calibration curve that can be measured routinely with acceptable precision (RSD < 20 %) and accuracy (80-120 %) was 80 ng/ml (Table 11).

Table 11: The limit of quantitation of the method for determination of sorafenib in mouse serum

Concentration (ng/ml)	Mean	SD*	Precision RSD* (%)	Accuracy (%)	Difference (%)
Inter-day (n = 6)					
80	84.7	15.2	17.9	105.8	5.87

* Standard deviation of the mean

* Relative standard deviation

3.3.4.5 Relative recovery

The recovery was quantified by the ratio of the slopes of the six calibration curves for extracted to non-extracted samples [282] Table 12.

Table 12: Recovery study for sorafenib (by ratio of slopes). The calibration curves were (n = 6) for each of the standard curve and extraction curve

	Standard curves	Extraction curves
Intercept	0.0055	0.024
Slope	0.000406	0.000379
Correlation coefficient (<i>r</i>)	0.9994	0.9933
Recovery by ratio of slopes	= 0.000379/0.000406 = 93.3 %	

3.3.4.6 Extraction efficiency

To determine extraction efficiency [283], mouse serum samples were spiked with sorafenib to achieve a final concentration of 100 and 1800 ng/ml. Six samples were extracted and analyzed for each concentration. Extraction efficiency was calculated according to the following equation:

$$\text{Extraction efficiency [\%]} = \frac{\text{peak area extracted sample for } \times \text{ ng/ml}}{\text{peak area neat sample for } \times \text{ ng/ml}} \times 100$$

Sorafenib peak areas were proportional over the mouse plasma concentrations ranges from 60-2000 ng/ml. Mean absolute recoveries of sorafenib from mouse plasma at concentrations of 100 and 1800 ng/ml were $71.8 \pm 6.25 \%$ and $74.2 \pm 8.52 \%$, respectively.

3.4. Histopathological evaluation of lungs from SP-C-craf BXB-23 mice

3.4.1 Materials

PCNA (Proliferating Cell Nuclear Antigen) antibody, mouse polyclonal antibody (Pharmlingen, Germany)

Biotinylated rabbit anti-mouse immunoglobulins (DAKO)

Caspase-3 (ASP 175, 5A19), rabbit anti-mouse monoclonal antibody (Cell signaling, Frankfurt, Germany)

Rabbit serum (Vector)

3.4.2 Preparation and staining of the lung tissues

Mice were sacrificed, subjected to complete autopsy and both gross and microscopic examinations were conducted. The dissected tissue samples were fixed overnight in 4 % formaldehyde. Specimens were washed in PBS then in 70 % ethanol and embedded in paraffin. Sections (6-10 μm thick) were fixed, deparaffinated using 100 % xylol 2 \times 10 min, 100 % ethanol (dipping), 96 % ethanol (dipping), 70 % ethanol 10 min and 5 min in distilled water. Sections were rehydrated and subsequently stained with hematoxylin (0.1 % in water) 5 min, washed under running tap water for 5 min, stained with eosin (1 % in water) 1 min and dipped in tap water. Afterwards, the slides were dehydrated using 70 % ethanol (dipping), 96 % ethanol (dipping), 100 % ethanol 10 min, xylol 100 % 10 min and mounted with entellan.

For morphometric studies three to four pieces of the lungs were serially sectioned in their entirety. Lung sections were stained with hematoxylin and eosin and evaluated by light microscopy. The average number of foci for 1 mm^2 area of the lungs of transgenic mice was counted by recording the number of individual foci on each section in several frames [72] and tumor percent was calculated by dividing the foci areas by the whole area using high power field (40 \times).

3.4.3 Immunohistochemistry

3.4.3.1 Proliferation test (Proliferating Cell Nuclear Antigen) (PCNA)

This protocol was performed according to Fedorov et al. [72] with some modifications. Paraffin-embedded 6- μ m thick lung sections were deparaffinized using a series of xylol and ethanol as described above in 3.4.2, rehydrated with water 2-5 min, and microwaved 6 min in 10 mM sodium citrate buffer (pH 6). Subsequently, the slides were washed in PBS (3 \times 5 min) and then incubated for 30 min at room temperature in peroxidase blocking solution (1.5 % H₂O₂ in PBS). The slides were washed in PBS (3 \times 5 min) and placed in blocking solution in PBS (0.1 % Triton -X + 1 % BSA + 5 % rabbit serum) for 30 min at room temperature. The slides were incubated with primary antibody PCNA which recognizes a nuclear antigen in the proliferating cells (dilution 1:3000) in blocking solution at 4 °C overnight. Then the slides were washed in PBS and incubated for 90 min with biotinylated secondary rabbit-antimouse antibody (dilution 1:400) in blocking solution. Afterwards, the slides were rinsed in PBS, incubated at room temperature for 45 min with AB-complex (20 μ l of solution A plus 20 μ l of solution B in 1 ml of PBS, this complex must prepared 30 min before use) and rinsed with PBS. DAB reaction was done by incubating the slides 4 min in 1 ml DAB (diaminobenzidine) + 0.8 μ l 30 % H₂O₂. The reaction was stopped by distilled water, the slides were counterstained using hematoxylin (0.1 %) for 1 min, dehydrated using a series of ethanol and xylol as described before in 3.4.2 with subsequent mounting in entellan.

3.4.3.2 Caspase-3 staining for apoptosis

Paraffin-embedded 6 μ m thick lung sections were deparaffinized using a series of xylol and ethanol, rehydrated with water 2-5 min, and microwaved 6 min in 10 mM sodium citrate buffer (pH 6). Subsequently, the slides were washed in PBS (3 \times 5 min) and then incubated for 30 min at room temperature in peroxidase blocking solution (1.5 % H₂O₂ in PBS). The slides were washed in PBS (3 \times 5 min) and placed in blocking solution in PBS (5 % goat serum) for 30 min at room temperature. The slides were incubated with primary caspase-3 antibody (dilution 1:200) in blocking solution at 4 °C overnight. Then the slides were washed in PBS, incubated for 45 min with biotinylated secondary goat anti-rabbit

antibody (dilution 1:300) in the blocking solution, rinsed in PBS and incubated at room temperature for 30 min with AB-complex as described under 3.4.3.1.

3.5. Preparation and characterization of sorafenib liposomes

3.5.1 Materials and devices

➤ Reagents used in liposome preparation and characterization

Dialysis tubing, molecular weight cut-off (MWCO) of 12,000-14,000 (Sigma)

Maltose monohydrate (Merck)

t-Butanol 99.5 % (Grüssing)

1, 2-dilauroyl-sn-glycero-3-phosphocholine (DLPC) > 95 % purity (LIPOID GmbH, Ludwigshafen, Germany)

Phosphate buffered saline (PBS) (Biochrom AG, Berlin, Germany)

➤ Reagents used in cell culture and western blot analysis

6 well plates (Sarstedt, Newton, USA)

Acrylamide 30 %, TEMED (tetramethylethylenediamine) (Roth)

Ammonium peroxydisulfate, APS (Sigma)

Dimethylsulfoxide, DMSO (Sigma)

Dulbecco's Essential Medium (DMEM), fetal calf serum (FCS), penicillin and L-glutamine (GIBCO Invitrogen, Karlsruhe, Germany)

ERK2 C-14, rabbit polyclonal antibody (Santa Cruz biotechnology, California, USA)

Nitrocellulose membrane (Bioscience, Dassel, Germany)

Phospho-ERK Thr 202/Tyr 204, rabbit polyclonal antibody (Cell Signaling Technology, Frankfurt, Germany)

Ponceau S (Sigma)

Prestained protein ladder, Benchmark™, it consists of 10 proteins ranging in apparent molecular weight 10-190 kDa (Invitrogen, Germany)

X-ray film (Amersham Biosciences)

➤ Devices used

Cell culture incubator (Heraeus)

Cell culture microscope (Leica DMIL, Portugal)

Incubator used in dialysis assay (Mettler, Heinse + Ziller 400, Schwalbach, Germany)

Shaker (Bellco biotechnology, Newjersy, USA)

3.5.2 Procedure of liposome preparation

This procedure was done as described earlier [70, 106] with some modifications of the solvents used. 30 mg of sorafenib and 225 mg of DLPC (ratio 1:7.5) were dissolved in 15 ml *t*-butanol. The respective solution was frozen using liquid nitrogen and lyophilized in freeze dryer overnight. Subsequently, the dried lipid film was hydrated with pre-warmed 3 ml PBS pH (7.4) containing 225 mg maltose [284] at a ratio lipid:maltose 1:1 by weight to get a final drug concentration of 10 mg/ml. The mixture was incubated for 30 min in a water bath at a temperature above the lipid melting temperature (T_m) at 37 °C with intermittent vortexing to produce multilamellar vesicular (MLV) liposomes. The liposomal suspension was maintained for another hour in a water bath at 37 °C to anneal the liposome structure. Subsequently, the suspension was sonicated for 10 min using a bath sonicator to obtain small multilamellar vesicles (SMLV). The liposomal suspensions were freeze-dried. Liposome dispersions were added to glass drying vessels, and frozen in a freezer at – 20 °C then dipped in liquid nitrogen. The vessels were then attached to the freeze-dryer and dried for 24 h. The freeze-dried samples were stored at – 20 °C until required. Before use the freeze-dried liposomes were rehydrated with suitable volume of PBS to get final concentration of 10 mg/ml, followed by 2 min sonication mixing to redisperse the liposomes.

3.5.3 Characterization of the liposomal suspension

3.5.3.1 Particle size measurement

The morphology of the empty and drug loaded liposomal suspension was observed with light microscope using LWD 40X lens. The mean particle size and size distribution were measured by coulter counter [53, 115, 116].

3.5.3.2 Determination of encapsulation efficiency

To determine the amount of sorafenib not associated with liposomes, i.e., “free” drug in suspension, 1 ml suspension aliquot was centrifuged for 20 min at $7833 \times g$ and decanted [120, 122]. 500 μ l supernatant and standard calibration samples were extracted as described under 3.3.2. The drug content was analyzed by HPLC according to 3.3.3. The difference between the total drug amount in the preparation and the drug content in the suspension supernatant was calculated. Encapsulation efficiency was expressed as percent of the drug encapsulated by the lipid in the liposome.

3.5.3.3 Stability of the liposomal suspension

The blank and sorafenib loaded liposomal suspension were stored at 4 and 25 °C for one month and followed by visual and microscopic observation. Encapsulation efficiency was determined at the end of 15 and 30 days from the date of preparation [126] by HPLC (see 3.3.3). Liposomal suspension was treated as described above in 3.5.3.2. The content of sorafenib was then determined. Moreover, the particle size was examined by coulter counter.

3.5.3.4 *In vitro* release of sorafenib from liposomes in a dialysis assay

30 μ l loaded liposomal suspension, contains 300 μ g sorafenib, was placed into dialysis tubing with a molecular weight cut-off of 12,000-14,000. The dialysis tubing was placed into a beaker containing 1000 ml of PBS (pH 7.4). The liposomes were incubated with stirring for 24 h at 37 °C [118, 129]. At various time points (30 min, 2 h, 6 h and 24 h), 2 ml aliquots were withdrawn from the beaker for drug analysis. The Raf inhibitor sorafenib concentration was determined by HPLC (3.3.3).

The drug solution was also assayed in the same manner explained above as a control. The drug was dissolved in methanol/PBS mixture and the concentration of the drug in the solution was the same as in the liposomal suspension. The assay was carried out in similar manner as described above.

3.5.3.5 *In vitro* release of sorafenib in a cell culture assay

NIH3T3 mouse fibroblast (ATCC American type culture collection) cells were maintained in Dulbecco's Essential Medium (DMEM) supplemented with 10 % (v/v) fetal calf serum (FCS), 100 IU penicillin per ml, 2 mM L-glutamine in a humidified atmosphere of 5 % CO₂ at 37 °C. The cells were harvested with trypsin-EDTA and seeded in 6-well plates (2.5×10^5 per well) containing 2 ml medium per well and allowed to attach overnight. After this time the medium was discarded and the cells were washed well twice with PBS. The cells were starved by adding DMEM medium containing 0.05 % FCS for 48 h, incubating them at 37 °C and 5 % CO₂. 2 h before the end of starvation period different concentrations of the sorafenib loaded in the liposome or dissolved in DMSO were added. The cells were stimulated by adding 20 % FCS in the medium. The cells were incubated for 30 min, then the medium was removed and the cells were washed 2 times with PBS. The cells were lysed using OTG lysis buffer in PBS (150 µl/well).

3.5.3.5.1 SDS-PAGE and Western blot analysis (Detection of p-ERK inhibition by sorafenib)

The protein concentration of cell lysate was determined using the Bradford assay [285]. A volume of cell lysate stored at -20 °C and containing 20 µg proteins was mixed with 5 µl 5 × Laemmli buffer.

All samples were heated at 95 °C for 5-10 min in thermocycler. They were then resolved by SDS-PAGE (sodium dodecyl sulfate polyacrylamide gel electrophoresis)

The SDS complexes with the denatured proteins were electrophoresed on a polyacrylamide gel in the form of a thin vertical slab.

Vertical gels were set in between 2 glass plates (10 cm × 12 cm) with an internal thickness of 1.5 mm between the two plates. These gels composed of two layers (Table 13), the first layer (separating gel) contained 12 % acrylamide gel (pH 8.8) that separates the proteins according to their size while the second layer (stacking gel) contained 4 % stacking gel (pH 6.8) that insures the simultaneous entry of the proteins into the separating gel and the sharpening stacking of the protein bands. The separating gel was poured in between two glass plates, leaving a space of about 1 cm plus the length of the teeth of the comb and left to polymerise for at least 30 min at room temperature. Millipore water was added to the surface of the gel to exclude air and after the separating gel was polymerised, the water

was removed. The stacking gel was poured on top of the separating gel, the comb was inserted and the gel was allowed to polymerise.

Table 13: Composition of Western blot gels

Acrylamide gel 12 %	Stacking gel 4 %
Tris 750 mM pH 8.8 (5 ml)	Tris 250 mM pH 6.8 (2.5 ml)
Distilled water (1.1 ml)	Distilled water (1.8 ml)
Acrylamide stock 30% (3.9 ml)	Acrylamide stock 30 % (650 μ l)
Temed (3 μ l)	Temed (4 μ l)
Ammonium peroxydisulfate (APS) 10 % (100 μ l)	APS 10 % (37.5 μ l)

The samples were loaded into the wells of the gel and running buffer (1 \times SDS-PAGE) was added to the chamber. A cover was then placed over the gel chamber and 45 mA was applied. SDS is an anionic detergent that disrupts nearly all non-covalent interactions in native proteins and β -Mercaptoethanol was also included in the sample buffer to reduce disulfide bonds.

The proteins were transferred onto nitrocellulose membrane by electroblotting SDS-PAGE gels at 260 mA (semidry method). The filter papers and the nitrocellulose membrane used in the blotting step were prewetted with blotting buffer.

Ponceau S fixative dye solution was used to check if the transfer was successful by staining the membrane for 1 min with subsequent washing with water to remove the excess colour. For Western blot analysis, the membranes were incubated in blocking buffer for 1 h at room temperature or overnight at 4 °C on a shaker. The membrane was probed with polyclonal rabbit antibody directed against phospho-ERK (diluted in TBST buffer, 1:1000) and then incubated overnight at 4 °C. The membrane was washed three times with TBST each time for 10 min. Positive antibody reactions were visualized using peroxidase-conjugated anti-rabbit immunoglobulin as secondary antibody (diluted in TBST, 1:5000) for 45 min at room temperature and subsequent washing (3 \times 10 min) with TBST buffer.

Proteins were visualized by enhanced chemiluminescence's reaction (ECL) by incubating the membrane in 1:1 mix of ECL reagent 1 and 2. This reaction is based on a peroxidase

catalysed oxidation of Luminol which leads to emission of light photons that can be detected on X-ray film. Thus, a positive signal indicated that the peroxidase conjugated secondary antibody bound to the primary antibody to detect the protein of interest. The removal of the primary and secondary antibodies from a membrane (stripping) was possible, so that it could be reprobbed with alternative antibodies. The membrane was incubated in 50 ml stripping buffer for 1 h at 50 °C and then washed with TBST buffer (3 × 5 min). The membrane was reprobbed with ERK2 antibody as a loading control as described above. Protein band intensity was quantitated using Adobe shop program version 6. The inhibition percent was calculated in comparison with the placebo in which the cells were incubated with non-drug containing liposomes.

3.6. Treatment of mice with sorafenib liposome intratracheally

3.6.1 Animals and materials

B6D2F1 wild- type mice (n = 50), three months old female, weighting between 20-30 g.

BXB-23 transgenic mice (n = 40), C57Bl6 background, male and female, 4 months old and weighing 20-30 g.

Isoflurane (Uniklinikum Apotheke, Würzburg, Germany)

3.6.2 Pharmacokinetic experiment

The procedure of intratracheal instillation was done as explained in [286]. Wild type mice were anesthetized in a plastic cage with gauze containing isoflurane until the animals did not react upon a tactile stimulus. They remained unconscious throughout the entire instillation procedure and had no cough reflex upon intubation. The animals were placed on their dorsum on a restraining board at a 45° angle with a rubber band to hold the mouth open and the tongue was moved. A ball-tipped 24-gauge animal feeding needle fitted with an insulin syringe was passed into the trachea via the mouth. 50 µl of sorafenib loaded liposome suspension containing 1 mg sorafenib was slowly instilled once followed by five boluses of air. The animals remained in the slanted position for 1 min after instillation to facilitate distribution in the lungs. The animals were returned to the cage woke up within 1-2 min and observed until consciousness was regained. After recovery from anaesthesia the animals were returned to the animal quarters until analysis. Blood and lung samples

were collected after sacrifice of the mice after 2 h, 24 h, 48 h, 72 h and one week. The lungs were weighed, frozen in liquid nitrogen and kept frozen at $-70\text{ }^{\circ}\text{C}$ until analysis. The concentration of the sorafenib was determined in serum samples using the HPLC analysis method, see 3.3.3.

3.6.3 Pharmacological effects of sorafenib liposome

The BXB-23 transgenic mice were intubated using the same procedure described in 3.6.2. 50 μl liposome suspension containing 1 mg sorafenib or an equal volume of empty liposome per mouse was instilled three times weekly for three weeks. A group of mice was sacrificed every week, blood and lung samples were collected to analyze the drug concentration by HPLC. For histological analysis, part of the lung was fixed in 4 % formaldehyde, washed in PBS and placed in 70 % ethanol. After paraffin embedding, 6 μm sections were cut and stained with hematoxylin and eosin (H&E) as described in 3.4.2. Random pictures were taken of each specimen. The tumor percent, number of adenoma foci/ mm^2 and the ratio between the lung weight and mouse body weight were calculated. Subsequently, the immunohistochemistry for proliferation of the cells (PCNA) and the apoptosis test (caspase-3 assay) was done as explained before in 3.4.3.1 and 3.4.3.2, respectively. Positive cells in adenoma foci were counted and expressed as percentage of total adenoma cells.

3.6.4 HPLC analytics of sorafenib in lung samples

3.6.4.1 Samples preparation

The frozen lung tissues were milled using liquid nitrogen in small porcelain mortar with pestle to get homogenous fine powder.

To 40 mg of powdered lung tissue, standard calibration or unknown samples, 20 μl from concentrated stock solution (3 mg/ml) tolinaftate in methanol was added to obtain a final concentration of 150 ng/mg lung. Sorafenib concentrations in the working standard solutions chosen for the calibration curve were 10, 25, 50, 100, 150, 300, 500 ng/mg lung by adding 10-50 μl from a concentrated stock solution (1 mg/ml) in methanol to blank mouse lung powder. After vortex-mixing, 1 ml acetonitrile was added and all samples were extracted by vortex-mixing for 2 min. Subsequently, all samples were centrifuged at

7833 × g for 10 min. The acetonitrile layer was transferred into a 5 ml flask and evaporated to dryness under a stream of nitrogen at 25 °C. The residue was reconstituted in 100 µl methanol.

3.6.4.2 HPLC conditions

The HPLC system and conditions were described before in 3.3.3. For subsequent chromatograms, the modified conditions demonstrated in Table 14 from 20 min to 41 min were applied.

Table 14: Time table of HPLC gradient elution of sorafenib

Time (min)	Solvent A	Solvent B	Comment
0	55	45	Begin of linear gradient
20	80	20	End of chromatogram, return to 55/45
21	55	45	Begin of equilibrium
41 = 0	55	45	End of equilibrium, begin next chromatogram

3.6.5 Immunohistochemistry for multidrug resistance (MDR) in BXB-23 lungs

3.6.5.1 Materials

Biotinylnlated antibody, goat anti-mouse, immunoglobulins (DAKO)

C219, anti-MDR1 P-gp mouse monoclonal antibody (Innovative diagnostic-system, Hamburg, Germany)

Ethylenediaminetetraacetic acid-disodium salt, EDTA (Sigma)

Normal mouse serum (Sigma)

Streptavidin_{HRP}, Streptavidin linked to horseradish peroxidase (DAKO)

3.6.5.2 Immunohistochemistry protocol

Paraffin wax embedded tissues (2-3 μm thick) were dewaxed using a series of xylol and ethanol, rehydrated with water 2-5 min, microwaved (3×5 min) in Tris/EDTA buffer (pH 9) and was left to cool for 20 min. Subsequently, the slides were incubated for 10 min at room temperature in peroxidase blocking solution (3 % H_2O_2 in methanol) and then washed in TBS (3×5 min). The immunoreaction was done by incubating the slides in TBS buffer solution of the primary antibody (C219) in biotinylated secondary antibody (1:75) for 15 min (this immunoreaction was done to reduce the background, because the source of the primary antibody (C219) was mouse and used in the immunohistochemistry for mouse tissues). The reaction was blocked by incubating the slides in 10 % mouse serum in TBS for 45 min. Then the slides were washed in TBS, incubated at room temperature for 20 min with horseradish peroxidase (HRP) conjugated labelled streptavidin (1:300) in TBS. Afterwards, the slides were washed with TBS (3×5 min). DAB reaction was done by incubating the slides 10 min in 1 ml DAB (diaminobenzidine) + 0.8 μl 30 % H_2O_2 . The reaction was stopped by distilled water, the slides were counterstained using hematoxylin (0.1 %) for 2 min, dehydrated using a series of ethanol and xylol as described before in 3.4.2 and then mounted in entellan. Positive cells in adenoma foci were counted and expressed as percentage of all adenoma cells. This protocol was done according to Scheffer et al. [157] with some modification in the reagents used to reduce the background.

3.7 Preparation and characterization of sorafenib microspheres

3.7.1 Materials and devices

0.2 μm syringe filter (Sartorius, Hannover, Germany)

Beckman centrifuge model J2-21 (Beckman CoulterTM, Unterschleissheim-Lohhof, Germany)

Centrifuge microfuge 22 R (Beckman CoulterTM, Unterschleissheim-Lohhof, Germany)

Dichloromethane p.a (Fisher Scientific, Schwerte, Germany)

Maltose monohydrate (Merck)

Polyvinyl alcohol (PVA), 87-89 % hydrolyzed and average molecular weight 13.000-23.000 (Aldrich, Steinline, Germany)

Resomer[®] RG 502 S, poly (L-lactide-co-glycolide) (PLGA) 50:50 lactide: glycolide was a gift from Boehringer Ingelheim (Ingelheim am Rhein, Germany)

Scanning electron microscope (SEM) Zeiss DSM 962 (Carl Zeiss, Oberkochen, Germany)

Sputter coater SCD 005 (BAL-TEC GmbH, Witten/Ruhr, Germany)

Ultraturrax mixer (Janke and Kunkel GmbH KG, Staufen, Germany)

3.7.2 Preparation of sorafenib PLGA microspheres

Microspheres were prepared by emulsion-diffusion-evaporation method as described earlier [188, 189] with some modifications in the used solvent as shown in Figure 39.

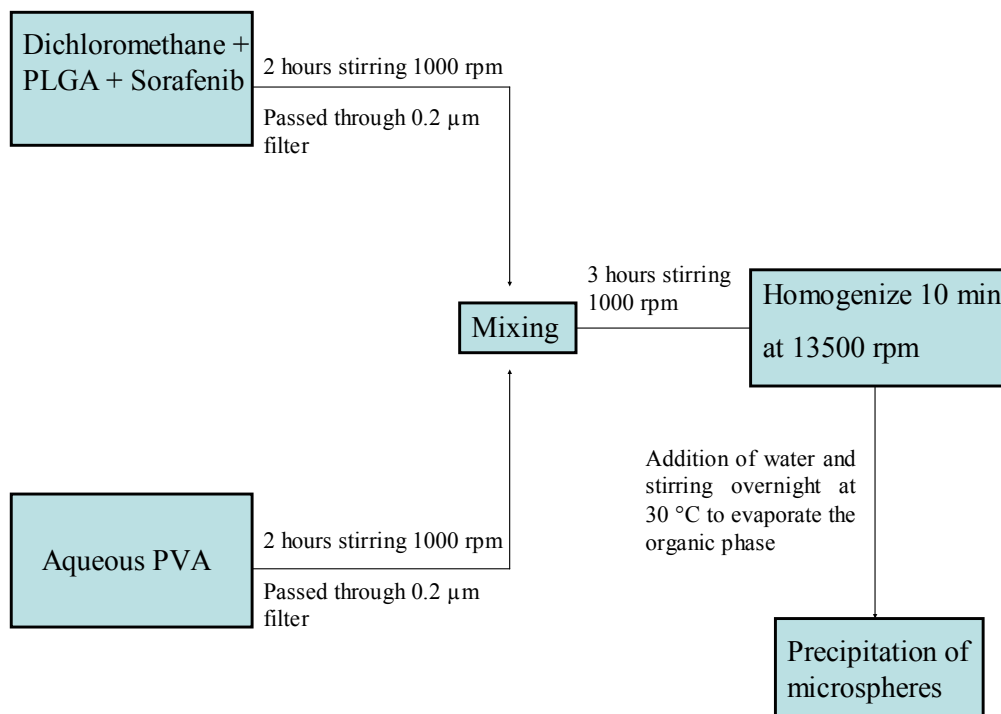


Figure 39: Schematic representation of PLGA microspheres preparation process.
 PLGA: poly (L-lactide-co-glycolide) PVA: Polyvinyl alcohol

The methodology was done as follows:

100 mg PLGA was dissolved alone or dispersed with 10 % sorafenib in 10 ml dichloromethane under stirring for 2 hours at room temperature then the organic phase was passed through 0.2 µm filter in case of plain microspheres preparation. The aqueous phase

contained 100 mg PVA in 10 ml water was also stirred for 2 hours at room temperature and then filtered through 0.2 μm filter. The organic phase was then added portionwise to the aqueous phase under stirring to obtain o/w emulsion. The emulsion was stirred at room temperature for 3 hours before homogenizing at 13500 rpm for 10 min in an ice bath using an Ultraturrax homogenizer. To precipitate the microspheres, 105.0 ml water was added to this emulsion. Stirring was continued on a water bath maintained at 30 °C to evaporate the organic solvent. The resulting suspension was centrifuged at $18000 \times g$ at 4 °C for 20 min. The pellets were washed two times with 15 ml water to remove the non-incorporated drug and PVA residue. The pellets were redispersed in 10 ml water by 1 min sonication. Maltose was added 0.1 % (w/v) to the suspension then the suspension was kept 2 hours at – 70 °C. The suspension was lyophilized overnight using the freeze dryer to get stable lyophilized powder.

3.7.3 Sorafenib microspheres characterization

3.7.3.1 Determination of particle size distribution

Particle size and size distribution of sorafenib-loaded and plain PLGA microspheres were measured using coulter counter LS 230 [176, 196, 197]. For measurement 1 mg of the lyophilized microspheres were resuspended in 1 ml distilled water. The apparatus was washed two times with isopropanol then several times with distilled water. After washing, it was a must to get rid of air bubbles then wait for calibration. Then the sample was added dropwise and the measuring was started. The results were reported as a volume size distribution by a computerized analysis.

3.7.3.2 Morphological studies of sorafenib microspheres

The shape and surface morphology of the sorafenib-loaded and plain PLGA microspheres was observed using the scanning electron microscope. The lyophilized microspheres were attached to holders. Furthermore, the specimens were coated with approximately 20 nm platinum/palladium using the sputter coater SCD 005. The surface morphology of the microspheres samples was then visualized under a scanning electron microscope (SEM) [192, 193] and digital images were recorded.

3.7.3.3 Determination of the actual drug loading and microspheres yield

The amount of non-incorporated sorafenib was determined by HPLC with UV detection set at 254 nm. The mobile phase consisted of acetonitrile:water and the flow rate was set at 1 ml/min. Separation was achieved using C18 column (Symmetry[®] C18, 5 μ m, 4.6 \times 150 mm HPLC column) as described earlier in 3.3.3. The supernatant (1 ml) was extracted two times with 3 ml diethyl ether (see 3.3.2). The free drug in the supernatant after microspheres preparation was determined (indirect method) [182] and then subtracted from the total amount of the drug added to the preparation. The percent was then calculated by dividing the result of subtraction to the total amount of the drug added. The percentage yield was calculated based on the amount of lyophilized microspheres of each formulation obtained to the amount of solid materials used in the dispersed phase (the PLGA or/and sorafenib) [178, 287].

3.7.3.4 *In vitro* release study of sorafenib from the microspheres preparation

The *in vitro* release study of sorafenib microspheres was done according to Hombreiro-Perez et al. [186] with some modification in the procedure strategy. The *in vitro* drug release from microparticles was studied in phosphate buffer pH 7.4, containing 0.01 % (w/v) tween 80 to increase the solubility of the poorly water-soluble drug sorafenib and the wettability of the microparticles in the dissolution medium. Accurately weighed amounts of the sorafenib loaded microspheres (10 mg) were suspended in 4.0 ml PBS and then 1.0 ml from this suspension containing 250 μ g sorafenib was withdrawn and transferred into 250.0 ml PBS. The phosphate buffer kept constant at 37 $^{\circ}$ C and stirred at 100 rpm. At predetermined time intervals, 1.5 ml samples were withdrawn (replaced with fresh medium), centrifuged at 4 $^{\circ}$ C 10 min at 13000 \times g. 1 ml supernatant was extracted with diethyl ether and analyzed with HPLC for sorafenib. The experiment was performed for three different batches in duplicate for each batch. The drug solution (250 μ g sorafenib dissolved in methanol) was assayed in the same manner and considered as a control. The *in vitro* release study for sorafenib solution was done in phosphate buffer containing 0.01 % tween 80 and the procedure was continued as described above.

3.8. *In vivo* application of transfection complex of a reporter gene using different vectors and different routes in tumor bearing BXB-23 mice

3.8.1 Materials and devices

➤ **Devices used**

Bacterial incubator (Heraeus B 6200)

Bacterial shaker (New Brunswick Scientific innova 4330, Nürtingen, Germany)

Centrifuge, Megafuge 1.0 R (Heraeus)

Cryosection cutting machine (Leica CM 1900)

Mega centrifuge (Sorvall, RC 5 B plus, Newtown, USA)

Microtome laser microscope (Leica CTR MIC)

UV visible spectrophotometer, ultrospec 3000 (Pharmacia Biotech, Uppsala, Sweden)

➤ **Reagent used in maxi-preparation of plasmid DNA**

Agar plates (Qbiogene, Heidelberg, Germany)

Agarose ultra pure and Ethidium bromide (life technologies, Inc)

Ampicillin (Sigma)

DH5 α , bacterial strain optimised for DNA transformation and replication (Bethesda Research Laboratories)

Isopropanol (Merck)

➤ **Reagents used in X-gal staining**

Dimethylformamide, DMF (Fluka, Steinheim, Germany)

Glutraldehyde (Roth)

Heparin sodium (Applichem)

Moviol, aqueous fluorescence mounting medium (Calbiochem, Darmstadt, Germany)

➤ Cationic vector and plasmids used

Linear polyethylenimine 22 kDa (PEI 22 lin solution 1 mg/ml) was obtained as a gift from Dr. Ogris (Department of Pharmacy Ludwig-Maximilians-Universität, München, Germany).

Plasmid coding GFP (Green Fluorescent Protein) pEGFPN1 (Clontech, Germany)

Plasmid coding β -galactosidase, CH10 LacZ, pSV40 promoter (Pharmacia, Germany)

3.8.2 Preparation of the transfection complex

This preparation procedure was done according to Kircheis et al. [278]

Plasmid DNA (200 μ g/ml) was mixed with the linear polyethylenimine (PEI 22 kDa) at molar ratio of PEI nitrogen to DNA phosphate (N/P) = 6 (40 μ g PEI per 50 μ g DNA).

Two solutions were prepared:

1) 200 μ g DNA diluted to 500 μ l with HBG (Hepes buffered glucose)

2) 156 μ g PEI diluted to 500 μ l with HBG

The PEI solution (2) was added to the DNA solution (1), mixed 10 times immediately with pipette. The complex had to be prepared 30 min-120 min before the injection.

3.8.3 Determination of GFP (Green Fluorescent Protein) reporter gene expression after systemic application via tail vein

3.8.3.1 Animals

BXB-23 transgenic mice (C57Bl6 background) were of 7 weeks of age, female, weighing between 15-20 g.

3.8.3.2 *In vivo* transfection efficiency in tumor bearing lungs using PEI (polyethylenimine)/GFP complex

Two groups of mice each group (n = 4) were injected once slowly into the tail vein with 250 μ l/mouse of the transfection complex (GFP/PEI in HBG buffer) which contained

50 µg of GFP DNA. One group was anesthetized after 24 h and the second group was anesthetized after 48 h using 300 µl/mouse ketamine solution intraperitoneally. A third group of mice (n = 4) was injected twice with 15 min interval between the two injection and the mice were anesthetized after 24 h. Another group of mice (n = 4) was injected with 250 µl of HBG and considered as a placebo.

The mice were scarified and lungs were perfused through the left ventricle of the heart with PBS for 10 min and then with 4 % formaldehyde in PBS for 10 min. The lungs were isolated and fixed in 4 % formalin overnight then transferred to 30 % sucrose solution in PBS and left overnight at 4 °C. The lungs were frozen by embedding them in tissue-tek (OCT compound) using dry ice and kept frozen at -70 °C. The tissues were not paraffin-embedded because GFP fluorescence is lost during treatment with organic solvents [288]. The cryosections (20 µm cut) were dried at room temperature for 30 min, fixed on the slides for 15 min in 4 % formalin in PBS, washed (3 × 5 min) in PBS, washed in water 5 min then mounted with moviol. The slides were examined for the green fluorescence by microtome microscope using I3 filter.

3.8.4 Determination of LacZ (β -galactosidase) reporter gene expression after systemic application via tail vein

3.8.4.1 Maxi-preparation of plasmid DNA (LacZ)

100 µl of (DH5 α) competent cells (these cells were prepared as described before [289]) were thawed on ice, followed by addition of 10 ng LacZ DNA and the mixture was incubated on ice for 30 min. Heat shock transformation of cells was performed at 42 °C in water bath for 90 seconds. The cells were returned to ice for 2 min and 900 µl LB medium without antibiotic was added. The cells were shaken using bacterial shaker at 200 rpm for 1 h at 37 °C. Selection of the transformed bacteria was done by plating 100 µl of the bacterial suspension on antibiotic (ampicillin) containing agar plates followed by incubation at 37 °C overnight for 16 h. Only bacteria that took up the desired plasmids, which contain an ampicillin resistance cassette, grow on the agar plates. A single colony was then be expanded in LB medium and used for DNA preparation.

One colony from the plate was picked. The bacteria were grown in 3 ml LB medium containing ampicillin (final concentration 100 µg/ml) at 37 °C in bacterial shaker at 200 rpm for 6 h. 250 µl from this cell suspension was transferred in a big volume of LB

medium (250 ml) containing ampicillin (final concentration 100 µg/ml) and the cells were grown overnight for 16 h at 37 °C with shaking.

The bacteria were collected by centrifugation and plasmid DNA was isolated by using a Qiagen Plasmid Maxi Kit. This extraction method is based on Birnboim's alkali lysis principle [290]. The bacterial pellets were resuspended in 10 ml of buffer P1, buffer P2 (10 ml) was added, gently mixed and incubated at room temperature for 5 min. 10 ml of chilled buffer P3 was added, immediately mixed, incubated on ice for 20 min and centrifuged at 12.000 rpm for 30 min at 4 °C. The supernatant was filtered over a pre-wetted folded filter paper, applied to equilibrated Qiagen-tip 500 column and allowed to enter the resin by gravity flow. The Qiagen-tip 500 was washed twice with buffer QC and DNA was eluted with 15 ml buffer QF. These processes result in the isolation of a DNA-salt pellet which was precipitated by addition of isopropanol (10.5 ml) and subsequent centrifugation at 4000 rpm for 30 min. The resulting pellets were washed twice with 70 % ethanol and dried on air at room temperature. The pellets were then carefully resuspended in TE buffer (pH 8).

3.8.4.2 Measurement of DNA concentration

The DNA concentration was determined by UV spectrophotometry at 260 nm. The absorption of OD (optical density) = 1 at 260 nm corresponds to a concentration of 50 µg/ml double stranded DNA.

Identity, integrity and possible purity of the DNA were subsequently analysed on an agarose gel. Purity of the DNA was determined by the ratio $OD_{260}/OD_{280} = 1.6$.

3.8.4.3 Electrophoresis of DNA on agarose gel

Double stranded DNA fragments with lengths between 0.5 kb and 10 kb can be separated according to their lengths on agarose gels. Agarose was added to 1 × TAE to obtain a final concentration between 0.7-2 %. The suspension was boiled in the microwave until the agarose was completely solubilised. The agarose was allowed to cool down to around 50 °C and then the ethidium bromide was added to obtain concentration of 0.5 µg/ml. The mixture was poured into the gel apparatus. DNA gel loading buffer was added to the DNA sample and applied on the gel. Electrophoresis was done at 100 volts. The DNA was visualised under UV-light.

3.8.4.4 Animals

Three months old, female BXB-23 transgenic mice (C57Bl6 background), weighting between 20-30 g.

3.8.4.5 *In vivo* transfection efficiency in tumor bearing lungs after intravenous injection of PEI/LacZ complex

The mice (n = 5) were injected once slowly into tail vein with cationic vector/DNA complex (250 μ l/mouse) containing 50 μ g LacZ DNA which was prepared as described in 3.8.2 using N/P ratio of 10 [238, 253]. A placebo group (n = 4) was injected with 250 μ l HBG (Hepes buffered glucose). Mice were anesthetized 24 h after injection using 300 μ l/mouse ketamine solution intraperitoneally (i.p.). The mice were scarified and the lung was perfused through the left ventricle of the heart with 5 mg/l heparin in saline 10 min, 2 % formaldehyde in PBS, saline 10 min and β -galactosidase solution 10 min. After perfusion, the lungs were dissected and the β -galactosidase reaction continued for 48 h by immersion in the X-gal staining solution in PBS at 30 °C as described earlier [236]. After staining the lungs were immersed overnight in 30 % sucrose in PBS. Then the lungs were embedded in tissue-tek (OCT) and frozen at -70 °C, this embedding was performed according to Bragonzi et al. [250].

Cryosections (8-10 μ m) were cutted using tissue tek cryostat at -20 °C and placed into glass slides. The sections were fixed for 10 min with 0.2 % glutaraldehyde and 2 % formaldehyde for 10 min, washed with PBS (3 \times 5 min) and placed in water for 5 min. The slides were stained with eosin for 2 min, mounted with moviol and examined under the light microscope.

3.8.5 Determination of LacZ reporter gene expression after intratracheal instillation

3.8.5.1 Animals

BXB-23 transgenic mice (C57Bl6 background), three months old female, weighting between 20-30 g.

3.8.5.2 *In vivo* transfection efficiency in tumor bearing lungs after intratracheal instillation of PEI/LacZ complex

The mice (n = 5) were instilled slowly once via the trachea with 150 µl transfection complex/mouse. This complex contained 50 µg LacZ DNA. The instillation procedure was done as described before in 3.6.2. The complex was prepared according to 3.8.2 at N/P 6. A placebo group (n = 4) was instilled with 150 µl HBG. Mice were anesthetized 24 h after intubation, sequentially the *in vivo* transfection efficiency was examined as described above in 3.8.4.5.

3.8.6 Determination of LacZ reporter gene expression after systemic application of two polyplexes via tail vein

3.8.6.1 Animals and materials

Anti-EGFR, anti-epidermal growth factor receptors, rabbit polyclonal antibody (Biogenex, the Hague, the Netherlands)

EGF-PEI25br (cationic vector) was obtained as gift from Dr.Ogris (Department of Pharmacy Ludwig-Maximilians-Universität München, Germany)

Three months old, male BXB-23 mice and weighting between 20-30 g.

Trypsin (Sigma)

EGF-PEG-PEI25/PEI22 polyplex was obtained as gift from Dr.Ogris (Department of Pharmacy Ludwig-Maximilians-Universität München, Germany)

Polyethylene glycol (PEG), branched polyethylenimine 25 kDa (PEI25), epidermal growth factor (EGF)

3.8.6.2 Preparation of transfection complex (EGF targeted polyplexes)

1) DNA solution

100 µg LacZ DNA was dissolved in HBG buffer to a final volume of 250 µl and the solution was mixed by up and down pipetting.

2) PEI solution

7.8 μg EGF-PEI25br and 70.2 μg linear polyethylenimine 22 kDa (PEI 22lin) (1 mg/ml) were diluted with HBG to 250 μl and the mixture was mixed by pipetting up and down.

This solution was added to DNA solution and mixed immediately by rapid up and down (5-10 times). It was necessary to mix the two solutions immediately to reduce the formation of large aggregates. The mixture was kept for 10 min at room temperature.

The stock solution of PEI22lin (9.28 mg/ml) was diluted with HBS to obtain solution of 1 mg/ml which was frozen in aliquots or stored at 4 °C.

3.8.6.3 *In vivo* transfection efficiency in tumor bearing lungs using EGF/PEI and EGF/PEG/PEI as cationic vectors

The mice ($n = 4$) were injected once slowly into the tail vein either with EGF/PEI25/PEI22 polyplex or EGF/PEG/PEI25/PEI22 polyplex (250 μl /mouse) which contained 50 μg LacZ DNA at N/P 6. A placebo group ($n = 4$) was injected with 250 μl HBG. Mice were anesthetized 24 h after the injection then the mice were scarified, sequentially the lung was perfused, stained and embedded as described before in 3.8.4.5.

3.8.6.4 Immunohistochemistry for EGFR in BXB-23 lungs

This protocol was done as described by Selvaggi et al. [270] with some modification of reagents used. Paraffin-embedded lung sections (6 μm thick) were deparaffinized using a series of xylol and ethanol, see 3.4.2, rehydrated with water for 2-5 min and incubated at 37 °C for 10 min in 0.1 % trypsin (pH 7.4). Subsequently, the slides were washed in PBS (3 \times 5 min) and then incubated for 30 min at room temperature in peroxidase blocking solution (3 % H_2O_2 in methanol). The slides were washed in PBS (3 \times 5 min) and placed in blocking solution in PBS (5 % goat serum) for 30 min at room temperature. The slides were incubated with primary antibody anti-EGFR (dilution 1:40) in the blocking solution for 2 h at room temperature. Afterwards, the slides were washed in PBS, incubated for 30 min with biotinylated secondary goat anti-rabbit antibody (dilution 1:500) in the blocking solution, rinsed in PBS and incubated at room temperature for 45 min with

AB-complex as described under 3.4.3.1. The slides were examined for expression of EGFR under the light microscope.

4. Tables

4. Tables

4.1 Treatment of BXB-23 mice with sorafenib emulsion peroral

4.1.1 Sorafenib concentration in mice serum after peroral treatment

Table 15: values of sorafenib serum concentrations

Sorafenib concentrations in the emulsion	The injected volume	Time of taking samples	Sorafenib concentrations in the serum samples
2 mg/ml	100 μ l	After 2 h from the tail	999.44 ng/ml
2 mg/ml	100 μ l	After 24 h after sacrifice	No drug
20 mg/ml	100 μ l	After 2 h from the tail	1776.80 ng/ml
20 mg/ml	100 μ l	After 24 h after sacrifice	96.31 ng/ml

4.1.2 Pharmacological effects on the lung adenoma after peroral treatment of BXB-23 mice with sorafenib emulsion

Table 16: The single values of tumor percent (%) study

Placebo	Sorafenib treated animals
16.0	10.5
10.0	7.8
13.3	6.6
11.5	7.8
12.7	8.4
8.0	10.3

Table 17: The single values of number of foci per mm² analysis

Placebo	Sorafenib treated animals
3.5	2.0
5.5	1.5
4.0	4.0
6.0	7.0
6.6	8.0
7.0	5.0

Table 18: The single values of Proliferating Cellular Nuclear Antigen (PCNA) immunohistochemistry (%)

Placebo	Sorafenib treated animals
28.0	22.0
27.3	20.5
30.0	21.7
26.5	23.0
29.3	19.0
27.0	22.9

Table 19: The single values of percent of activated caspase-3 positive cells (%)

Placebo	Sorafenib treated animals
3.0	3.0
2.8	3.6
3.5	2.3
3.4	2.8
2.6	2.6
3.2	2.2

Table 20: The single values of the lung weights (g)

Control	Placebo	Sorafenib treated animals
0.19	0.18	0.19
0.23	0.14	0.17
0.21	0.16	0.15
0.17	0.20	0.20
	0.22	0.20
	0.18	0.20

4.2 Characterization of sorafenib liposome preparation

Table 21: The single values of *in vitro* release study of sorafenib (%)

Time	Sorafenib loaded liposome	Sorafenib solution
30 min	50.7	69.8
	52.4	78.9
	50.8	75.0
	61.0	70.8
	61.5	
	61.7	
	69.0	
2 h	51.3	83.0
	52.6	82.5
	61.8	80.7
	61.6	75.8
	76.0	
	62.5	
	74.0	
6 h	53.2	85.7
	57.1	90.5
	62.0	87.9
	61.4	95.9
	76.0	
	62.7	
	77.0	
24 h	55.0	96.5
	58.2	95.8
	62.6	97.8
	61.4	99.8
	80.0	
	63.5	
	78.0	

Table 22: The single values of the particle size (μm) of liposome preparation

Empty liposome	Sorafenib loaded liposome
8.5	8.2
7.4	8.9
7.0	8.7

Table 23: The single values of the percent encapsulation efficiency (%) after storage of the liposome preparation

Storage period	4 °C	25 °C
After 15 days	99.0	97.9
	98.0	97.5
	97.0	96.9
After 30 days	97.0	87.0
	97.8	89.7
	98.0	90.4

4.3 Pharmacokinetics of sorafenib after intratracheal instillation

Table 24: The single values of sorafenib concentrations in BXB-23 mice lungs and blood samples after intratracheal instillation of 1 mg in 50 μ l of liposome suspension

	Lung				Serum
	Time	Sorafenib concentration (μ g/g lung)	Lung weight in (g)	Sorafenib concentration in whole lung in (μ g)	Sorafenib concentration in blood (μ g/ml)
2 hours group	2 hours	157.2	0.289	45.43	15.656
	2 hours	141.1	0.242	34.15	12.775
	2 hours	140.0	0.346	48.44	15.462
	2 hours	159.0	0.261	41.40	16.600
24 hours group	24 hours	20.5	0.382	7.83	2.8414
	24 hours	20.1	0.286	5.75	1.943
	24 hours	23.0	0.289	6.65	2.453
48 hours group	48 hours	24.0	0.206	4.94	Less than LOQ
	48 hours	15.0	0.304	4.56	
	48 hours	17.4	0.260	4.52	
One week group	one week	14.9	0.208	3.09	Less than LOQ
	one week	14.9	0.140	2.09	
	one week	15.0	0.283	4.25	

4.4 Antitumor effect of liposomal sorafenib after intratracheal instillation

Table 25: single values of lung weight/body weight (mg/g)

Control	Placebo	One week	Two weeks	Three weeks	Recovery placebo	Recovery control	Recovery treated
9	16	15	17	13	13	12	10
7.6	26	18	20	16	12	12	10
10	16	15	30	20	11	11	13
8	13	20	15	17	10	13	10
9	18	16	14	19	10	10	11
	11		16	19			
	16			30			
	10			16			
	12			17			

Table 26: Single values for tumor percent (%)

Control	Placebo	One week	Two weeks	Three weeks	Recovery placebo	Recovery control	Recovery treated
15	12	5	10	6.9	26	23	15
13	18	8	12	10	22	22	10
18	16	7	15	14	25	24	14
15	12	6.5	11	14	23	28	10
12	13	4.5	8.7	10	24	25	12
	15		11	16	25		
	15			11			
	18			15			

Table 27: Single values for percent of PCNA positive cells (%)

Placebo	One week	Two weeks	Three weeks	Recovery placebo	Recovery treated
30	25	30	31	29	35
27	30	35	34	44	31
27.5	29	40	41	35	40
25	26	29	45	28	38
28	28	27	29	40	29
26		24	26		
35			35		
39					
40					

Table 28: Single values for percent of activated caspase-3 positive cells (%)

Placebo	One week	Two weeks	Three weeks	Recovery placebo	Recovery treated
1.8	11	4	5	4	3
1.9	7	2	1.9	1.8	1.9
2	11	1.9	2	2	1.8
3	10	1.8	1.8	3.5	2
2.5	8	2	1.6	2.5	2.5
1.8		2.5	4		
4			3.6		
2.5					
1.8					

Table 29: Single values of percent of positive MDR cells (%)

Placebo	One week	Two weeks	Three weeks	Recovery placebo	Recovery treated
6	7	14	21	6	5
10	8	17	24	9	4
5	6	20	18	3	7
3	7	15	14	7	6
9	5	19	20	5	2.5
7		22	19		
7			23		
8			25		
6.5					
5.9					

4.5 Characterization of sorafenib microspheres

Table 30: Single values for sorafenib encapsulation efficiency (%)

Batch number	Encapsulation efficiency (%)
Batch (1)	99.5
Batch (2)	98.4
Batch (3)	99.6
Batch (4)	95.7
Batch (5)	99.2
Batch (6)	99.1

Table 31: Single values of the *in vitro* release study of sorafenib microspheres and sorafenib solution

Time (h)	Released sorafenib (%)					
	Sorafenib microspheres			Sorafenib solution		
	Batch A	Batch B	Batch C	Solution A	Solution B	Solution C
0.5	4.0	10.0	5.0	17.5	20.1	19.2
1	8.3	14.7	9.3	21.3	22.4	24.5
2	11.0	20.2	12.3	31.0	31.9	32.2
6	13.7	23.2	16.3	60.2	59.4	61.2
24	18.5	25.4	19.4	69.3	70.4	68.5
48	20.3	26.0	21.0	69.8	71.2	69.0
120	22.0	28.4	22.6	72.2	73.0	70.8

Table 32: The single values of the particle size (μm) of microspheres

Plain microspheres	Sorafenib loaded microspheres
1.3	1.6
1.2	1.3
1.7	1.6
	2.2
	1.6

4.6 Validation of sorafenib HPLC method

Table 33: Single values of inter-day assay

100 ng/ml	600 ng/ml	1800 ng/ml
91.8	801	1797
96.5	709	1921
94.0	675	1928
91.8	621	1653
99.0	656	1779
94.4		1805

Table 34: Single values of intra-day assay

100 ng/ml	600 ng/ml	1800 ng/ml
99.0	601.5	1689
84.4	643.0	1805
101.0	621.5	1839
116.0	695.0	1862
99.1	668.0	1856

Table 35: Single values of low limit of quantitation (LOQ)

80 ng/ml
100.4
108.9
76.0
74.8
73.7
74.9

Table 36: Single values of the recovery study

Standard curves		Extraction curves	
Slops	Intercepts	Slops	Intercepts
0.000402	0.00546	0.00044	0.0635
0.000400	0.00550	0.00040	0.0097
0.000404	0.00532	0.00038	0.0161
0.000420	0.00560	0.00036	0.0024
0.000380	0.00540	0.00038	0.0237
0.000430	0.00600	0.00031	0.0289

5. Summary

5. Summary

The aim of the present study was to design different dosage forms as carrier systems to deliver sorafenib to the lung of BXB-23 transgenic mice using different routes of administration. Three dosage forms were used one of them was an oil-in-water emulsion and the oral route was chosen for this experiment. The other delivery system was a liposome preparation for intratracheal instillation. In this case the oral route was considered as a control experiment. The last dosage form was PLGA microspheres.

Before sorafenib administration it was important to develop a HPLC method to assess sorafenib absorption after its administration and to determine its concentrations in mouse serum. The HPLC method allowed sorafenib quantification in small volumes (30 μ l) of mouse serum and tissues. The developed HPLC method was validated resulting in satisfactory selectivity, good linearity, good accuracy and precision over the concentration range examined.

Sorafenib was successfully incorporated in a fat emulsion (o/w) using a traditional method resulting in a white homogenous emulsion and no particle aggregation was observed. Sorafenib exhibited antitumor activity on the lung adenoma in BXB-23 transgenic mice when administered orally (2 mg sorafenib per mouse) in the emulsion preparation. The determined effect was an approximately 29 % reduction in the tumor area of the adenoma foci and a proliferation reduction.

In order to improve the pharmacological effects of sorafenib on the lung adenoma in BXB-23 mice, the targeting of sorafenib directly to the site of action (the lung) was an attractive concept. For this purpose the intratracheal route was used. Since sorafenib administration by instillation required incorporation of sorafenib in a dosage form suitable for its lipophilic nature, a liposome suspension was the second dosage form used. A lyophilization method was employed for sorafenib liposome preparation utilizing dilauroylphosphatidylcholine (DLPC) which is safe and tolerable for the lung. Incorporation of sorafenib in the liposomes did not influence the particle size and its distribution. The sorafenib liposomes showed high encapsulation efficiency, good stability at 4 °C for one month and satisfactory *in vitro* release properties and inhibited Raf-1 mediated activation of ERK in cell culture assay.

In a pharmacokinetic experiment sorafenib loaded liposomes were instilled directly into the lung. The results revealed that a significant level of sorafenib was achieved in the lung tissues after 2 hours and then reduced after 48 h and remained nearly constant for one

week. On the other hand, only traces of sorafenib were found in the mice serum up to 48 h. Subsequently, the pharmacological activity of sorafenib (1 mg per mouse) was studied when delivered in a liposomal suspension intratracheally to treat the lung adenoma of BXB-23 mice. The data of this experiment demonstrated that sorafenib intratracheal instillation resulted in a reduction of tumor area of adenoma foci (67 %) and an elevation of the percent of apoptotic cells. In contrast, prolongation of the treatment period did not further enhance sorafenib activity on the lung adenoma. This previous finding suggested a development of multidrug resistance (MDR) by the adenoma foci cells against sorafenib instillation, which was examined by immunohistochemistry staining. The percent of MDR positive cells was higher after two and three weeks sorafenib liposome instillation treatment than that after one week treatment.

The last dosage form used for sorafenib was microspheres, which were prepared by emulsion-diffusion-evaporation method using biodegradable PLGA 50:50 resulting in a white lyophilized powder. The system was characterized physicochemically and revealed a good microspheres yield, high encapsulation efficiency, a homogenous particle size distribution and slow *in vitro* release of sorafenib.

The other strategy studied in the present research project was gene delivery to target the lung bearing tumor of BXB-23 mice using a non-viral vector (polyethylenimine). Polyethylenimine (PEI) was used to investigate its efficiency in transfecting lung bearing tumor of BXB-23 mice model and its ability to transfect the adenoma foci cells. LacZ, which encodes β -galactosidase was used in the present study as a reporter gene and was complexed with PEI before delivered intravenously. A high LacZ expression in the alveolar region with some expression in the adenoma foci was observed. On contrary, a low LacZ expression in the alveoli and in the adenoma foci was achieved after instillation of the same polyplex intratracheally.

Epidermal growth factor (EGF) was extensively used as a ligand because its receptors are overexpressed in many human tumors. In the present study the aim was to investigate the ability of two polyplexes in targeting the lung and/or the adenoma foci of BXB-23 mice when delivered intravenously. Polyethylenimine was used as macromolecular cationic polymer conjugated either with EGF as a ligand or with EGF and polyethyleneglycol (PEG) as a shielding agent to reduce the non-specific interaction with the blood components. LacZ was further used as a reporter gene. The results revealed that there was very poor expression in the lung tissues in the alveoli in comparison with using of PEI alone and no expression was found in the adenoma foci. This poor expression was attributed to the

absence of EGFR expression in the adenoma foci of BXB-23 mice which was proven immunohistochemically. Additionally, PEG probably masked the positive charge of the polyplex which was responsible for the high transfection efficiency of PEI in the lung tissues.

In conclusion, sorafenib was successfully incorporated in three different dosage forms. Sorafenib exhibited antitumor activity on lung adenoma of BXB-23 mice model when given orally in an emulsion. Targeting of sorafenib directly to the lung in a liposome preparation showed antitumor effect on lung adenoma after one week treatment. Regardless of multidrug resistance developed by adenoma foci cells after two and three weeks sorafenib instillation, targeting of sorafenib directly to the lung proved to be a promising route of administration for treatment of lung adenoma of BXB-23 mice model. In addition, microspheres loaded sorafenib revealed good and auspicious properties *in vitro* and can be further used *in vivo*. Moreover, lung adenoma foci of BXB-23 mice did not express epidermal growth factor receptors (EGFR). Polyethylenimine showed its efficiency as a cationic vector in transfecting the lung bearing tumor of BXB-23 mice model and showed LacZ expression in the adenoma foci when delivered intravenously and intratracheally.

Zusammenfassung

Das Ziel der vorliegenden Dissertation war es, verschiedene galenische Darreichungsformen als Trägersystem für Sorafenib zu entwickeln, um den direkten Transport des Arzneistoffes zum Zielorgan Lunge von BXB-23 transgenen Mäusen zu ermöglichen. Für die verschiedenen Applikationswege wurden drei Darreichungsformen gewählt. Eine Öl-in-Wasser-Emulsion sollte oral verabreicht werden. Für die intratracheale Instillation wurde ein liposomales Präparat gewählt. Hierfür diente der orale Weg als Kontrolle. Die letzte Darreichungsform stellten PLGA Mikrosphären dar.

Um die Absorption von Sorafenib nach Administration bestimmen zu können, wurde die Konzentration des Arzneistoffes im Mäuseserum gemessen. Da zur Quantifizierung von Sorafenib nur ein sehr geringes Volumen (30 µl) von Mäuseserum bzw. Gewebe zur Verfügung stand, musste eine geeignete HPLC-Methode entwickelt werden. Diese HPLC-Methode wurde validiert und lieferte im betrachteten Konzentrationsbereich eine zufriedenstellende Selektivität, gute Linearität, gute Genauigkeit und Präzision.

Sorafenib wurde erfolgreich in eine Fettemulsion (o/w) mittels einer traditionellen Methode eingearbeitet und ergab eine weiße, homogene Emulsion ohne Partikelaggregation. Nach oraler Verabreichung der Emulsion (2 mg/Maus) zeigte Sorafenib auf Lungenadenome eine Antitumor-Aktivität in BXB-23 transgenen Mäusen. Es konnte eine Reduktion der Tumorfläche der Adenomfoci um etwa 29 % verzeichnet werden, sowie eine Reduktion der Proliferation.

Um die pharmakologischen Effekte von Sorafenib auf die Lungenadenome in BXB-23 Mäusen zu verbessern, sollte Sorafenib direkt dem Zielorgan Lunge verabreicht werden. Zu diesem Zweck wurde der intratracheale Administrationsweg gewählt. Da die Instillation von Sorafenib aufgrund seiner lipophilen Natur nur durch Einschluß in eine andere Darreichungsform zu erreichen ist, wurde für die zweite Darreichungsform eine Liposomen-Suspension verwendet. Für die Zubereitung von Sorafenib in Liposomen wurde eine Lyophilisierungsmethode unter Verwendung von DPLC erarbeitet, welches sich durch eine gute Sicherheit und pulmonale Verträglichkeit auszeichnet. Der Einschluß von Sorafenib in die Liposomen hatte keinen Einfluss auf die Partikelgröße und Verteilung. Die Einkapselung-Fähigkeit der Sorafenib-beladenen Liposomen war hoch und zeigte bei 4°C eine gute Stabilität für einen Monat. Die erzielten Effekte bei der *in vitro* Freisetzung und die Hemmung der von Raf1-induzierten Aktivierung von ERK in Zellkulturexperimenten lieferten zufrieden stellende Ergebnisse.

In einem pharmakokinetischen Experiment wurden mit Sorafenib beladenen Liposomen direkt in die Lunge appliziert. Die Ergebnisse zeigten, dass nach 2 h eine signifikante Konzentration von Sorafenib im Lungengewebe erreicht wurde. Nach 48 h nahm diese Konzentration ab und blieb dann für eine Woche fast konstant. Andererseits wurden bis zu 48 h nach Gabe des Arzneistoffes nur Spuren von Sorafenib im Mäuseserum gefunden. Folglich wurde die pharmakologische Aktivität von Sorafenib (1 mg/Maus) bei intratrachealer Verabreichung in einer liposomalen Suspension untersucht. Die Ergebnisse zeigten, dass die intratracheale Gabe von Sorafenib eine Reduktion der Tumorfläche der Adenomfoci um 67 % bewirkte, sowie eine Erhöhung des prozentualen Anteils apoptotischer Zellen. Im Gegensatz dazu bewirkte eine Verlängerung der Behandlungszeit keine zusätzliche Verbesserung der durch Sorafenib erzielten Effekte. Dies lässt vermuten, dass hier eine Entwicklung von Multidrug-Resistenz in den Adenomfociszellen gegenüber der Instillation von Sorafenib erfolgte. Dies wurde in immunochemischen Anfärbexperimenten untersucht. Die Prozentzahl von MDR-positiven Zellen war nach zwei und drei Wochen Instillation von Sorafenib-Liposomen höher als nach einer Woche.

Die letzte verwendete Darreichungsform für Sorafenib waren Mikrosphären, die durch Emulsions-Diffusions-Evaporations-Methoden in biologisch abbaubarem PLGA 50:50 hergestellt wurden. Dies ergab ein weißes, lyophilisiertes Pulver. Das System wurde physiochemisch charakterisiert und ergab ein gutes Mikrosphären-Ergebnis, hohe Einkapselung-Fähigkeit, eine homogene Verteilung der Partikelgrößen und eine langsame *in vitro* Freisetzung von Sorafenib.

Die andere untersuchte Strategie war Gen-Delivery, um den Lungentumor von BXB-23 Mäusen mittels eines nicht-viralen Vektors (Polyethylenimin, PEI) anzuzielen. PEI wurde verwendet, um die Effektivität der Transfektion des Lungentumors zu untersuchen und seine Fähigkeit, die Adenomfociszellen zu transfizieren. LacZ, das β -Galactosidase codiert, diente bei diesem Experiment als Reportergen und wurde vor intravenöser Gabe mit PEI komplexiert. Eine hohe LacZ-Expression in der alveolaren Region, aber nur eine geringe Expression in den Adenomfoci wurde beobachtet. Im Gegensatz dazu wurde eine geringe Expression von LacZ in den Alveolen und den Adenomfoci nach intratrachealer Instillation des gleichen Polyplex erreicht.

Der epidermale Wachstumsfaktor (EGF) wird umfassend als Ligand verwendet, da seine Rezeptoren in vielen humanen Tumoren überexprimiert werden. Das Ziel unserer Untersuchung war es, die Fähigkeit von zwei Polyplexen zu untersuchen, das Zielorgan Lunge nach intravenöser Gabe und/oder die Adenomfoci von BXB-23 Mäusen zu

erreichen. Polyethylenimin wurde als makromolekulares, kationisches Polymer verwendet, konjugiert an EGF als Ligand oder EGF und Polyethylenglycol (PEG) als abschirmendes Agenz, um die nicht-spezifische Interaktion mit Blutkomponenten zu reduzieren. Desweiteren wurde LacZ als Reporter gen eingesetzt. Die Ergebnisse zeigten, dass es im Vergleich zur Verwendung von PEI alleine nur eine geringe Expression im Lungengewebe der Alveolen gab, und keine Expression in den Adenomfoci erfolgte. Diese geringe Expression wurde dem Fehlen einer EGFR-Expression in den Adenomfoci von BXB-23 Mäusen zugeschrieben, die immunohistochemisch nachgewiesen wurde. Darüber hinaus hat PEG vermutlich die positive Ladung des Polyplex maskiert, die für die hohe Transfektionsfähigkeit von PEI im Lungengewebe verantwortlich ist.

Zusammenfassen kann man feststellen, dass Sorafenib erfolgreich in Emulsion, Liposomen und Mikrosphären als Darreichungsform eingeschlossen wurde. Sorafenib zeigte nach oraler Gabe eines Emulsionpräparates Antitumor-Aktivität in Lungenadenomen eines BXB-23 Mäusemodells. Wohingegen die zielgerichtete Verabreichung von Sorafenib in die Lunge in einer liposomalen Darreichungsform nur nach einer Woche Behandlung Antitumor-Aktivität auf Lungenadenome zeigte. Ungeachtet der Multidrug-Resistenz, die durch Adenomfocizellen nach zwei und drei Wochen Sorafenib-Behandlung entwickelt wurde, zeigte sich die zielgerichtete Administration von Sorafenib in die Lunge als vielversprechende Route zur Behandlung von Lungenadenomen in BXB-23 Mäusen. Zusätzlich zeigten mit Sorafenib beladenen Mikrosphären gute und vielversprechende Eigenschaften *in vitro* und können weiter *in vivo* verwendet werden. Desweiteren exprimierten Lungenadenomfoci in BXB-23 Mäusen keine epidermalen Wachstumsfaktorrezeptoren (EGFR). Polyethylenimin zeigte seine Effektivität als kationischer Vektor bei der Transfektion von Lungentumoren in BXB-23 Mäusen und zeigte Expression von LacZ in Adenomfoci bei intravenöser und intratrachealer Verabreichung.

6. Abbreviations

6. Abbreviations

ABC	ATP-binding cassettes
APS	Ammoniumpersulfate
ATP	Adenosine-5'-triphosphate
AUC	Area under the curve
bid	Twice daily
BSA	Bovine Serum Albumin
C_{\max}	Maximum plasma concentration
DAB	3, 3' diaminobenzidine
DLPC	Dilauroylphosphatidylcholine
DMEM	Dulbecco's Modified Eagle Medium
DMF	Dimethylformamide
DMSO	Dimethylsulfoxide
ECL	Enhanced Chemiluminescence
EDTA	Ethylendiamintetra acetic acid
EE	Encapsulation efficiency
EGF	Epidermal growth factor
EGFR	Epidermal growth factor receptor
ERK	Extracellular signal regulated kinase
FCS	Fetal calf serum
GFP	Green fluorescent protein
h	Hours
H&E	Hematoxylin and eosin
HBG	Hepes buffered glucose
HBS	Hepes buffered saline
HEPES	4-(2-hydroxyethyl)-1-piperazineethanesulfonic acid
HPLC	High performance liquid chromatography
i.p.	Intraperitoneal
i.v.	Intravenous
IC	Inhibitory concentration
IT	Intratracheal instillation
Kb	Kilobasepairs
kDa	Kilo Dalton

LOQ	Low limit of quantitation
MAPK	Mitogen activate protein kinase
MDR	Multidrug resistance
MEK	Mitogen-activated protein kinase kinase (MAPK/ERK activating kinase)
min	Minutes
MTD	Maximum tolerated dose
MWCO	Molecular weight cut-off
NP40	Nonidet 40
OD	Optical density
PAGE	Polyacrylamide-Gel electrophoresis
PBS	Phosphate buffered saline
PCNA	Proliferating cell nuclear antigen
PDGFR	Platelet-derived growth factor receptor
PEG	Polyethylene glycol
PEI	Polyethylenimine
P-gp	P-glycoprotein
Pharm. Helv	Pharmacopea Helvetica
PLGA	Poly (L-lactide-co-glycolide)
PVA	Polyvinyl alcohol
QC	Quality control
r	Correlation coefficient
s.c.	Subcutaneous
SD	Standard deviation
SDS	Sodium Dodecylsulfate
SEM	Standard error of the mean
SEM	Scanning electron microscope
$t_{1/2}$	Terminal half-life
t_{max}	Time of maximum plasma concentration
UV	Ultraviolet
VEGFR	Vascular endothelial growth factor receptor
X-gal	5-Bromo-4-Chloro-3-Indolyl- β -D-Galactopyranosid
β -Gal	β -Galactosidase

7. Bibliography

7. Bibliography

1. Lodish H, Berk A, Zipursky SL, Matsudaira P, Baltimore D, Darnell J: **Cancer**. In: *Molecular cell biology*. United States of America: W. H. Freeman and company, New York, England; 2001: pp.1054-1056.
2. Jemal A, Tiwari RC, Murray T, Ghafoor A, Samuels A, Ward E, Feuer EJ, Thun MJ: **Cancer statistics, 2004**. *CA Cancer J Clin* 2004, **54**(1):8-29.
3. Wikenheiser KA, Clark JC, Linnoila RI, Stahlman MT, Whitsett JA: **Simian virus 40 large T antigen directed by transcriptional elements of the human surfactant protein C gene produces pulmonary adenocarcinomas in transgenic mice**. *Cancer Res* 1992, **52**(19):5342-5352.
4. Isselbacher KJ, Braunwald E, Wilson JD, Martin JB, Fauci AS, Kasper DL: **Neoplasms of the lung**. In: *Harrison's principles of internal medicine*. New York: Mc-Graw-Hill; 1994: pp.1221-1229.
5. Frederiksen KS, Petri A, Abrahamsen N, Poulsen HS: **Gene therapy for lung cancer**. *Lung Cancer* 1999, **23**(3):191-207.
6. McManus K: **Thoracic tumors**. In: *Oncology*. Edited by Spence RAJ, Johnston PG. United States: Oxford University; 2001: pp. 295-309.
7. Yousem SA, Hochholzer L: **Alveolar adenoma**. *Hum Pathol* 1986, **17**:1066-1071.
8. Menet E, Etchandy-Laclau K, Corbi P, Levillain P, Babin P: **[Alveolar adenoma: a rare peripheral pulmonary tumor]**. *Ann Pathol* 1999, **19**(4):325-328.
9. Bohm J, Fellbaum C, Bautz W, Prauer HW, Hofler H: **Pulmonary nodule caused by an alveolar adenoma of the lung**. *Virchows Arch* 1997, **430**(2):181-184.
10. Koppl H, Freudenberg N, Berwanger I, Frenzer K, Bohm N: **[Alveolar adenoma of the lung. Immunohistochemical characterization of type II pneumocytes]**. *Pathologe* 1996, **17**(2):150-153.
11. Mountain CF: **A new international staging system for lung cancer**. *Chest* 1986, **89**:225s-233s.
12. Mountain CF: **Histologic and anatomic classification of lung cancer and regional lymph nodes**. In: *Tumors and tumor-like lesions of the lung*. Edited by Carter D, Patchefsky AS, Mountain CF, vol. 36: W.B. Saunders Company, USA; 1998: pp. 5-10.
13. Lee JT, McCubrey JA: **BAY-43-9006 Bayer/Onyx**. *Curr Opin Investig Drugs* 2003, **4**(6):757-763.
14. Lyons JF, Wilhelm S, Hibner B, Bollag G: **Discovery of a novel Raf kinase inhibitor**. *Endocr Relat Cancer* 2001, **8**(3):219-225.
15. Lowinger TB, Riedl B, Dumas J, Smith RA: **Design and discovery of small molecules targeting raf-1 kinase**. *Curr Pharm Des* 2002, **8**(25):2269-2278.
16. Adnane L, Trail PA, Taylor I, Wilhelm SM: **Sorafenib (BAY 43-9006, Nexavar((R))), a Dual-Action Inhibitor That Targets RAF/MEK/ERK Pathway in Tumor Cells and Tyrosine Kinases VEGFR/PDGFR in Tumor Vasculature**. *Methods Enzymol* 2005, **407**:597-612.
17. Dumas J: **Protein kinase inhibitors from the urea class**. *Curr Opin Drug Discov Devel* 2002, **5**(5):718-727.
18. Arora A, Scholar EM: **Role of tyrosine kinase inhibitors in cancer therapy**. *J Pharmacol Exp Ther* 2005, **315**(3):971-979.

19. Strumberg D, Seeber S: **Raf kinase inhibitors in oncology.** *Onkologie* 2005, **28**(2):101-107.
20. Wilhelm SM, Carter C, Tang L, Wilkie D, McNabola A, Rong H, Chen C, Zhang X, Vincent P, McHugh M *et al*: **BAY 43-9006 exhibits broad spectrum oral antitumor activity and targets the RAF/MEK/ERK pathway and receptor tyrosine kinases involved in tumor progression and angiogenesis.** *Cancer Res* 2004, **64**(19):7099-7109.
21. Wakelee HA, Schiller JH: **Targeting angiogenesis with vascular endothelial growth factor receptor small-molecule inhibitors: novel agents with potential in lung cancer.** *Clin Lung Cancer* 2005, **7 Suppl 1**:S31-38.
22. Zakarija A, Soff G: **Update on angiogenesis inhibitors.** *Curr Opin Oncol* 2005, **17**(6):578-583.
23. Hotte SJ, Hirte HW: **BAY 43-9006: early clinical data in patients with advanced solid malignancies.** *Curr Pharm Des* 2002, **8**(25):2249-2253.
24. Wilhelm S, Carter C, Lynch M, Lowinger T, Dumas J, Smith RA, Schwartz B, Simantov R, Kelley S: **Discovery and development of sorafenib: a multikinase inhibitor for treating cancer.** *Nat Rev Drug Discov* 2006, **5**(10):835-844.
25. Branca MA: **Multi-kinase inhibitors create buzz at ASCO.** *Nat Biotechnol* 2005, **23**(6):639.
26. Beeram M, Patnaik A, Rowinsky EK: **Raf: a strategic target for therapeutic development against cancer.** *J Clin Oncol* 2005, **23**(27):6771-6790.
27. Wilhelm S, Housley T: **A novel diphenyl-urea raf kinase inhibitor (RKI) blocks the Raf/MEK/ERK pathway in tumor cells.** *Proc Am Assoc Cancer Res* 2001, **41**(abstr).
28. Rahmani M, Davis EM, Bauer C, Dent P, Grant S: **Apoptosis induced by the kinase inhibitor BAY 43-9006 in human leukemia cells involves down-regulation of Mcl-1 through inhibition of translation.** *J Biol Chem* 2005, **280**(42):35217-35227.
29. Wilhelm S, Chien DS: **BAY 43-9006: preclinical data.** *Curr Pharm Des* 2002, **8**(25):2255-2257.
30. Gianopaolo-Ostravage C, Carter C, Hibner B: **Anti-tumor efficacy of the orally active Raf kinase inhibitor BAY 43-9006 in human tumor xenograft models.** *Proc Am Assoc Cancer Res* 2001, **42**:(abstr).
31. Kramer BW, Gotz R, Rapp UR: **Use of mitogenic cascade blockers for treatment of C-Raf induced lung adenoma in vivo: CI-1040 strongly reduces growth and improves lung structure.** *BMC Cancer* 2004, **4**:24.
32. Karasarides M, Chiloechos A, Hayward R, Niculescu-Duvaz D, Scanlon I, Friedlos F, Ogilvie L, Hedley D, Martin J, Marshall CJ *et al*: **B-RAF is a therapeutic target in melanoma.** *Oncogene* 2004, **23**(37):6292-6298.
33. Strumberg D, Schuehly U, Moeller J, Hedley D, Hilger R, Stellberg W, Richly H, Heinig R, Ahr G, Wensing G *et al*: **phase I clinical pharmacokinetic, and pharmacodynamic study of Raf kinase inhibitor BAY 43-9006 in patients with locally advanced or metastatic cancer.** In: *Book of abstracts 37th ASCO meeting, 2001*: poster 330.
34. Strumberg D, Voliotis D, Moeller JG, Hilger RA, Richly H, Kredtke S, Beling C, Scheulen ME, Seeber S: **Results of phase I pharmacokinetic and pharmacodynamic studies of the Raf kinase inhibitor BAY 43-9006 in patients with solid tumors.** *Int J Clin Pharmacol Ther* 2002, **40**(12):580-581.

35. Strumberg D, Richly H, Hilger RA, Schleucher N, Korfee S, Tewes M, Faghieh M, Brendel E, Voliotis D, Haase CG *et al*: **Phase I clinical and pharmacokinetic study of the Novel Raf kinase and vascular endothelial growth factor receptor inhibitor BAY 43-9006 in patients with advanced refractory solid tumors.** *J Clin Oncol* 2005, **23**(5):965-972.
36. Moore M, Hirte HW, Siu L, Oza A, Hotte SJ, Petrenciuc O, Cihon F, Lathia C, Schwartz B: **Phase I study to determine the safety and pharmacokinetics of the novel Raf kinase and VEGFR inhibitor BAY 43-9006, administered for 28 days on/7 days off in patients with advanced, refractory solid tumors.** *Ann Oncol* 2005, **16**(10):1688-1694.
37. Awada A, Hendlisz A, Gil T, Bartholomeus S, Mano M, de Valeriola D, Strumberg D, Brendel E, Haase CG, Schwartz B *et al*: **Phase I safety and pharmacokinetics of BAY 43-9006 administered for 21 days on/7 days off in patients with advanced, refractory solid tumours.** *Br J Cancer* 2005, **92**(10):1855-1861.
38. Clark JW, Eder JP, Ryan D, Lathia C, Lenz HJ: **Safety and pharmacokinetics of the dual action Raf kinase and vascular endothelial growth factor receptor inhibitor, BAY 43-9006, in patients with advanced, refractory solid tumors.** *Clin Cancer Res* 2005, **11**(15):5472-5480.
39. Lathia C, Lettieri J, Cihon F, Gallentine M, Radtke M, Sundaresan P: **Lack of effect of ketoconazole-mediated CYP3A inhibition on sorafenib clinical pharmacokinetics.** *Cancer Chemother Pharmacol* 2006, **57**(5):685-692.
40. Ratain MJ, Eisen T, Stadler WM, Flaherty KT, Kaye SB, Rosner GL, Gore M, Desai AA, Patnaik A, Xiong HQ *et al*: **Phase II placebo-controlled randomized discontinuation trial of sorafenib in patients with metastatic renal cell carcinoma.** *J Clin Oncol* 2006, **24**(16):2505-2512.
41. Ahmad T, Eisen T: **Kinase inhibition with BAY 43-9006 in renal cell carcinoma.** *Clin Cancer Res* 2004, **10**(18 Pt 2):6388S-6392S.
42. Gore ME, Escudier B: **Emerging efficacy endpoints for targeted therapies in advanced renal cell carcinoma.** *Oncology (Williston Park)* 2006, **20**(6 Suppl 5):19-24.
43. Strumberg D, Awada A, Hirte H, Clark JW, Seeber S, Piccart P, Hofstra E, Voliotis D, Christensen O, Brueckner A *et al*: **Pooled safety analysis of BAY 43-9006 (sorafenib) monotherapy in patients with advanced solid tumours: Is rash associated with treatment outcome?** *Eur J Cancer* 2006, **42**(4):548-556.
44. Veronese ML, Mosenkis A, Flaherty KT, Gallagher M, Stevenson JP, Townsend RR, O'Dwyer PJ: **Mechanisms of hypertension associated with BAY 43-9006.** *J Clin Oncol* 2006, **24**(9):1363-1369.
45. Siu LL, Awada A, Takimoto CH, Piccart M, Schwartz B, Giannaris T, Lathia C, Petrenciuc O, Moore MJ: **Phase I trial of sorafenib and gemcitabine in advanced solid tumors with an expanded cohort in advanced pancreatic cancer.** *Clin Cancer Res* 2006, **12**(1):144-151.
46. Richly H, Henning BF, Kupsch P, Passarge K, Grubert M, Hilger RA, Christensen O, Brendel E, Schwartz B, Ludwig M *et al*: **Results of a Phase I trial of sorafenib (BAY 43-9006) in combination with doxorubicin in patients with refractory solid tumors.** *Ann Oncol* 2006, **17**(5):866-873.
47. Kupsch P, Henning BF, Passarge K, Richly H, Wiesemann K, Hilger RA, Scheulen ME, Christensen O, Brendel E, Schwartz B *et al*: **Results of a phase I trial of sorafenib (BAY 43-9006)**

- in combination with oxaliplatin in patients with refractory solid tumors, including colorectal cancer.** *Clin Colorectal Cancer* 2005, **5**(3):188-196.
48. Flaherty KT, Brose M, Schuchter L, Tuveson D, Lee R, Schwartz B, Lathia C, Weber B, O'Dwyer PJ: **Phase I/II trial of BAY 43-9006, carboplatin (C) and paclitaxel (P) demonstrates preliminary antitumor activity in the expansion cohort of patients with metastatic melanoma.** In: *American Society of Clinical Oncology 40th Annual Meeting Proceedings, J Clin Oncol, 2004*; 22:suppl, abstr 7507.
49. Ahmed T, Marais R, Pyle L, James M, Schwartz B, Gore M, Eisen T: **BAY 43-9006 in patients with advanced melanoma.** In: *American Society of Clinical Oncology 40th Annual Meeting Proceedings, J Clin Oncol, 2004*: abstr. 7506.
50. Carter CA, Chen C, Brink C, Vincent P, Maxuitenko YY, Gilbert KS, Waud WR, Zhang X: **Sorafenib is efficacious and tolerated in combination with cytotoxic or cytostatic agents in preclinical models of human non-small cell lung carcinoma.** *Cancer Chemother Pharmacol* 2006.
51. Reddy GK, Bukowski RM: **Sorafenib: recent update on activity as a single agent and in combination with interferon-alpha2 in patients with advanced-stage renal cell carcinoma.** *Clin Genitourin Cancer* 2006, **4**(4):246-248.
52. Kan P, Chen Z-B, Kung R-Y, Lee C-J, Chu I-M: **study on the formulation of o/w emulsion as carriers for lipophilic drugs.** *colloids and surfaces B* 1999, **15**(2):117-125.
53. Jurima-Romet M, Shek PN: **Lung uptake of liposome-entrapped glutathione after intratracheal administration.** *J Pharm Pharmacol* 1991, **43**(1):6-10.
54. Tokui T, Takatori T, Shinozaki N, Ishigami M, Shiraishi A, Ikeda T, Tsuruo T: **Delivery and cytotoxicity of RS-1541 in St-4 human gastric cancer cells in vitro by the low-density-lipoprotein pathway.** *Cancer Chemother Pharmacol* 1995, **36**(1):1-6.
55. Collins-Gold LC, Lyons RT, Bartholow LC: **Parenteral emulsions for drug delivery.** *Adv Drug Deliv Rev* 1990, **5**(3):189-208.
56. Kurihara A, Shibayama Y, Mizota A, Yasuno A, Ikeda M, Hisaoka M: **Pharmacokinetics of highly lipophilic antitumor agent palmitoyl rhizoxin incorporated in lipid emulsions in rats.** *Biol Pharm Bull* 1996, **19**(2):252-258.
57. Tamilvanan S: **Oil-in-water lipid emulsions: implications for parenteral and ocular delivering systems.** *Prog Lipid Res* 2004, **43**(6):489-533.
58. Tabibi SE, Rhodes CT: **Disperse systems.** In: *Modern pharmaceuticals*. Edited by Banker GS, Rhodes CT. New York: Marcel Dekker, Inc.; 1996: pp. 319-323.
59. Nakano M: **Places of emulsions in drug delivery.** *Adv Drug Deliv Rev* 2000, **45**(1):1-4.
60. de Baere T, Zhang X, Aubert B, Harry G, Lagrange C, Ropers J, Dufaux J, Lumbroso J, Rougier P, Ducreux M *et al*: **Quantification of tumor uptake of iodized oils and emulsions of iodized oils: experimental study.** *Radiology* 1996, **201**(3):731-735.
61. Pouton CW: **Lipid formulations for oral administration of drugs: non-emulsifying, self-emulsifying and 'self-microemulsifying' drug delivery systems.** *Eur J Pharm Sci* 2000, **11** Suppl 2:S93-98.

62. Lawrence MJ, Rees GD: **Microemulsion-based media as novel drug delivery systems.** *Adv Drug Deliv Rev* 2000, **45**(1):89-121.
63. Piemi MP, Korner D, Benita S, Marty JP: **Positively and negatively charged submicron emulsions for enhanced topical delivery of antifungal drugs.** *J Control Release* 1999, **58**(2):177-187.
64. Khopade AJ, Nandakumar KS, Jain NK: **Lectin-functionalized multiple emulsions for improved cancer therapy.** *J Drug Target* 1998, **6**(4):285-292.
65. Rehfeldt SJ: **Stability of hydrocarbon-in-water emulsions during centrifugation. Influence of dispersed phase composition.** *Journal of colloid and interface science* 1974, **48**(3):448-459.
66. Li J, Caldwell KD, Anderson BD: **A method for the early evaluation of the effects of storage and additives on the stability of parenteral fat emulsions.** *Pharm Res* 1993, **10**(4):535-541.
67. Clause M: **Encyclopedia of emulsion technology**, vol. 1; 1983.
68. Afify S, Rapp UR, Högger P: **Validation of a liquid chromatography assay for the quantification of the Raf kinase inhibitor BAY 43-9006 in small volumes of mouse serum.** *J Chromatogr B Analyt Technol Biomed Life Sci* 2004, **809**(1):99-103.
69. Koshkina NV, Kleinerman ES, Waidrep C, Jia SF, Worth LL, Gilbert BE, Knight V: **9-Nitrocamptothecin liposome aerosol treatment of melanoma and osteosarcoma lung metastases in mice.** *Clin Cancer Res* 2000, **6**(7):2876-2880.
70. Koshkina NV, Waldrep JC, Roberts LE, Golunski E, Melton S, Knight V: **Paclitaxel liposome aerosol treatment induces inhibition of pulmonary metastases in murine renal carcinoma model.** *Clin Cancer Res* 2001, **7**(10):3258-3262.
71. Kerkhoff E, Fedorov LM, Siefken R, Walter AO, Papadopoulos T, Rapp UR: **Lung-targeted expression of the c-Raf-1 kinase in transgenic mice exposes a novel oncogenic character of the wild-type protein.** *Cell Growth Differ* 2000, **11**(4):185-190.
72. Fedorov LM, Tyrsin OY, Papadopoulos T, Camarero G, Gotz R, Rapp UR: **Bcl-2 determines susceptibility to induction of lung cancer by oncogenic CRaf.** *Cancer Res* 2002, **62**(21):6297-6303.
73. Travali S, Ku DH, Rizzo MG, Ottavio L, Baserga R, Calabretta B: **Structure of the human gene for the proliferating cell nuclear antigen.** *J Biol Chem* 1989, **264**(13):7466-7472.
74. Haapasalo HK, Sallinen PK, Helen PT, Rantala IS, Helin HJ, Isola JJ: **Comparison of three quantitation methods for PCNA immunostaining: applicability and relation to survival in 83 astrocytic neoplasms.** *J Pathol* 1993, **171**(3):207-214.
75. Tanioka F, Hiroi M, Yamane T, Hara H: **Proliferating cell nuclear antigen (PCNA), immunostaining and flow cytometric DNA analysis of renal cell carcinoma.** *Zentralbl Pathol* 1993, **139**(3):185-193.
76. Duan WR, Garner DS, Williams SD, Funckes-Shippy CL, Spath IS, Blomme EA: **Comparison of immunohistochemistry for activated caspase-3 and cleaved cytokeratin 18 with the TUNEL method for quantification of apoptosis in histological sections of PC-3 subcutaneous xenografts.** *J Pathol* 2003, **199**(2):221-228.

77. Gown AM, Willingham MC: **Improved detection of apoptotic cells in archival paraffin sections: immunohistochemistry using antibodies to cleaved caspase 3.** *J Histochem Cytochem* 2002, **50**(4):449-454.
78. Slee EA, Adrain C, Martin SJ: **Executioner caspase-3, -6, and -7 perform distinct, non-redundant roles during the demolition phase of apoptosis.** *J Biol Chem* 2001, **276**(10):7320-7326.
79. Panka DJ, Wang W, Atkins MB, Mier JW: **The Raf inhibitor BAY 43-9006 (Sorafenib) induces caspase-independent apoptosis in melanoma cells.** *Cancer Res* 2006, **66**(3):1611-1619.
80. Murphy DA, Makonnen S, Lassoued W, Feldman MD, Carter C, Lee WM: **Inhibition of Tumor Endothelial ERK Activation, Angiogenesis, and Tumor Growth by Sorafenib (BAY43-9006).** *Am J Pathol* 2006, **169**(5):1875-1885.
81. Cohen PT, Browne GJ, Delibegovic M, Munro S: **Assay of protein phosphatase I complexes.** *Methods Enzymol* 2003, **366**:135-144.
82. Hall-Jackson CA, Eyers PA, Cohen P, Goedert M, Boyle FT, Hewitt N, Plant H, Hedge P: **Paradoxical activation of Raf by a novel Raf inhibitor.** *Chem Biol* 1999, **6**:559-568.
83. Kumar V, Banker GS: **Target-oriented drug delivery systems.** In: *Modern pharmaceuticals*. Edited by Banker GS, Rhodes CT. New York: Marcel Dekker, Inc.; 1996: pp. 613-614.
84. Gilbert BE, Knight C, Alvarez FG, Waldrep C, Rodarte JR, Knight V, Eschenbacher WL: **Tolerance of volunteers to cyclosporine A-dilauroylphosphatidylcholine liposome aerosol.** *Am J Respir Crit Care Med* 1997, **156**(6):1789-1793.
85. Gilbert BE, Knight V: **Pulmonary delivery of antiviral drugs in liposome aerosol.** *Semin Pediatr Infect Dis* 1996, **7**:148-154.
86. Vidgren M, Waldrep JC, Arrpe J, Black M, Rodarte JA, Cole W, Knight V: **A study of ^{99m}technetium-labelled beclomethane dipropionate dilauroylphosphatidylcholine liposome aerosol in normal volunteers.** *Int J Pharm* 1995, **115**:209-216.
87. Meisner D, Pringle J, Mezei M: **Liposomal pulmonary drug delivery. I. In vivo disposition of atropine base in solution and liposomal form following endotracheal instillation to the rabbit lung.** *J Microencapsul* 1989, **6**(3):379-387.
88. Demaeyer P, Akodad EM, Gravet E, Schietecat P, Van Vooren JP, Drowart A, Yernault JC, Legros FJ: **Disposition of liposomal gentamicin following intrabronchial administration in rabbits.** *J Microencapsul* 1993, **10**(1):77-88.
89. Suntres ZE, Hepworth SR, Shek PN: **Pulmonary uptake of liposome-associated alpha-tocopherol following intratracheal instillation in rats.** *J Pharm Pharmacol* 1993, **45**(6):514-520.
90. Juliano RL, McCullough HN: **Controlled delivery of an antitumor drug: localized action of liposome encapsulated cytosine arabinoside administered via the respiratory system.** *J Pharmacol Exp Ther* 1980, **214**(2):381-387.
91. Gonzalez-Rothi RJ, Suarez S, Hochhaus G, Schreier H, Lukyanov A, Derendorf H, Costa TD: **Pulmonary targeting of liposomal triamcinolone acetonide phosphate.** *Pharm Res* 1996, **13**(11):1699-1703.

92. Sharma A, Straubinger RM: **Novel taxol formulations: preparation and characterization of taxol-containing liposomes.** *Pharm Res* 1994, **11**(6):889-896.
93. Darwis Y, Kellaway IW: **Nebulisation of rehydrated freeze-dried beclomethasone dipropionate liposomes.** *Int J Pharm* 2001, **215**(1-2):113-121.
94. Goyal P, Goyal K, Vijaya Kumar SG, Singh A, Katare OP, Mishra DN: **Liposomal drug delivery systems--clinical applications.** *Acta Pharm* 2005, **55**(1):1-25.
95. Taylor KM, Newton JM: **Liposomes as a vehicle for drug delivery.** *Br J Hosp Med* 1994, **51**(1-2):55-60.
96. Drummond DC, Meyer O, Hong K, Kirpotin DB, Papahadjopoulos D: **Optimizing liposomes for delivery of chemotherapeutic agents to solid tumors.** *Pharmacol Rev* 1999, **51**(4):691-743.
97. Schreier H, Gonzalez-Rothi RJ, Stecenko AA: **pulmoary delivery of liposomes.** *J Control Release* 1993, **24**(1-3):209-223.
98. Taylor KMG, Farr SJ: **Liposomes for drug delivery to the respiratory tract.** *drug development and industrial pharmacy* 1993, **19**(1-2):123-142.
99. Poznansky MJ, Juliano RL: **Biological approaches to the controlled delivery of drugs: a critical review.** *Pharmacol Rev* 1984, **36**(4):277-336.
100. Jamil H, Sheikh S, Ahmad I: **liposomes: the next generation.** *modern drug discovery* 2004(1):37-39.
101. Krishna R, Webb MS, St Onge G, Mayer LD: **Liposomal and nonliposomal drug pharmacokinetics after administration of liposome-encapsulated vincristine and their contribution to drug tissue distribution properties.** *J Pharmacol Exp Ther* 2001, **298**(3):1206-1212.
102. Asai T, Shuto S, Matsuda A, Kakiuchi T, Ohba H, Tsukada H, Oku N: **Targeting and anti-tumor efficacy of liposomal 5'-O-dipalmitoylphosphatidyl 2'-C-cyano-2'-deoxy-1-beta-D-arabino-pentofuranosylcytosine in mice lung bearing B16BL6 melanoma.** *Cancer Lett* 2001, **162**(1):49-56.
103. Sharma A, Sharma US: **Liposomes in drug delivery: progress and limitations.** *Int J Pharm* 1997, **154**:123-140.
104. Pagano RE, Weinstein JN: **Interactions of liposomes with mammalian cells.** *Annu Rev Biophys Bioeng* 1978, **7**:435-468.
105. Chandran S, Roy A, Mishra B: **Recent trends in drug delivery systems: liposomal drug delivery system--preparation and characterisation.** *Indian J Exp Biol* 1997, **35**(8):801-809.
106. Waldrep JC, Arppe J, Jansa KA, Knight V: **high dose cyclosporin A and budesonide-liposome aerosols.** *Int J Pharm* 1997, **152**:27-36.
107. Waldrep JC, Arppe J, Jansa KA, Vidgren M: **Experimental pulmonary delivery of cyclosporin A by liposome aerosol.** *Int J Pharm* 1998, **160**:239-249.
108. Saari M, Vidgren MT, Koskinen MO, Turjanmaa VM, Nieminen MM: **Pulmonary distribution and clearance of two beclomethasone liposome formulations in healthy volunteers.** *Int J Pharm* 1999, **181**(1):1-9.

109. Knight V, Koshkina NV, Waldrep JC, Giovanella BC, Gilbert BE: **Anticancer effect of 9-nitrocamptothecin liposome aerosol on human cancer xenografts in nude mice.** *Cancer Chemother Pharmacol* 1999, **44**(3):177-186.
110. Gilbert BE, Black MB, Waldrep JC, Bennick J, Montgomery C, Knight V: **Cyclosporin A liposome aerosol: lack of acute toxicity in rats with high incidence of underlying pneumonitis.** *Inhal Toxicol* 1997, **9**:717-730.
111. Waldrep JC, Gilbert BE, Knight CM, Black MB, Scherer PW, Knight V, Eschenbacher W: **Pulmonary delivery of beclomethasone liposome aerosol in volunteers. Tolerance and safety.** *Chest* 1997, **111**(2):316-323.
112. Kulkarni SB, Singh M, Betageri GV: **Encapsulation, stability and in-vitro release characteristics of liposomal formulations of colchicine.** *J Pharm Pharmacol* 1997, **49**(5):491-495.
113. Boulmedarat L, Grossiord JL, Fattal E, Bochot A: **Influence of methyl-beta-cyclodextrin and liposomes on rheological properties of Carbopol 974P NF gels.** *Int J Pharm* 2003, **254**(1):59-64.
114. Bridges PA, Taylor KM: **The effects of freeze-drying on the stability of liposomes to jet nebulization.** *J Pharm Pharmacol* 2001, **53**(3):393-398.
115. Khalil RM, Murad FE, Yehia SA, El-Ridy MS, Salama HA: **Free versus liposome-entrapped streptomycin sulfate in treatment of infections caused by Salmonella enteritidis.** *Pharmazie* 1996, **51**(3):182-184.
116. Fielding RM, Abra RM: **Factors affecting the release rate of terbutaline from liposome formulations after intratracheal instillation in the guinea pig.** *Pharm Res* 1992, **9**(2):220-223.
117. Zhigaltsev IV, Maurer N, Akhong QF, Leone R, Leng E, Wang J, Semple SC, Cullis PR: **Liposome-encapsulated vincristine, vinblastine and vinorelbine: a comparative study of drug loading and retention.** *J Control Release* 2005, **104**(1):103-111.
118. Ugwu S, Zhang A, Parmar M, Miller B, Sardone T, Peikov V, Ahmad I: **Preparation, characterization, and stability of liposome-based formulations of mitoxantrone.** *Drug Dev Ind Pharm* 2005, **31**(2):223-229.
119. Shahiwala A, Misra A: **Pulmonary absorption of liposomal levonorgestrel.** *AAPS PharmSciTech* 2004, **5**(1):E13.
120. Lambros MP, Bourne DW, Abbas SA, Johnson DL: **Disposition of aerosolized liposomal amphotericin B.** *J Pharm Sci* 1997, **86**(9):1066-1069.
121. Vorauer-Uhl K, Wagner A, Borth N, Katinger H: **Determination of liposome size distribution by flow cytometry.** *Cytometry* 2000, **39**(2):166-171.
122. Gabriels M, Plaizier-Vercammen J: **Physical and chemical evaluation of liposomes, containing artesunate.** *J Pharm Biomed Anal* 2003, **31**(4):655-667.
123. Manosroi A, Kongkaneramt L, Manosroi J: **Characterization of amphotericin B liposome formulations.** *Drug Dev Ind Pharm* 2004, **30**(5):535-543.
124. Crosasso P, Ceruti M, Brusa P, Arpicco S, Dosio F, Cattel L: **Preparation, characterization and properties of sterically stabilized paclitaxel-containing liposomes.** *J Control Release* 2000, **63**(1-2):19-30.

125. Paavola A, Kilpelainen I, Yliruusi J, Rosenberg P: **Controlled release injectable liposomal gel of ibuprofen for epidural analgesia.** *Int J Pharm* 2000, **199**(1):85-93.
126. Nagarsenker MS, Londhe VY: **Preparation and evaluation of a liposomal formulation of sodium cromoglicate.** *Int J Pharm* 2003, **251**(1-2):49-56.
127. Al-Angary AA, Bayomi MA, Khidr SH, Al-Meshal MA, Al-Dardiri M: **Characterization, stability and in vivo targeting of liposomal formulation containing cyclosporin.** *Int J Pharm* 1994, **114**:221-225.
128. Xiao C, Qi X, Maitani Y, Nagai T: **Sustained release of cisplatin from multivesicular liposomes: potentiation of antitumor efficacy against S180 murine carcinoma.** *J Pharm Sci* 2004, **93**(7):1718-1724.
129. Shabbits JA, Chiu GN, Mayer LD: **Development of an in vitro drug release assay that accurately predicts in vivo drug retention for liposome-based delivery systems.** *J Control Release* 2002, **84**(3):161-170.
130. Driscoll KE, Costa DL, Hatch G, Henderson R, Oberdorster G, Salem H, Schlesinger RB: **Intratracheal instillation as an exposure technique for the evaluation of respiratory tract toxicity: uses and limitations.** *Toxicol Sci* 2000, **55**(1):24-35.
131. Brain JD, Knudson DE, Sorokin SP, Davis MA: **pulmonary distribution of particles given by intratracheal instillation or by aerosol inhalation.** *Environ Res* 1976, **11**:13-33.
132. Schanker LS, Mitchell EW, Brown RA, Jr.: **Species comparison of drug absorption from the lung after aerosol inhalation or intratracheal injection.** *Drug Metab Dispos* 1986, **14**(1):79-88.
133. Sabaitis CP, Leong BK, Rop DA, Aaron CS: **Validation of intratracheal instillation as an alternative for aerosol inhalation toxicity testing.** *J Appl Toxicol* 1999, **19**(2):133-140.
134. Costa DL, Lehmann JR, Harold WM, Drew RT: **Transoral tracheal intubation of rodents using a fiberoptic laryngoscope.** *Lab Anim Sci* 1986, **36**(3):256-261.
135. Pritchard JN, Holmes A, Evans JC, Evans N, Evans RJ, Morgan A: **The distribution of dust in the rat lung following administration by inhalation and by single intratracheal instillation.** *Environ Res* 1985, **36**(2):268-297.
136. Mauderly JL: **Bronchopulmonary lavage of small laboratory animals.** *Lab Anim Sci* 1977, **27**(2):255-261.
137. Hatch GE, Slade R, Boykin E, Hu PC, Miller FJ, Gardner DE: **Correlation of effects of inhaled versus intratracheally injected males on susceptibility to respiratory infection in mice.** *Am Rev Respir Dis* 1981, **124**(2):167-173.
138. Driscoll KE, Lindenschmidt RC, Maurer JK, Higgins JM, Ridder G: **Pulmonary response to silica or titanium dioxide: inflammatory cells, alveolar macrophage-derived cytokines, and histopathology.** *Am J Respir Cell Mol Biol* 1990, **2**(4):381-390.
139. Driscoll KE, Lindenschmidt RC, Maurer JK, Perkins L, Perkins M, Higgins J: **Pulmonary response to inhaled silica or titanium dioxide.** *Toxicol Appl Pharmacol* 1991, **111**(2):201-210.
140. Driscoll KE, Maurer JK, Poynter J, Higgins J, Asquith T, Miller NS: **Stimulation of rat alveolar macrophage fibronectin release in a cadmium chloride model of lung injury and fibrosis.** *Toxicol Appl Pharmacol* 1992, **116**(1):30-37.

141. Damon EG, Halliwell WH, Henderson TR, Mokler BV, Jones RK: **Acute toxicity of polyethylene glycol p-isooctylphenol ether in syrian hamsters exposed by inhalation or bronchopulmonary lavage.** *Toxicol Appl Pharmacol* 1982, **63**(1):53-61.
142. Muhle H, Bellmann B, Creutzenberg O, Dasenbrock C, Ernst H, Kilpper R, MacKenzie JC, Morrow P, Mohr U, Takenaka S *et al*: **Pulmonary response to toner upon chronic inhalation exposure in rats.** *Fundam Appl Toxicol* 1991, **17**(2):280-299.
143. Koshkina NV, Waldrep JC, Knight V: **Camptothecins and lung cancer: improved delivery systems by aerosol.** *Curr Cancer Drug Targets* 2003, **3**(4):251-264.
144. Kastl S, Kotschenreuther U, Hille B, Schmidt J, Gepp H, Hohenberger W: **Simplification of rat intubation on inclined metal plate.** *Adv Physiol Educ* 2004, **28**(1-4):29-32.
145. Omri A, Beaulac C, Bouhajib M, Montplaisir S, Sharkawi M, Lagace J: **Pulmonary retention of free and liposome-encapsulated tobramycin after intratracheal administration in uninfected rats and rats infected with Pseudomonas aeruginosa.** *Antimicrob Agents Chemother* 1994, **38**(5):1090-1095.
146. Postnov AA, Meurrens K, Weiler H, Van Dyck D, Xu H, Terpstra P, De Clerck NM: **In vivo assessment of emphysema in mice by high resolution X-ray microtomography.** *J Microsc* 2005, **220**(Pt 1):70-75.
147. Muensterer OJ, Till H, Bergmann F, Klis VJ, Metzger R, Deprest JA, Simbruner G: **Lung growth induced by prenatal instillation of perfluorocarbon into the fetal rabbit lung.** *Pediatr Surg Int* 2004, **20**(4):248-252.
148. Dean M, Rzhetsky A, Allikmets R: **The human ATP-binding cassette (ABC) transporter superfamily.** *Genome Res* 2001, **11**(7):1156-1166.
149. Beaulieu E, Demeule M, Ghitescu L, Beliveau R: **P-glycoprotein is strongly expressed in the luminal membranes of the endothelium of blood vessels in the brain.** *Biochem J* 1997, **326** (Pt 2):539-544.
150. Nielsen DL: **Mechanisms and functional aspects of multidrug resistance in Ehrlich ascites tumour cells.** *Dan Med Bull* 2004, **51**(4):393-414.
151. Borst P, Evers R, Kool M, Wijnholds J: **The multidrug resistance protein family.** *Biochim Biophys Acta* 1999, **1461**(2):347-357.
152. Borst P, Zelcer N, van Helvoort A: **ABC transporters in lipid transport.** *Biochim Biophys Acta* 2000, **1486**(1):128-144.
153. Rosati A, Maniori S, Decorti G, Candussio L, Giraldi T, Bartoli F: **Physiological regulation of P-glycoprotein, MRP1, MRP2 and cytochrome P450 3A2 during rat ontogeny.** *Dev Growth Differ* 2003, **45**(4):377-387.
154. Edwards G: **Ivermectin: does P-glycoprotein play a role in neurotoxicity?** *Filaria J* 2003, **2 Suppl 1**:S8.
155. Thomas H, Coley HM: **Overcoming multidrug resistance in cancer: an update on the clinical strategy of inhibiting p-glycoprotein.** *Cancer Control* 2003, **10**(2):159-165.
156. Georges E, Bradley G, Garipey J, Ling V: **Detection of P-glycoprotein isoforms by gene-specific monoclonal antibodies.** *Proc Natl Acad Sci U S A* 1990, **87**(1):152-156.

157. Scheffer GL, Pijnenborg AC, Smit EF, Muller M, Postma DS, Timens W, van der Valk P, de Vries EG, Scheper RJ: **Multidrug resistance related molecules in human and murine lung.** *J Clin Pathol* 2002, **55**(5):332-339.
158. Paredes A, Lobo C, Izquierdo JM, Egana L, Aldama L, Aldazabal P, Sarasqueta C, Abad T, Scheper RJ, Izquierdo MA: **Immunohistochemical expression of multidrug resistance (MDR) proteins in non-small cell lung cancer (NSCLC).** *Annals of oncology* 2000, **11**:124-126.
159. Komdeur R, Klunder J, Van Der Graaf WTA, Van Den Berg E, Hoekstra HJ, De Bont Eveline SJM, Molenaar WM: **Multidrug resistance proteins in rhabdomyosarcoms: comparison between children and adults.** *Cancer* 2003, **97**(8):1999-2005.
160. Links M, Brown R: **Clinical relevance of the molecular mechanisms of resistance to anti-cancer drugs.** *Mol Med* 1999:1-21.
161. Krishna R, Mayer LD: **Multidrug resistance (MDR) in cancer mechanisms, reversal using modulators of MDR and the role of MDR modulators in influencing the pharmacokinetics of anticancer drugs.** *Eur J Cancer Sci* 2000, **11**:265-283.
162. Jang SH, Wientjes MG, Lu D, Au JL: **Drug delivery and transport to solid tumors.** *Pharm Res* 2003, **20**(9):1337-1350.
163. Jain RK: **Determinants of tumor blood flow: a review.** *Cancer Res* 1988, **48**(10):2641-2658.
164. Folkman J: **What is the evidence that tumors are angiogenesis dependent?** *J Natl Cancer Inst* 1990, **82**(1):4-6.
165. Richly H, Kupsch P, Passage K, Grubert M, Hilger RA, Kredtke S, Voliotis D, Scheulen ME, Seeber S, Strumberg D: **A phase I clinical and pharmacokinetic study of the Raf kinase inhibitor (RKI) BAY 43-9006 administered in combination with doxorubicin in patients with solid tumors.** *Int J Clin Pharmacol Ther* 2003, **41**(12):620-621.
166. Richly H, Kupsch P, Passage K, Grubert M, Hilger RA, Voigtmann R, Schwartz B, Brendel E, Christensen O, Haase CG *et al*: **Results of a phase I trial of BAY 43-9006 in combination with doxorubicin in patients with primary hepatic cancer.** *Int J Clin Pharmacol Ther* 2004, **42**(11):650-651.
167. Lavie Y, Cao H, Volner A, Lucci A, Han TY, Geffen V, Giuliano AE, Cabot MC: **Agents that reverse multidrug resistance, tamoxifen, verapamil, and cyclosporin A, block glycosphingolipid metabolism by inhibiting ceramide glycosylation in human cancer cells.** *J Biol Chem* 1997, **272**(3):1682-1687.
168. Nobili S, Landini I, Giglioni B, Mini E: **Pharmacological strategies for overcoming multidrug resistance.** *Curr Drug Targets* 2006, **7**(7):861-879.
169. Chen LM, Liang YJ, Ruan JW, Ding Y, Wang XW, Shi Z, Gu LQ, Yang XP, Fu LW: **Reversal of P-gp mediated multidrug resistance in-vitro and in-vivo by FG020318.** *J Pharm Pharmacol* 2004, **56**(8):1061-1066.
170. Jin J, Wang FP, Wei H, Liu G: **Reversal of multidrug resistance of cancer through inhibition of P-glycoprotein by 5-bromotetrandrine.** *Cancer Chemother Pharmacol* 2005, **55**(2):179-188.
171. Shen LZ, Hua YB, Yu XM, Xu Q, Chen T, Wang JH, Wu WX: **Tamoxifen can reverse multidrug resistance of colorectal carcinoma in vivo.** *World J Gastroenterol* 2005, **11**(7):1060-1064.

172. Brigger I, Dubernet C, Couvreur P: **Nanoparticles in cancer therapy and diagnosis.** *Adv Drug Deliv Rev* 2002, **54**:631-651.
173. Vauthier C, Dubernet C, Chauvierre C, Brigger I, Couvreur P: **Drug delivery to resistant tumors: the potential of poly(alkyl cyanoacrylate) nanoparticles.** *J Control Release* 2003, **93**(2):151-160.
174. Cuvier C, Roblot-Treupel L, Millot JM, Lizard G, Chevillard S, Manfait M, Couvreur P, Poupon MF: **Doxorubicin-loaded nanospheres bypass tumor cell multidrug resistance.** *Biochem Pharmacol* 1992, **44**(3):509-517.
175. Huo D, Deng S, Li L, Ji J: **Studies on the poly (lactic-co-glycolic) acid microspheres of cisplatin for lung-targeting.** *Int J Pharm* 2005, **289**(1-2):63-67.
176. Boisdron-Celle M, Menei P, Benoit JP: **Preparation and characterization of 5-fluorouracil-loaded microparticles as biodegradable anticancer drug carriers.** *J Pharm Pharmacol* 1995, **47**(2):108-114.
177. Ertl B, Platzer P, Wirth M, Gabor F: **Poly(D,L-lactic-co-glycolic acid) microspheres for sustained delivery and stabilization of camptothecin.** *J Control Release* 1999, **61**(3):305-317.
178. Gupte A, Ciftci K: **Formulation and characterization of Paclitaxel, 5-FU and Paclitaxel + 5-FU microspheres.** *Int J Pharm* 2004, **276**(1-2):93-106.
179. Liggins RT, D'Amours S, Demetrick JS, Machan LS, Burt HM: **Paclitaxel loaded poly(L-lactic acid) microspheres for the prevention of intraperitoneal carcinomatosis after a surgical repair and tumor cell spill.** *Biomaterials* 2000, **21**(19):1959-1969.
180. Jain RA: **The manufacturing techniques of various drug loaded biodegradable poly (lactide-co-glycolide) (PLGA) devices.** *Biomaterials* 2000, **21**:2475-2490.
181. Benny O, Duvshani-Eshet M, Cargioli T, Bello L, Bikfalvi A, Carroll RS, Machluf M: **Continuous delivery of endogenous inhibitors from poly(lactic-co-glycolic acid) polymeric microspheres inhibits glioma tumor growth.** *Clin Cancer Res* 2005, **11**(2 Pt 1):768-776.
182. Mainardes RM, Evangelista RC: **PLGA nanoparticles containing praziquantel: effect of formulation variables on size distribution.** *Int J Pharm* 2005, **290**(1-2):137-144.
183. Yue IC, Poff J, Cortes ME, Sinisterra RD, Faris CB, Hildgen P, Langer R, Shastri VP: **A novel polymeric chlorhexidine delivery device for the treatment of periodontal disease.** *Biomaterials* 2004, **25**(17):3743-3750.
184. Herrmann J, Bodmeier R: **Biodegradable, somatostatin acetate containing microspheres prepared by various aqueous and non-aqueous solvent evaporation methods.** *Eur J Pharm Biopharm* 1998, **45**(1):75-82.
185. Lee WK, Park JY, Yang EH, Suh H, Kim SH, Chung DS, Choi K, Yang CW, Park JS: **Investigation of the factors influencing the release rates of cyclosporin A-loaded micro- and nanoparticles prepared by high-pressure homogenizer.** *J Control Release* 2002, **84**(3):115-123.
186. Hombreiro-Perez M, Siepmann J, Zinutti C, Lamprecht A, Ubrich N, Hoffman M, Bodmeier R, Maincent P: **Non-degradable microparticles containing a hydrophilic and/or a lipophilic drug: preparation, characterization and drug release modeling.** *J Control Release* 2003, **88**(3):413-428.

187. Martinez-Sancho C, Herrero-Vanrell R, Negro S: **Optimisation of aciclovir poly(D,L-lactide-co-glycolide) microspheres for intravitreal administration using a factorial design study.** *Int J Pharm* 2004, **273**(1-2):45-56.
188. Hariharan S, Bhardwaj V, Bala I, Sitterberg J, Bakowsky U, Ravi Kumar MN: **Design of estradiol loaded PLGA nanoparticulate formulations: a potential oral delivery system for hormone therapy.** *Pharm Res* 2006, **23**(1):184-195.
189. Ravi Kumar MN, Bakowsky U, Lehr CM: **Preparation and characterization of cationic PLGA nanospheres as DNA carriers.** *Biomaterials* 2004, **25**(10):1771-1777.
190. Wichert B, Rohdewald P: **A new method for the preparation of drug containing polylactic acid microparticles without using organic solvents.** *J Control Release* 1990, **14**:269-283.
191. Wichert B, Rohdewald P: **Low molecular weight PLA: a suitable polymer for pulmonary administered microparticles?** *J Microencapsul* 1993, **10**(2):195-207.
192. Tomoda K, Kojima S, Kajimoto M, Watanabe D, Nakajima T, Makino K: **Effects of pulmonary surfactant system on rifampicin release from rifampicin-loaded PLGA microspheres.** *Colloids Surf B Biointerfaces* 2005, **45**(1):1-6.
193. Lin R, Ng LS, Wang CH: **In vitro study of anticancer drug doxorubicin in PLGA-based microparticles.** *Biomaterials* 2005, **26**(21):4476-4485.
194. Panyam J, Dali MM, Sahoo SK, Ma W, Chakravarthi SS, Amidon GL, Levy RJ, Labhasetwar V: **Polymer degradation and in vitro release of a model protein from poly (D,L-lactide-co-glycolide) nano- and microparticles.** *J Control Release* 2003, **92**(1-2):173-187.
195. Lu B, Wu W: **Optimization of preparation of dexamethasone acetate-loaded poly (D,L-lactide) microspheres by central composite design.** *Acta pharm Sin* 1999, **34**:387-391.
196. Lagarce F, Renaud P, Faisant N, Nicolas G, Cailleux A, Richard J, Menei P, Benoit JP: **Baclofen-loaded microspheres: preparation and efficacy testing in a new rabbit model.** *Eur J Pharm Biopharm* 2005, **59**(3):449-459.
197. Lagarce F, Faisant N, Desfontis JC, Marescaux L, Gautier F, Richard J, Menei P, Benoit JP: **Baclofen-loaded microspheres in gel suspensions for intrathecal drug delivery: in vitro and in vivo evaluation.** *Eur J Pharm Biopharm* 2005, **61**(3):171-180.
198. Hou D, Xie C, Huang K, Zhu C: **The production and characteristics of solid lipid nanoparticles (SLNs).** *Biomaterials* 2003, **24**(10):1781-1785.
199. Le Corre P, Rytting JH, Gajan V, Chevanne F, Le Verge R: **In vitro controlled release kinetics of local anaesthetics from poly(D,L-lactide) and poly(lactide-co-glycolide) microspheres.** *J Microencapsul* 1997, **14**(2):243-255.
200. Galeska I, Kim TK, Patil SD, Bhardwaj U, Chattopadhyay D, Papadimitrakopoulos F, Burgess DJ: **Controlled release of dexamethasone from PLGA microspheres embedded within polyacid-containing PVA hydrogels.** *Aaps J* 2005, **7**(1):E231-240.
201. Bodmeier R, Chen H: **The preparation and characterization of microspheres containing the anti-inflammatory agents indomethacin, ibuprofen and ketoprofen.** *J Control Release* 1989, **10**(2):167-175.

202. Mu L, Feng SS: **Fabrication, characterization and in vitro release of paclitaxel (Taxol®) loaded poly (lactic-co-glycolic acid) microspheres prepared by spray drying technique with lipid/cholesterol emulsifiers.** *J Control Release* 2001, **76**:239-254.
203. Kissel T, Brich Z, Bantle S, Lancranjan I, Nimmerfall F, Vit P: **Parenteral depot system on the basis of biodegradable polyesters.** *J Control Release* 1991, **16**:27-42.
204. Crotts G, Park TG: **Protein delivery from poly(lactic-co-glycolic acid) biodegradable microspheres: release kinetics and stability issues.** *J Microencapsul* 1998, **15**:699-713.
205. Igartua M, Hernandez RM, Esquisabel A, Gascon AR, Calvo MB, Pedraz JL: **Influence of formulation variables on the in-vitro release of albumin from biodegradable microparticulate systems.** *J Microencapsul* 1997, **14**(3):349-356.
206. Shive MS, Anderson JM: **Biodegradation and biocompatibility of PLA and PLGA microspheres.** *Adv Drug Deliv Rev* 1997, **28**(1):5-24.
207. Gautam A, Waldrep CJ, Densmore CL: **Delivery systems for pulmonary gene therapy.** *Am J Respir Med* 2002, **1**(1):35-46.
208. Roth JA, Nguyen D, Lawrence DD, Kemp BL, Carrasco CH, Ferson DZ, Hong WK, Komaki R, Lee JJ, Nesbitt JC *et al*: **Retrovirus-mediated wild-type p53 gene transfer to tumors of patients with lung cancer.** *Nat Med* 1996, **2**(9):985-991.
209. Gautam A, Densmore CL, Waldrep JC: **Inhibition of experimental lung metastasis by aerosol delivery of PEI-p53 complexes.** *Mol Ther* 2000, **2**(4):318-323.
210. Vile RG, Russell SJ: **Retroviruses as vectors.** *Br Med Bull* 1995, **51**:12-30.
211. Curiel DT: **Strategies to adapt adenoviral vectors for targeted delivery.** *Ann N Y Acad Sci* 1999, **886**:158-171.
212. Flotte TR, Afione SA, Conrad C, McGrath SA, Solow R, Oka H, Zeitlin PL, Guggino WB, Carter BJ: **Stable in vivo expression of the cystic fibrosis transmembrane conductance regulator with an adeno-associated virus vector.** *Proc Natl Acad Sci U S A* 1993, **90**(22):10613-10617.
213. Balter M: **Gene therapy on trial.** *Science* 2000, **288**(5468):951-957.
214. De Smedt SC, Demeester J, Hennink WE: **Cationic polymer based gene delivery systems.** *Pharm Res* 2000, **17**(2):113-126.
215. Brown MD, Schatzlein AG, Uchegbu IF: **Gene delivery with synthetic (non viral) carriers.** *Int J Pharm* 2001, **229**(1-2):1-21.
216. Kircheis R, Schuller S, Brunner S, Ogris M, Heider KH, Zauner W, Wagner E: **Polycation-based DNA complexes for tumor-targeted gene delivery in vivo.** *J Gene Med* 1999, **1**(2):111-120.
217. Ogris M, Wagner E: **Targeting tumors with non-viral gene delivery systems.** *Drug Discov Today* 2002, **7**(8):479-485.
218. Templeton NS, Lasic DD, Frederik PM, Strey HH, Roberts DD, Pavlakis GN: **Improved DNA: liposome complexes for increased systemic delivery and gene expression.** *Nat Biotechnol* 1997, **15**(7):647-652.
219. Szala S, Missol E, Sochanik A: **The use of cationic liposomes DC/Chol/DOPE and DDAB/DOPE for direct transfer of Escherichia coli cytosine deaminase gene into growing melanoma tumors.** *Gene Ther* 1996, **3**:1026-1031.

220. Pedroso de Lima MC, Simoes S, Pires P, Faneca H, Duzgunes N: **Cationic lipid-DNA complexes in gene delivery: from biophysics to biological applications.** *Adv Drug Deliv Rev* 2001, **47**(2-3):277-294.
221. Felgner PL, Ringold GM: **Cationic liposome-mediated transfection.** *Nature* 1989, **337**(6205):387-388.
222. Felgner JH, Kumar R, Sridhar CN, Wheeler CJ, Tsai YJ, Border R, Ramsey P, Martin M, Felgner PL: **Enhanced gene delivery and mechanism studies with a novel series of cationic lipid formulations.** *J Biol Chem* 1994, **269**(4):2550-2561.
223. Farhood H, Serbina N, Huang L: **The role of dioleoyl phosphatidylethanolamine in cationic liposome mediated gene transfer.** *Biochim Biophys Acta* 1995, **1235**(2):289-295.
224. Nishikawa M, Takemura S, Yamashita F, Takakura Y, Meijer DK, Hashida M, Swart PJ: **Pharmacokinetics and in vivo gene transfer of plasmid DNA complexed with mannosylated poly(L-lysine) in mice.** *J Drug Target* 2000, **8**(1):29-38.
225. Shapiro JT, Leng M, Felsenfeld G: **Deoxyribonucleic acid-polylysine complexes. Structure and nucleotide specificity.** *Biochemistry* 1969, **8**(8):3219-3232.
226. Demeneix B, Behr JP: **Polyethylenimine (PEI).** *Adv Genet* 2005, **53**:217-230.
227. Lungwitz U, Breunig M, Blunk T, Gopferich A: **Polyethylenimine-based non-viral gene delivery systems.** *Eur J Pharm Biopharm* 2005, **60**(2):247-266.
228. Gautam A, Densmore CL, Xu B, Waldrep JC: **Enhanced gene expression in mouse lung after PEI-DNA aerosol delivery.** *Mol Ther* 2000, **2**(1):63-70.
229. Ernst N, Ulrichskotter S, Schmalix WA, Radler J, Galneder R, Mayer E, Gersting S, Plank C, Reinhardt D, Rosenecker J: **Interaction of liposomal and polycationic transfection complexes with pulmonary surfactant.** *J Gene Med* 1999, **1**(5):331-340.
230. Kichler A, Leborgne C, Coeytaux E, Danos O: **Polyethylenimine-mediated gene delivery: a mechanistic study.** *J Gene Med* 2001, **3**(2):135-144.
231. Boussif O, Lezoualc'h F, Zanta MA, Mergny MD, Scherman D, Demeneix B, Behr JP: **A versatile vector for gene and oligonucleotide transfer into cells in culture and in vivo: polyethylenimine.** *Proc Natl Acad Sci U S A* 1995, **92**(16):7297-7301.
232. Tang MX, Szoka FC: **The influence of polymer structure on the interactions of cationic polymers with DNA and morphology of the resulting complexes.** *Gene Ther* 1997, **4**(8):823-832.
233. Abdallah B, Hassan A, Benoist C, Goula D, Behr JP, Demeneix BA: **A powerful nonviral vector for in vivo gene transfer into the adult mammalian brain: polyethylenimine.** *Hum Gene Ther* 1996, **7**:1947-1954.
234. Bragonzi A, Dina G, Villa A, Calori G, Biffi A, Bordignon C, Assael BM, Conese M: **Biodistribution and transgene expression with nonviral cationic vector/DNA complexes in the lungs.** *Gene Ther* 2000, **7**(20):1753-1760.
235. Goula D, Remy JS, Erbacher P, Wasowicz M, Levi G, Abdallah B, Demeneix BA: **Size, diffusibility and transfection performance of linear PEI/DNA complexes in the mouse central nervous system.** *Gene Ther* 1998, **5**(5):712-717.

236. Goula D, Benoist C, Mantero S, Merlo G, Levi G, Demeneix BA: **Polyethylenimine-based intravenous delivery of transgenes to mouse lung.** *Gene Ther* 1998, **5**(9):1291-1295.
237. Goula D, Becker N, Lemkine GF, Normandie P, Rodrigues J, Mantero S, Levi G, Demeneix BA: **Rapid crossing of the pulmonary endothelial barrier by polyethylenimine/DNA complexes.** *Gene Ther* 2000, **7**(6):499-504.
238. Zou SM, Erbacher P, Remy JS, Behr JP: **Systemic linear polyethylenimine (L-PEI)-mediated gene delivery in the mouse.** *J Gene Med* 2000, **2**(2):128-134.
239. Chalfie M, Tu Y, Euskirchen G, Ward WW, Prasher DC: **Green fluorescent protein as a marker for gene expression.** *Science* 1994, **263**(5148):802-805.
240. Bout A, Valerio D, Scholte BJ: **In vivo transfer and expression of the lacZ gene in the mouse lung.** *Exp Lung Res* 1993, **19**(2):193-202.
241. Zinselmeyer BH, Beggbie N, Uchegbu IF, Schatzlein AG: **Quantification of beta-galactosidase activity after non-viral transfection in vivo.** *J Control Release* 2003, **91**(1-2):201-208.
242. Griesenbach U, Chonn A, Cassady R, Hannam V, Ackerley C, Post M, Tanswell AK, Olek K, O'Brodovich H, Tsui LC: **Comparison between intratracheal and intravenous administration of liposome-DNA complexes for cystic fibrosis lung gene therapy.** *Gene Ther* 1998, **5**(2):181-188.
243. Boucher RC: **Status of gene therapy for cystic fibrosis lung disease.** *J Clin Invest* 1999, **103**(4):441-445.
244. Blezinger P, Freimark BD, Matar M, Wilson E, Singhal A, Min W, Nordstrom JL, Pericle F: **Intratracheal administration of interleukin 12 plasmid-cationic lipid complexes inhibits murine lung metastases.** *Hum Gene Ther* 1999, **10**(5):723-731.
245. Zou Y, Zong G, Ling YH, Perez-Soler R: **Development of cationic liposome formulations for intratracheal gene therapy of early lung cancer.** *Cancer Gene Ther* 2000, **7**(5):683-696.
246. Chishima T, Miyagi Y, Wang X, Yamaoka H, Shimada H, Moossa AR, Hoffman RM: **Cancer invasion and micrometastasis visualized in live tissue by green fluorescent protein expression.** *Cancer Res* 1997, **57**(10):2042-2047.
247. Akerman ME, Chan WC, Laakkonen P, Bhatia SN, Ruoslahti E: **Nanocrystal targeting in vivo.** *Proc Natl Acad Sci U S A* 2002, **99**(20):12617-12621.
248. Kishimoto J, Ehama R, Ge Y, Kobayashi T, Nishiyama T, Detmar M, Burgeson RE: **In vivo detection of human vascular endothelial growth factor promoter activity in transgenic mouse skin.** *Am J Pathol* 2000, **157**(1):103-110.
249. Wightman L, Kircheis R, Rossler V, Carotta S, Ruzicka R, Kurska M, Wagner E: **Different behavior of branched and linear polyethylenimine for gene delivery in vitro and in vivo.** *J Gene Med* 2001, **3**(4):362-372.
250. Bragonzi A, Boletta A, Biffi A, Muggia A, Sersale G, Cheng SH, Bordignon C, Assael BM, Conese M: **Comparison between cationic polymers and lipids in mediating systemic gene delivery to the lungs.** *Gene Ther* 1999, **6**(12):1995-2004.
251. Uduehi AN, Stammberger U, Frese S, Schmid RA: **Efficiency of non-viral gene delivery systems to rat lungs.** *Eur J Cardiothorac Surg* 2001, **20**(1):159-163.

252. Ferrari S, Pettenazzo A, Garbati N, Zacchello F, Behr JP, Scarpa M: **Polyethylenimine shows properties of interest for cystic fibrosis gene therapy.** *Biochim Biophys Acta* 1999, **1447**(2-3):219-225.
253. Coll JL, Chollet P, Brambilla E, Desplanques D, Behr JP, Favrot M: **In vivo delivery to tumors of DNA complexed with linear polyethylenimine.** *Hum Gene Ther* 1999, **10**(10):1659-1666.
254. Allo JC, Midoux P, Merten M, Souil E, Lipecka J, Figarella C, Monsigny M, Briand P, Fajac I: **Efficient gene transfer into human normal and cystic fibrosis tracheal gland serous cells with synthetic vectors.** *Am J Respir Cell Mol Biol* 2000, **22**(2):166-175.
255. Densmore CL: **Polyethyleneimine-based gene therapy by inhalation.** *Expert Opin Biol Ther* 2003, **3**(7):1083-1092.
256. Rudolph C, Lausier J, Naundorf S, Muller RH, Rosenecker J: **In vivo gene delivery to the lung using polyethylenimine and fractured polyamidoamine dendrimers.** *J Gene Med* 2000, **2**(4):269-278.
257. Rudolph C, Ortiz A, Schillinger U, Jauernig J, Plank C, Rosenecker J: **Methodological optimization of polyethylenimine (PEI)-based gene delivery to the lungs of mice via aerosol application.** *J Gene Med* 2005, **7**(1):59-66.
258. Wiseman JW, Goddard CA, McLelland D, Colledge WH: **A comparison of linear and branched polyethylenimine (PEI) with DCChol/DOPE liposomes for gene delivery to epithelial cells in vitro and in vivo.** *Gene Ther* 2003, **10**(19):1654-1662.
259. Dif F, Djediat C, Alegria O, Demeneix B, Levi G: **Transfection of multiple pulmonary cell types following intravenous injection of PEI-DNA in normal and CFTR mutant mice.** *J Gene Med* 2006, **8**(1):82-89.
260. Blessing T, Kursa M, Holzhauser R, Kircheis R, Wagner E: **Different strategies for formation of pegylated EGF-conjugated PEI/DNA complexes for targeted gene delivery.** *Bioconjug Chem* 2001, **12**(4):529-537.
261. Ferrari S, Moro E, Pettenazzo A, Behr JP, Zacchello F, Scarpa M: **ExGen 500 is an efficient vector for gene delivery to lung epithelial cells in vitro and in vivo.** *Gene Ther* 1997, **4**(10):1100-1106.
262. Densmore CL, Orson FM, Xu B, Kinsey BM, Waldrep JC, Hua P, Bhogal B, Knight V: **Aerosol delivery of robust polyethyleneimine-DNA complexes for gene therapy and genetic immunization.** *Mol Ther* 2000, **1**(2):180-188.
263. Finsinger D, Remy JS, Erbacher P, Koch C, Plank C: **Protective copolymers for nonviral gene vectors: synthesis, vector characterization and application in gene delivery.** *Gene Ther* 2000, **7**(14):1183-1192.
264. Ogris M, Brunner S, Schuller S, Kircheis R, Wagner E: **PEGylated DNA/transferrin-PEI complexes: reduced interaction with blood components, extended circulation in blood and potential for systemic gene delivery.** *Gene Ther* 1999, **6**(4):595-605.
265. Ogris M, Walker G, Blessing T, Kircheis R, Wolschek M, Wagner E: **Tumor-targeted gene therapy: strategies for the preparation of ligand-polyethylene glycol-polyethylenimine/DNA complexes.** *J Control Release* 2003, **91**(1-2):173-181.

266. Arteaga CL: **The epidermal growth factor receptor: from mutant oncogene in nonhuman cancers to therapeutic target in human neoplasia.** *J Clin Oncol* 2001, **19**(18 Suppl):32S-40S.
267. Kim ES, Khuri FR, Herbst RS: **Epidermal growth factor receptor biology (IMC-C225).** *Curr Opin Oncol* 2001, **13**(6):506-513.
268. Cerny T, Barnes DM, Hasleton P, Barber PV, Healy K, Gullick W, Thatcher N: **Expression of epidermal growth factor receptor (EGF-R) in human lung tumours.** *Br J Cancer* 1986, **54**(2):265-269.
269. Cristiano RJ, Roth JA: **Epidermal growth factor mediated DNA delivery into lung cancer cells via the epidermal growth factor receptor.** *Cancer Gene Ther* 1996, **3**(1):4-10.
270. Selvaggi G, Novello S, Torri V, Leonardo E, De Giuli P, Borasio P, Mossetti C, Ardisson F, Lausi P, Scagliotti GV: **Epidermal growth factor receptor overexpression correlates with a poor prognosis in completely resected non-small-cell lung cancer.** *Ann Oncol* 2004, **15**(1):28-32.
271. Smith GJ, Morris C, Leigh D, Rhodes GC, Wong A: **EGF-receptor and extracellular matrix changes in mouse pulmonary carcinogenesis.** *Exp Lung Res* 1991, **17**(2):327-340.
272. Tanno S, Ohsaki Y, Nakanishi K, Toyoshima E, Kikuchi K: **Small cell lung cancer cells express EGFR and tyrosine phosphorylation of EGFR is inhibited by gefitinib ("Iressa", ZD1839).** *Oncol Rep* 2004, **12**(5):1053-1057.
273. Veale D, Ashcroft T, Marsh C, Gibson GJ, Harris AL: **Epidermal growth factor receptors in non-small cell lung cancer.** *Br J Cancer* 1987, **55**(5):513-516.
274. Wolschek MF, Thallinger C, Kursa M, Rossler V, Allen M, Lichtenberger C, Kircheis R, Lucas T, Willheim M, Reinisch W *et al*: **Specific systemic nonviral gene delivery to human hepatocellular carcinoma xenografts in SCID mice.** *Hepatology* 2002, **36**(5):1106-1114.
275. Frederiksen KS, Abrahamsen N, Cristiano RJ, Damstrup L, Poulsen HS: **Gene delivery by an epidermal growth factor/DNA polyplex to small cell lung cancer cell lines expressing low levels of epidermal growth factor receptor.** *Cancer Gene Ther* 2000, **7**(2):262-268.
276. Porebska I, Harlozinska A, Bojarowski T: **Expression of the tyrosine kinase activity growth factor receptors (EGFR, ERB B2, ERB B3) in colorectal adenocarcinomas and adenomas.** *Tumour Biol* 2000, **21**(2):105-115.
277. Kim H, Muller WJ: **The role of the epidermal growth factor receptor family in mammary tumorigenesis and metastasis.** *Exp Cell Res* 1999, **253**(1):78-87.
278. Kircheis R, Ostermann E, Wolschek MF, Lichtenberger C, Magin-Lachmann C, Wightman L, Kursa M, Wagner E: **Tumor-targeted gene delivery of tumor necrosis factor-alpha induces tumor necrosis and tumor regression without systemic toxicity.** *Cancer Gene Ther* 2002, **9**(8):673-680.
279. Hsieh ET, Shepherd FA, Tsao MS: **Co-expression of epidermal growth factor receptor and transforming growth factor-alpha is independent of ras mutations in lung adenocarcinoma.** *Lung Cancer* 2000, **29**(2):151-157.
280. Zhou S, Paxton JW, Tingle MD, Kestell P: **Determination of the covalent adducts of the novel anti-cancer agent 5,6-dimethylxanthenone-4-acetic acid in biological samples by high-performance liquid chromatography.** *J Chromatogr B Biomed Sci Appl* 2001, **757**(2):343-348.

-
281. Shah VP, Midha KK, Dighe S, McGilveray IJ, Skelly JP, Yacobi A, Layloff T, Viswanathan CT, Cook CE, McDowall RD *et al*: **Analytical methods validation: bioavailability, bioequivalence and pharmacokinetic studies. Conference report.** *Eur J Drug Metab Pharmacokinet* 1991, **16**(4):249-255.
282. Gan SH, Ismail R, Wan Adnan WA, Wan Z: **Method development and validation of a high-performance liquid chromatographic method for tramadol in human plasma using liquid-liquid extraction.** *J Chromatogr B Analyt Technol Biomed Life Sci* 2002, **772**(1):123-129.
283. Gonzales J, Jim Yeung SC, Smith JA: **High-performance liquid chromatographic assay validation of Manumycin A in mouse plasma.** *J Chromatogr B Analyt Technol Biomed Life Sci* 2002, **776**(2):177-182.
284. Tanaka K, Takeda T, Fujii K, Miyajima K: **Cryoprotective mechanism of saccharides on freeze-drying of liposome.** *chemical & Pharmaceutical Bulletin* 1992, **40**(1):1-5.
285. Bradford MM: **A rapid and sensitive method for the quantitation of microgram quantities of protein utilizing the principle of protein-dye binding.** *Anal Biochem* 1976, **72**:248-254.
286. Tchou-Wong KM, Jiang Y, Yee H, LaRosa J, Lee TC, Pellicer A, Jagirdar J, Gordon T, Goldberg JD, Rom WN: **Lung-specific expression of dominant-negative mutant p53 in transgenic mice increases spontaneous and benzo(a)pyrene-induced lung cancer.** *Am J Respir Cell Mol Biol* 2002, **27**(2):186-193.
287. Murakami H, Kobayashi M, Takeuchi H, Kawashima Y: **Preparation of poly(DL-lactide-co-glycolide) nanoparticles by modified spontaneous emulsification solvent diffusion method.** *Int J Pharm* 1999, **187**(2):143-152.
288. Naumov GN, Wilson SM, MacDonald IC, Schmidt EE, Morris VL, Groom AC, Hoffman RM, Chambers AF: **Cellular expression of green fluorescent protein, coupled with high-resolution in vivo videomicroscopy, to monitor steps in tumor metastasis.** *J Cell Sci* 1999, **112** (Pt 12):1835-1842.
289. Tyrsin O: **Role of Raf family members in mouse development.** *Dissertation.* Würzburg: Bayerische Julius-Maximilians-Universität Würzburg; 2003.
290. Birnboim HC, Doly J: **A rapid alkaline extraction procedure for screening recombinant plasmid DNA.** *Nucleic Acids Res* 1979, **7**(6):1513-1523.

Curriculum Vitae

Personal information:

Name: Samar Afify

Sex: female

Date and place of birth: December 6, 1970, Doha, Qatar

Marital status: Married, 1997

Citizenship: Egyptian

Education:

September 76-Jun 82: Primary school

September 82-Jun 85: Preparatory school

September 85-Jun 89: Secondary school

September 89-May 93: Faculty of Pharmacy, Cairo University, Egypt (Bachelor of Pharmaceutical Sciences)

April 94-September 98: Research assistant at the Pharmaceutics Department, National Organization of Drug Control and research (NODCAR), Cairo, Egypt

March 2003: Starting Ph.D. work under supervision of Prof. Dr. U. Rapp, Institut für Medizinische Strahlenkunde und Zellforschung and Prof. Dr. P. Högger, Institut für Pharmazie und Lebensmittelchemie, Universität Würzburg.

Language skills:

Arabic: Writing excellent, reading excellent

English: Writing good, reading very well

German: Good communication ability

ERKLÄRUNG

Hiermit erkläre ich an Eides statt, dass ich die Dissertation

Drug targeting delivery systems for treatment of Raf-1 induced lung tumors in mice

selbständig angefertigt und keine anderen als die von mir angegebenen Quellen und Hilfsmittel benutzt habe.

Ich erkläre außerdem, dass diese Dissertation weder in gleicher noch in anderer Form bereits in einem anderen Prüfungsverfahren vorgelegen hat.

Ich habe früher, außer den urkundlich vorgelegten und anerkannten Graden, keine weiteren akademischen Grade erworben oder zu erwerben versucht.

Würzburg, den

Samar Afify